

STRUCTURE AND DEFORMATION
ACROSS THE QUESNELLIA-OMINECA
TERRANE BOUNDARY, MT. PERSEUS AREA,
EAST-CENTRAL BRITISH COLUMBIA

By

DARREN C. ELSBY
B.A. POMONA COLLEGE, 1981

A THESIS SUBMITTED IN PARTIAL FULFILLMENT OF
THE REQUIREMENTS FOR THE DEGREE OF
MASTER OF SCIENCE

in

THE FACULTY OF GRADUATE STUDIES
Department of Geological Sciences

We accept this thesis as conforming
to the required standard

THE UNIVERSITY OF BRITISH COLUMBIA
OCTOBER 1985

© Darren C. Elsby, 1985

90

In presenting this thesis in partial fulfilment of the requirements for an advanced degree at the University of British Columbia, I agree that the Library shall make it freely available for reference and study. I further agree that permission for extensive copying of this thesis for scholarly purposes may be granted by the head of my department or by his or her representatives. It is understood that copying or publication of this thesis for financial gain shall not be allowed without my written permission.

Department of GEOLOGICAL Sciences

The University of British Columbia
1956 Main Mall
Vancouver, Canada
V6T 1Y3

Date 09 October, 1985

ABSTRACT

Detailed structural mapping near Mt. Perseus, British Columbia, provides an overview of the nature of deformation across a portion of the Quesnellia-Omineca terrance boundary.

Rocks within the Omineca Belt are comprised of the Hadrynian to mid-Paleozoic Snowshoe Group. These rocks are structurally overlain by and act as basement to accreted rocks of the Intermontane Belt (Quesnellia): the Upper Paleozoic Slide Mountain Group (Antler Formation), Upper Triassic Black Phyllite (unnamed), and Jurassic volcanic rocks of Takla Group equivalence.

Within the Snowshoe Group, four phases of regionally significant deformation have been established. Both basement and cover have common phases of deformation wherein the first phase of deformation present within the cover sequence is equivalent to the second phase within the basement. In general, deformation within the cover is less well developed with respect to the basement.

Earliest structures, only observed within the Snowshoe Group are east-verging rootless isoclinal folds accompanied by a transposed foliation of a regional nature. Associated with this event is the intrusion of a large tabular granitic body, later metamorphosed into the Mt. Perseus Gneiss. Second phase structures are easterly verging

and comprise large recumbent nappe structures. Third phase westerly verging folds dip moderately to the northeast. It is these large scale structures which control the present regional map pattern and local configuration of the Omineca-Quesnellia boundary, which in this study, is manifest in the Mt. Perseus antiformal culmination. Small scale crenulations and easterly verging buckle folds comprise the fourth deformational phase and do not appreciably affect earlier geometries.

Second phase deformation marks the obduction of the easterly converging Quesnellia accretionary package onto the Omineca terrane. This tectonic contact is flanked by narrow longitudinal ductile shear zones containing mylonites, which in Snowshoe rocks are often associated with isolated fault bounded slivers of oceanic cover rock (ophiolite). These tectonic slivers are thought to be related to geometry resulting from the eastward subduction of oceanic Quesnellia rocks beneath the Omineca craton during the third deformational phase. The development of the late crenulation cleavage is likely a consequence of late eastward thrusting of early Jurassic volcanics during the later deformation stages of the underlying phyllites.

Mineral assemblages describe a Barrovian metamorphic sequence which ranges from the middle to upper greenschist facies in cover rocks to the lower amphibolite in the Snowshoe basement. The earliest recorded metamorphism is associated with phase 1 deformation but details regarding this event remain ambiguous as most textures have been destroyed by successive metamorphism. Microscopic textures

indicate that the peak of metamorphism is synchronous with phase 2 deformation followed by a reduction to the middle greenschist facies during the third deformational phase.

Both obduction and subduction processes and their associated deformation and metamorphism were most likely the result of mid Mesozoic tectonics related to the Columbian Orogeny.

TABLE OF CONTENTS

ABSTRACT	ii
LIST OF TABLES	vii
LIST OF ILLUSTRATIONS	viii
ACKNOWLEDGEMENTS	xv
 I. INTRODUCTION	 1
Physiography	3
Regional Geology	3
 II. STRATIGRAPHY	 9
Snowshoe Group	11
Antler Formation	27
Upper Triassic Formation	35
- Lower Unit	36
- Middle Unit	37
- Upper Unit	37
 III. STRUCTURE	 39
Phase 1 (D_1)	43
Phase 2 (D_2)	43
Phase 3 (D_3)	61
Phase 4 (D_4)	85
Phase 5 (D_5)	86
Phase 6 (D_6)	94

IV. MICROTEXTURES	95
Snowshoe Group	97
- Meta-pelitic - Psammitic Rocks	97
- Non-pelitic Rock Types	111
Antler Formation	124
Upper Triassic Formation	145
- Lower Unit	150
- Middle Unit	153
- Upper Unit	156
General Conclusions	158
V. SUMMARY AND DISCUSSION	161
Structure: General Conclusions	161
Regional Implications and Tectonic Conclusions	167
Bibliography	173

LIST OF TABLES

	PAGE
TABLE 3-1 Characteristic Deformational Fabrics associated with the proposed deformation sequence	42
TABLE 4-1 Relevant stratigraphy, metamorphic rock types, and typical mineral constituents within the Snowshoe Group	96
4-2 Relation of mineral growth to the proposed deformation scheme in Snowshoe metapelites	110
4-3 Relevant stratigraphy, metamorphic rock types, and typical mineral constituents within the Antler Formation	125
4-4 Relation of mineral growth to the proposed deformation scheme in the Antler Formation	144
4-5 Relevant stratigraphy, metamorphic rock types, and typical mineral constituents within Upper Triassic Formation	146
4-6 Relation of mineral growth to the proposed deformation scheme in the Upper Triassic Formation	157

LIST OF FIGURES

Figure 1-1	Location map of the Mt. Perseus area	2
1-2	Regional geology of the Cariboo Mountains, British Columbia	5
Figure 2-1	Schematic structural succession across the Mt. Perseus area	10
2-2	Regional geology of the Cariboo Mountains showing the spatial relations of the Snowshoe and Kaza Groups	12
2-3	Garnet-muscovite biotite schist of the Snowshoe Group	16
2-4	Complexly folded calcareous metapelite of the upper Snowshoe Group	19
2-5	Micaceous quartzite of the Snowshoe Group	21
2-6	Xenoliths contained within the Mt. Perseus Gneiss	26
2-7	Coarse pegmatite containing xenoliths of garnet-biotite schist	28
Figure 3-1	Map of the Quesnel Lake region showing the present configuration of the Quesnellia-Omineca terrane boundary	40
3-2a	F_1 isoclinal folds in Snowshoe Group garnet-biotite schist	44
3-2b	F_2 isoclinal folds in Snowshoe Group micaceous quartzite	45
3-3	Lower hemisphere stereo projections of the present geometry of phase 1 deformation as deformed by phase 2 and phase 3 folding	46
3-4a	F_2 isoclinal folds in the Mt. Perseus Gneiss	48

3-4b	F_2 isoclinal folds in the Mt. Perseus Gneiss within the overturned limb of the Perseus antiform	49
3-5	Map view of Perseus Gneiss within the Snowshoe Group and F_2 fold vergence at various structural levels around the Perseus Antiform	50
3-6	Schematic cross-section through the phase 3 Perseus Antiform	52
3-7a	Flattened F_2 folds within the Perseus Gneiss	53
3-7b	F_2 isoclinal fold within Snowshoe garnet-biotite schist	54
3-8	Mesoscopic F_3 fold refolding an F_2 isocline	55
3-9	Mesoscopic F_2 fold contained within the hinge region of the Perseus Antiform	56
3-10	F_2 isoclinal folds contained within the Perseus Gneiss	57
3-11	Large F_2 folds within shallowly dipping Snowshoe metapelite in the southeastern portion of the Perseus Antiform hinge zone	58
3-12	Steeply inclined F_2 isoclinal folds overprinted by shallowly dipping open F_4 folds	59
3-13	Schematic illustrating the unfolding of the superposed phase 3 Perseus Antiform	60
3-14	Map and schematic cross-section through the Perseus Antiform showing the nature and orientation of phase 2 and phase 3 axial surfaces and axial traces	62
3-15	Phase 2 isoclinal fold within a chlorite schist of the Antler Formation	63

3-16	Lower hemisphere stereo projections of F ₂ minor fold geometry	64
3-17	Schematic cross-section illustrating the changing style of F ₃ folding across the Perseus Antiform	67
3-18a	Mesoscopic F ₃ folds in micaceous quartzite of the Snowshoe Group	68
3-18b	Phase 3 mesoscopic folds contained within the upright limb of the Perseus Antiform	69
3-19	Photograph of the superposition of phase 3 folds onto phase 2 geometry	70
3-20	Phase 3 folds characteristic of the Perseus Antiform core zone	71
3-21	F ₃ folds contained within calcareous metapelites adjacent to the Perseus Antiform hinge zone	72
3-22	Superposition of phase 3 onto phase 2 structures within the antiform hinge zone	73
3-23	Small scale phase 3 disharmonic folds contained within calcareous metapelite	74
3-24	Isoclinal F ₂ minor fold refolded by tight F ₃ folds	75
3-25	Isoclinal phase 2 minor fold refolded around a phase 3 minor fold	77
3-26	Phase 3 disharmonic folding adjacent to a small shear zone in garnet-biotite schist of the Snowshoe Group	78
3-27	Isoclinal phase 3 minor fold adjacent to a minor shear zone	79
3-28a	Mesoscopic phase 3 antiform in Snowshoe micaceous quartzite immediately adjacent to the Quesnellia-Omineca boundary	80
3-28b	Phase 3 antiform situated immediately adjacent to Figure 3-28a	81

3-28c	Mesoscopic phase 3 antiform immediately adjacent to Figure 3-28b	82
3-28d	Mesoscopic phase 3 isocline adjacent to Figure 3-28c	83
3-29	Talus blocks containing interfolded Antler amphibolite and Snowshoe garnet metapelite	86
3-30	Schematic cross-section of phase 3 folding throughout the contact zone between the Black Phyllite and Antler Formations and the Snowshoe Group	87
3-31	Lower hemisphere stereo projection of phase 3 minor fold geometry	88
3-32	Phase 4 recumbent folds refolding steeply inclined phase 2 isoclines	89
3-33	Nearly recumbent phase 4 folds deforming phase 2 isoclinal folds	90
3-34	Phase 4 minor folds contained within Snowshoe garnet-biotite schist	91
3-35	Lower hemisphere stereo projection of phase 4 fold geometry	92
3-36	Large kink-band structure within the Perseus Gneiss	93
Figure 4-1	Photomicrograph of a Snowshoe Group quartz-muscovite schist	99
4-2	Photomicrograph of a Snowshoe micaceous quartzite	100
4-3	Photomicrograph of a Snowshoe Group garnet-muscovite-biotite schist	102
4-4	Photomicrograph of a phase 2 microfold in Snowshoe micaceous quartzite	103
4-5	Photomicrograph of a helicitic phase 1 type garnet in garnet-muscovite-biotite schist	104

4-6	Schematic illustration of the timing of garnet growth with respect to deformation episodes and styles in the Snowshoe Group	105
4-7	Photomicrograph of small idioblastic phase 2 type garnets in garnet-biotite-muscovite schist	106
4-8	Photomicrograph of altered hornblende in Snowshoe amphibolite	107
4-9	Photograph of a thin section of Snowshoe augen gneiss	112
4-10a	Photomicrograph of a K-feldspar-quartz augen in Figure 4-9	113
4-10b	Cross-nicols view of Figure 4-10a	114
4-11a	Photomicrograph of the Perseus Gneiss	118
4-11b	Partially cross-nicols view of Figure 4-11a showing detail of idioblastic garnet form	119
4-12a	Photomicrograph of the Perseus Gneiss	121
4-12b	Photograph of the thin section appearing in Figure 4-12a	122
4-13a	Photomicrograph of basal Antler Formation actinolite-tremolite-talc schist	127
4-13b	Cross-nicols view of Figure 4-13a	128
4-14a	Photomicrograph of actinolite-tremolite-antigorite-talc schist of the lowermost Antler unit	130
4-14b	Tremolite-twins within Figure 4-14a	131
4-15a	Photomicrograph of a rotated biotite porphyroblast in Antler chlorite-biotite schist	138
4-15b	Cross-nicols view of Figure 4-15a	139
4-16	Sketch of a thin section of an Antler chlorite-biotite schist	140

4-17a	Photomicrograph of rootless intrafolial microfolds within micaceous quartzite of the Antler Formation	141
4-17b	Cross-nicols view of Figure 4-17a	142
4-18a	Photomicrograph of basal micaceous quartzite of the Upper Triassic Assemblage	148
4-18b	Photomicrograph of basal micaceous quartzite of the Upper Triassic Assemblage	149
4-18c	Photomicrograph of basal micaceous quartzite of the Upper Triassic Assemblage	149
4-19	Photomicrograph of an Upper Triassic graphitic phyllonite	151
4-20a	Photomicrograph of a typical graphitic phyllite of the Upper Triassic assemblage	152
4-20b	Photomicrograph of a typical graphitic phyllite of the Upper Triassic assemblage	152
4-21a	Photomicrograph of a deformed quartz filled hydraulic fracture within graphitic phyllite	154
4-21b	Cross-nicols view of Figure 4-21a	155
Figure 5-1	Schematic cross-sections across the Quesnellia-Omineca boundary during the time of initial convergence (obduction)	170
5-2	Schematic cross-sections across the Quesnellia-Omineca boundary after initial convergence and during a reversal in subduction	172

LIST OF PLATES

- | | | |
|-----------|--|---|
| PLATE I | Geologic map of the Mt. Perseus area | <i>in Special Collections</i>
(in-pocket) |
| PLATE II | Structural Geology of the Mt. Perseus area | <i>in Special Collections</i>
(in-pocket) |
| PLATE III | Cross-section A-A' across the Mt. Perseus area | <i>in Special Collections</i>
(in-pocket) |
| PLATE IV | Cross-section B-B' across the Mt. Perseus area | <i>in Special Collections</i>
(in-pocket) |

ACKNOWLEDGEMENTS

This study was done under the supervision of Dr. J.V. Ross who originally suggested the Crooked Lake area for a study of this kind. Technical assistance was provided by G.E. Montgomery and B. Cranston. Able field assistance was provided by W.H.G Matthews III and P. Baier. The structural presentation has been improved through discussions with Dr. J.V. Ross, J. Montgomery and J. Fillipone.

Field and laboratory expenses were covered by NSERC 67-2134 awarded to Dr. J.V. Ross.

Finally, I wish to acknowledge and gratefully thank my wife Elisabeth for all typing and moral support given throughout the course of this study.

INTRODUCTION

The southwestern margin of the Cariboo Mountains, situated in east central British Columbia, is located within a tectonic assemblage consisting of rocks of both the Omineca Crystalline Belt and Intermontane Zone, which in this study is represented by the Quesnellia Terrane. A location map (Fig. 1-1) outlines the extent of the thesis area which includes the tectonic boundary. The area is characterized by polyphase deformation involving Late Proterozoic (Hadrynian?) metasediments and gneisses of the Snowshoe Group, Upper- Paleozoic amphibolites of the Slide Mountain Group, and un-named Upper Triassic phyllites and Lower Jurassic metavolcanics of probable Takla Group equivalence (Struik, 1984). This study provides a detailed structural and metamorphic analysis immediately adjacent to this tectonic zone. Deformation styles, their trends, and metamorphic assemblages are compared, and the relations between deformation and metamorphism are presented across this marginal boundary.

The specific area of study, the Mt. Perseus area, comprises some 66 square miles within the southern Cariboo Mountains, approximately 28 miles southeast of Quesnel Lake, British Columbia. The eastern extent of the area is contained within the Wells Gray Provincial Park

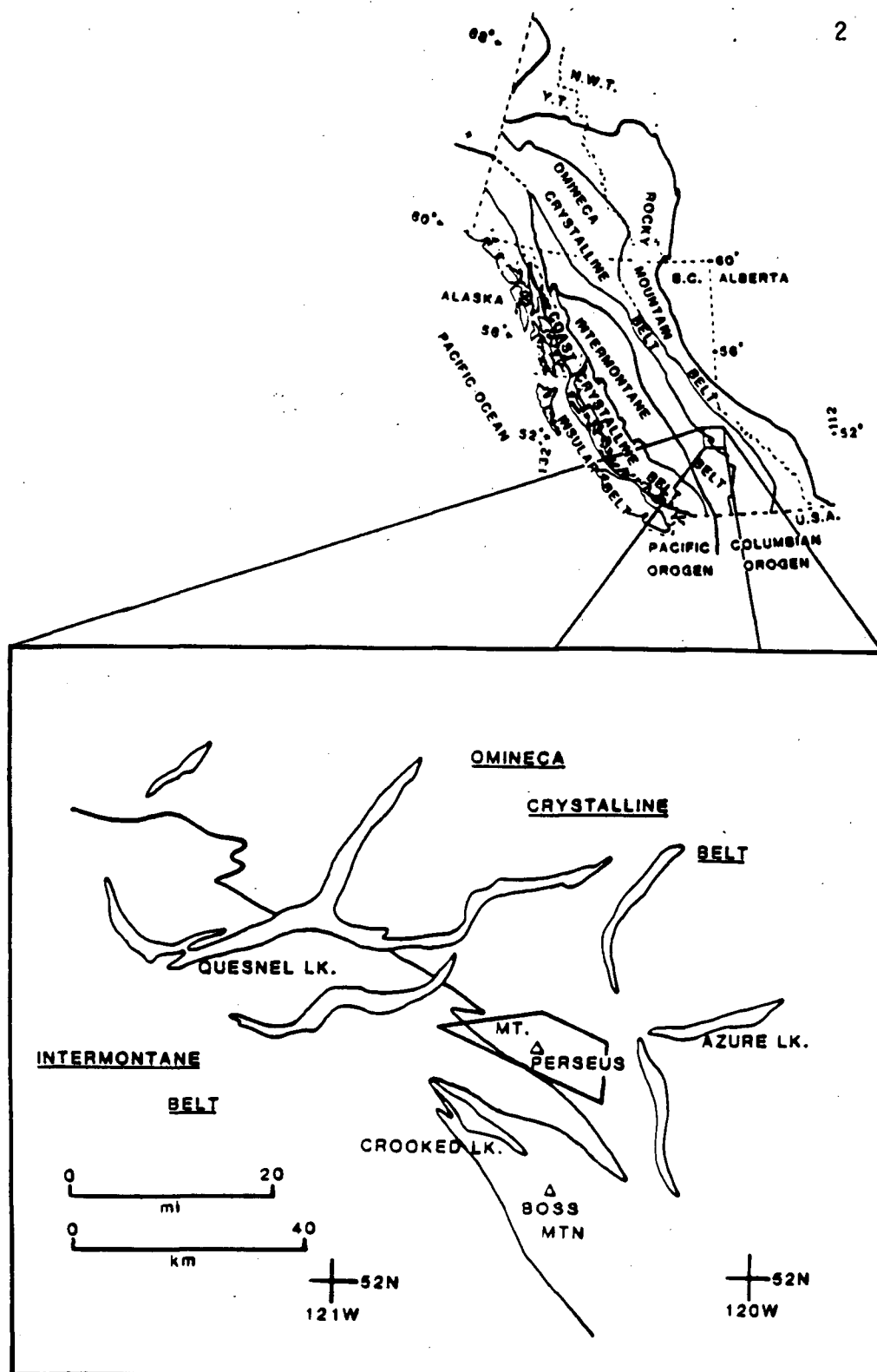


Figure 1-1. Location map of the Mt. Perseus area. Inset map shows relation to the major structural elements of the Canadian Cordillera. Modified from Wheeler and Gabrielse (1972).

boundary. Detailed geologic mapping on the scale of 1:15,000 was completed during the summer of 1982.

Physiography

Total relief within the area is approximately 4,400 feet (1,341 metres). The present physiography is the result of both structural control and glaciation. The ridges are often aligned with the metamorphic foliation. Abundant glacial striations, tarn lakes, and cirques indicate that much of the present topography resulted from north westerly directed ice flow.

Regional Geology

The Cariboo Mountains form the northwesternmost part of the Columbia Mountains and lie in the central part of the Omineca Geanticline; the core zone of the eastern fold belt of the Canadian Cordillera (Campbell, 1970).

The relatively unmetamorphosed and little deformed rocks of the northern Cariboo Mountains lie between and along strike with the intensely deformed, moderate to highly metamorphosed Shuswap metamorphic complex to the southeast and the Wolverine complex to the northwest. Northwest of the Shuswap metamorphic complex, a general though somewhat erratic decrease in metamorphic grade is accompanied by simplification of fold patterns (Campbell, 1970, 1977).

The Shuswap metamorphic complex, as originally defined, forms the core of the Omineca Crystalline Belt and represents the highest grade zone of a wide zone of metamorphic rocks in southwestern British Columbia. The complex includes probable Hudsonian crystalline basement together with Proterozoic - early Paleozoic miogeoclinal strata and Mesozoic eugeoclinal rocks as young as Late Triassic (Ross, 1968; Campbell, 1977). Borders of the complex were originally defined by the sillimanite isograd (Fig. 1-2). The position of this isograd has since changed as the result of detailed mapping in surrounding areas (Montgomery, 1985; Fillipone, 1985). Rocks of sillimanite grade have been found throughout the Quesnel Lake area, a fact which necessitates a re-definition of the present Shuswap metamorphic complex boundary.

In central British Columbia, the Omineca Geanticline consists mainly of late Proterozoic metasediments of the Kaza Group and Cariboo Group, including the Hadrynian Snowshoe Formation (Sutherland-Brown 1957, 1963), most recently updated to Group status (Struik, 1984). Protolith rock types in both groups are of shallow water marine origin and were most likely deposited in a basin west of the existing cratonic platform in the late Proterozoic to early Paleozoic (Campbell and Tipper, 1970). Monger and Price (1979) infer that these Western-most clastics within the Omineca Belt are part of a continental margin terrace wedge that prograded into a marginal basin in which there was intermittent volcanic activity.

In the southern Cariboo Mountains, Kaza Group rocks are in

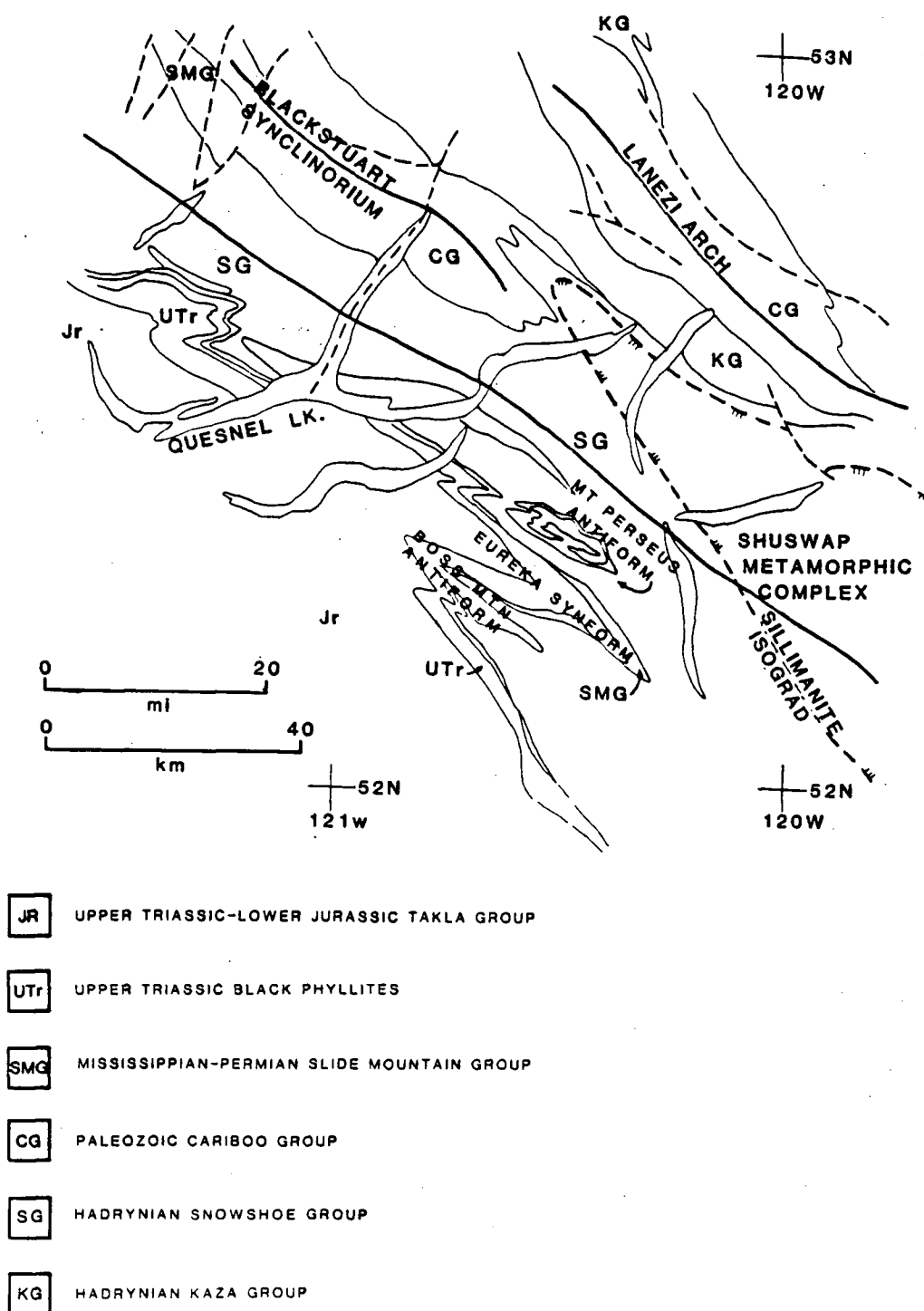


Figure 1-2. Regional geology of the Cariboo Mountains, British Columbia. Modified from Wheeler, R.B. Campbell, Reesor, and Mountjoy (1972).

conformable contact with the overlying Snowshoe Group (Fig. 1-2) (Sutherland-Brown 1957; Campbell 1970; Struik 1981, 1982, 1984). The nature of this contact is discussed by Fletcher and Greenwood (1978) and Pigage (1978) in which they conclude that the Snowshoe Group is in part correlative with the Kaza Group.

Recent classifications by Struik (1984, 1985) divide the Omineca Crystalline Belt into two different zones termed the Barkerville and Cariboo Terranes. Hadrynian to Paleozoic Barkerville rocks, bounded on the west by the Quesnellia Terrane, underly the Cariboo Terrane and are comprised solely of the Snowshoe Group. The overlying Hadrynian to Paleozoic Cariboo Terrane is separated from Barkerville rocks by the Pleasant Valley Thrust within the McBride map area, and by an unnamed southwest dipping ductile fault surface (Campbell, 1970; Fletcher and Greenwood, 1978; Pigage, 1978) within the Wells Gray area. Stratigraphies within the Cariboo Terrane include the Jurassic Hobson Pluton and the Late Proterozoic Cariboo and Kaza Groups. The eastern boundary of this terrane has not yet been firmly established.

Snowshoe rocks enclose several distinct bodies of quartzofeldspathic and augen gneiss. Okulitch (personal communication, 1983) interprets some of these rocks as orthogneiss of possible Devonian age. Campbell (1971), suggests that gneissic outcrops south of Quesnel Lake contain both orthogneiss and paragneiss components. Recent work by Montgomery (1985) and Fillipone (1985) infers that these gneisses represent highly deformed mid-Paleozoic granitic bodies.

The Slide Mountain Group comprises rocks at least in part of Mississippian age and overlies with regional discordance older rocks in the Cariboo Mountains (Snowshoe Formation and Cariboo Group) (Sutherland-Brown, 1957). North of Quesnel Lake, the Guyet Formation, a basal conglomerate of the Slide Mountain Group, rests unconformably on the Cariboo Group. South of Quesnel Lake, including the study area, Antler Formation equivalents of the Slide Mountain Group, discordantly overlie Snowshoe rocks (Campbell, 1971; Campbell, 1973; Montgomery, 1978; Rees, 1981). Within the Intermontane Belt, Mesozoic metasediments and metavolcanics are the oldest exposed rocks and are contained within the north-south aligned Quesnel Trough. These rocks consist of unnamed Upper Triassic phyllites and Lower Jurassic Takla Group volcanoclastics of basaltic to andesitic composition (Campbell, 1971; Bailey, 1976; Morton, 1976) which structurally overlie the Slide Mountain Group. Takla rocks conformably overlie the Upper Triassic phyllites and in several localities the depositional record appears continuous between the two rock types (Campbell, 1971). Undeformed granitic rock, intrusive into the Takla Group, has been radiometrically dated at 100 m.y. (Campbell and Tipper, 1970) and is believed to postdate all structures in the Quesnel and Omineca Geanticline, with the exception of Tertiary faults. Tertiary clastics and olivine basalts unconformably overlie Takla rocks and cover large areas within the region.

The earliest recorded deformation within Omineca rocks occurred during the Hadrynian East Kootenay orogeny, followed by additional

deformation in the late Devonian to Mississippian Caribooan orogeny. The Omineca Geanticline was the site of renewed uplift in the Triassic Tahltanian Orogeny and plutonism and metamorphism in the Columbian Orogeny (Wheeler, 1970; Campbell, 1971). This resulted in a regional map pattern characterized by structural culminations frequently associated with high grade metamorphism. Most structures are arched over regional northwest trending anticlinoria (Campbell, 1970) (Fig. 1-2). Structural style ranges from early large scale ductile shear zones and associated ductile "flow" folding to late stage buckle folding and brittle fracturing.

Within the Crooked Lake area of the southwest Cariboo Mountains, the present map pattern configuration is dominated by large scale southwest verging folds, termed the Mt. Perseus Antiform, Eureka Synform, and Boss Mountain Antiform (Fig. 1-2).

STRATIGRAPHY

The stratigraphic framework and regional correlation of units within the Mt. Perseus area are based on early studies by Holland (1954) and Sutherland-Brown (1957). Recent work within the Quesnel Lake area was performed by Campbell (1971), Campbell, (1973), Campbell (1978), Struik (1981, 82, 83, 84), and Rees (1982, 1983). A detailed schematic structural succession for the Mt. Perseus area is presented in Figure 2-1.

The study area contains Late Proterozoic (Hadrynian?) meta-sediments and gneisses of the Snowshoe Group which are unconformably overlain by Mississippian to Permian amphibolites and metavolcanics of the Antler Formation. These rocks are in turn unconformably overlain by unnamed Upper Triassic graphitic phyllites, schists and Jurassic Takla volcaniclastics (outside of the field area). Within the study area all contacts are tectonic and metamorphic grade increases from lower greenschist in the southwest to at least lower amphibolite in the northeast part of the study area. Snowshoe rocks have been interpreted by Campbell (1971) to be miogeoclinal derivatives of the Omineca Geanticline. Textural evidence and facies relations within the Snowshoe metapelites in the Quesnel Lake and McBride map areas indicate a northern cratonic source for the original sediments (Campbell et. al, 1973).

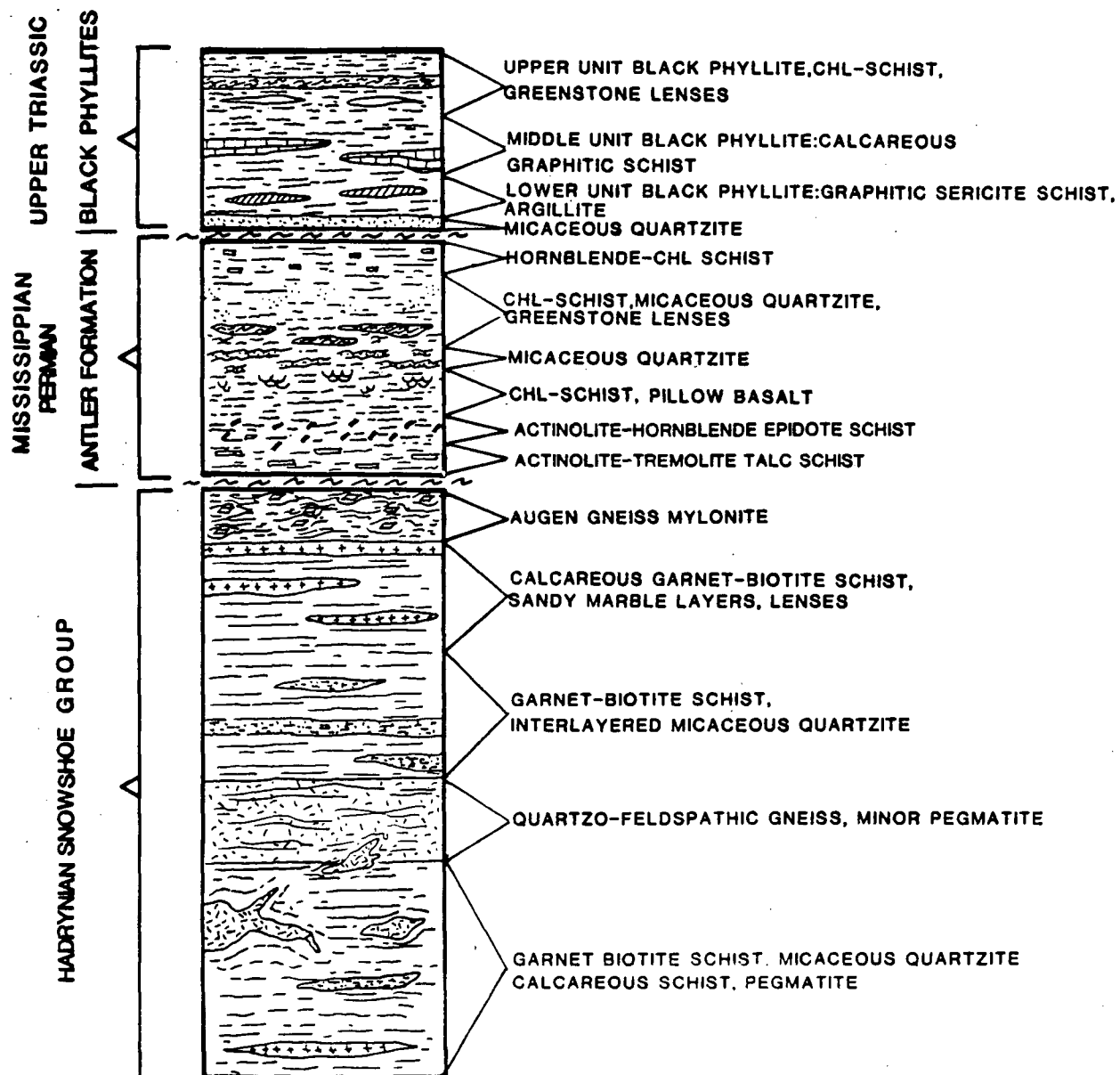


Figure 2-1. Schematic structural succession across the Mt. Perseus area.

Monger and Price (1979) in their discussion of the geodynamic evolution of the Canadian Cordillera infer that western-most clastics within the Omineca Belt (which includes the Snowshoe Group) are part of a regional northeasterly tapering sedimentary wedge that overlaps precambrian structures of the cratonic basement. This continental margin terrace wedge (miogeoclinal wedge) is believed to have prograded into an intermittantly tectonically active back-arc type marginal basin based upon the stratigraphic incorporation of coarse feldspathic wackes and volcanics in a dominantly shale facies.

The overlying Antler Formation of the Slide Mountain Group and Upper Triassic assemblages show evidence of eugeoclinal affinity; their structural juxtaposition believed to be largely a result of regional wrench fault tectonics (Campbell, 1971; Monger and Price, 1979; Monger et al., 1982). All rock units within the study area have been multiply deformed and therefore, owing to the complex nature of the deformation, any original depositional contacts have in large part been completely transposed.

Snowshoe Group

The Snowshoe Group within the map area contains a sequence of pelitic metasediments and quartzo-feldspathic gneisses of Late Proterozoic (Hadrynian?) age. Upper most units of the Snowshoe Group within the Quesnel Lake area are tectonically overlain by Antler Formation amphibolites. Lowermost units of the Snowshoe are in fault

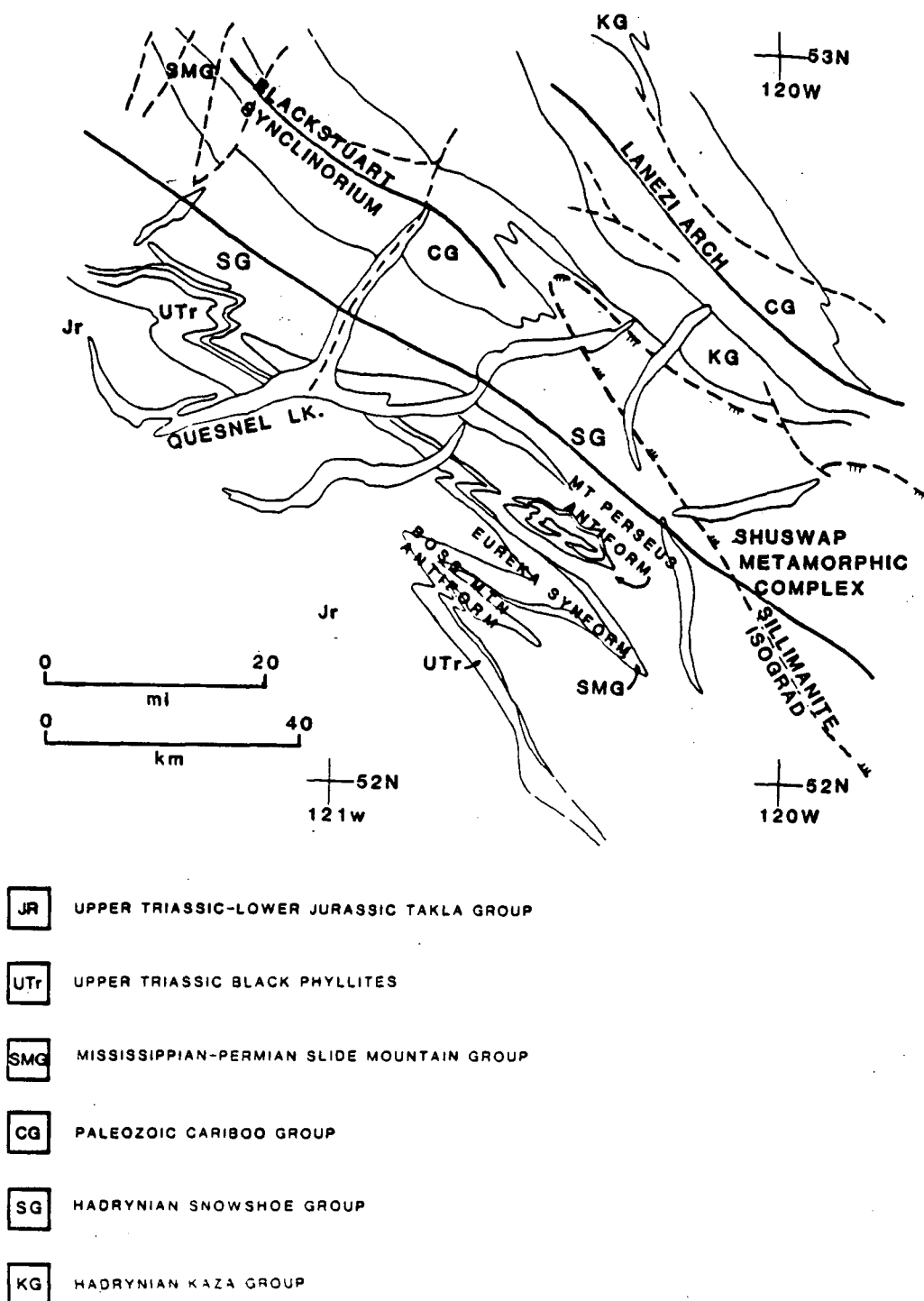


Figure 2-2 Regional geology of the Cariboo Mountains showing the spatial relations between Snowshoe and Kaza Groups.

contact with the Kaza Group (Fletcher and Greenwood, 1978; Pigage 1978) (Fig. 2-2). The total present tectonic thickness of the Snowshoe Formation is believed to be in excess of 27,000 metres as original stratigraphic thickness has not yet been estimated. Exact ages and correlations of Snowshoe rocks with regional units are controversial and still under current investigation. Mapping performed by Struik (1982, 1983), northeast of the Quesnel Lake classifies rocks resembling the Snowshoe Group as part of the Cariboo Group which within the study area may be in part correlative with these strata but insufficient mapping exists between the respective field areas to provide a conclusive correlation. Recent work by Struik (1984, 1985) reclassifies and divides the Omineca Crystalline Belt into two distinct zones separated by a prominent fault zone. These zones are termed the Barkerville and Cariboo Terranes. Rocks of the Barkerville Terrane contain Hadrynian and Paleozoic metasediments and gneisses of the Snowshoe Group. The Cariboo Terrane is comprised of Hadrynian and Paleozoic rocks of the Cariboo and Kaza Groups and the Jurassic Hobson Pluton. Further correlations have been made between the Snowshoe Group and rocks of the Horsethief Creek and Miette Group based upon similar structural position and stratigraphy. Price and Douglas (1972) believe that Kaza Group rocks (including the Snowshoe Group) are in part a northern extension of the Horsethief Creek Group and a western continuation of the lower and middle Miette Group (of the Rocky Mountain fold belt).

Work performed by Fletcher and Greenwood (1978) and Pigage (1978)

provides evidence that the Snowshoe Group may be a higher metamorphic grade equivalent of the Kaza Group which may imply that the Snowshoe is a westerly facies of the Kaza.

The 5000 metre present tectonic thickness of exposed Snowshoe Formation within the study area is largely composed of garnetiferous quartz-mica schist, micaceous quartzites, calcareous schist, augen gneiss, and quartzo-feldspathic gneiss. A well exposed layer of this gneiss provides a continuous marker horizon throughout the field area. Present map pattern geometry indicates that all units have been folded into an overturned doubly-plunging, southwest verging antiform (Plates II and III). The upper 2400 metres of Snowshoe rock consist of carbonate horizons which contain distinct layers of calcareous schist and numerous smaller intercalations of marble. Calcareous zones are repeated on both limbs of the antiform at similar structural levels. The appearance of garnet within Snowshoe rocks is controlled by the garnet isograd and in large part by compositional variation within the above lithologies. The order and stratigraphic position of the following descriptions may be found in figure 2-1.

Quartz-Mica Schist

Light tan to dark brown weathering schists composed of quartz, plagioclase, K-feldspar, biotite, muscovite, hornblende, calcite, and garnet (almandine) comprise approximately 60 percent of the exposed Snowshoe Formation. The development of garnet in these rocks is

strongly dependent upon composition and are therefore often confined to local layers. As a general rule, porphyroblast sizes increase in a northeasterly direction from the Snowshoe-Antler contact. Lithologies within this group include garnet-biotite schist, micaceous quartzite, calcareous mica schists, sandy marble, and amphibole bearing schists.

All units contain a well developed penetrative foliation defined by mica layers and discontinuous quartz intercalations. Much evidence indicates that metamorphic crystallization outlasted deformation: randomly oriented biotite porphyroblasts, strongly annealed quartz, and helicitic garnet. Present contacts between all units are believed to be the result of multiple transposition.

Garnet-Biotite Schist

Schist composed dominantly of biotite, muscovite, garnet, and quartz occurs as an ubiquitous rock type throughout the study area. This rock type consists of alternating thin laminae (1 to 5 mm) of biotite, muscovite, and quartz with garnet porphyroblasts ranging in diameter from 1 mm to 4 cm (Fig. 2-3). Adjacent to the Snowshoe-Antler contact schists become mylonitic and contain numerous randomly oriented biotite porphyroblasts; evidence of post-deformational metamorphic overgrowth. Similar field textures are observed within the core region of the Perseus antiform such that schists of similar composition appear mylonitic and are often restricted to small tabular

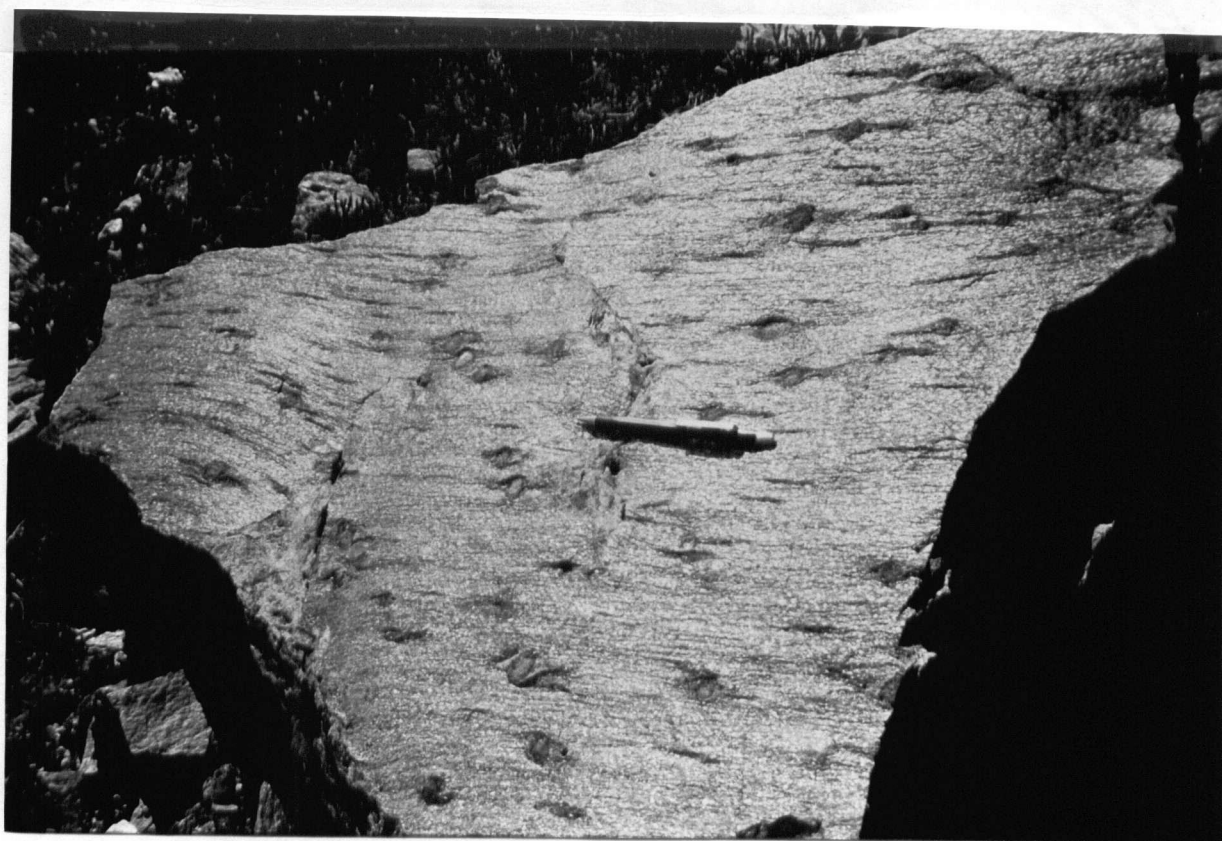


Figure 2-3. Photograph of a garnet-muscovite-biotite schist of the Snowshoe Group. Large early garnets, flanked by pressure shadows, are contained and have grown within the regional foliation.

zones. Quartz grains within these rocks are entirely polygonized and thus one can infer that zones of concentrated shear and flattening strain exist within the Snowshoe Group. The nature and significance of this geometry will be discussed in later sections.

Two generations of garnet are present within these rocks. An early phase of garnet displays helicitic textures and rotation of up to 90 degrees. These garnets are contained and have grown within the regional foliation. A later garnet phase confined to local layers is typically smaller than the large helicitic garnets, contains random inclusions, and has overgrown the primary crystallization foliation. Rocks containing these two garnet growths crop out in random layers throughout the Snowshoe and little can be said concerning their stratigraphic/structural continuity.

Calcareous Schist

The upper 2400 metres of Snowshoe Group schists within the study area are composed dominantly of calcareous metapelite which contains distinct layers of sandy marble and calcareous quartz-mica schist. These schists contain numerous minor lenses of amphibolite, calcareous gneiss and thin discontinuous quartz intercalations.

Quartz-mica-schist containing calcite comprises the dominant rock type within this calcareous zone (Fig. 2-4). Mineral phases include quartz, biotite, calcite, muscovite and localized K-feldspar,

plagioclase and garnet. Contained within these schists are layers of sandy marble composed almost exclusively of quartz, calcite, and muscovite. Layer thicknesses range from 10 to 120 metres. The sandy marble is light tan in color, high in outcrop relief with respect to surrounding schists and is repeated in several localities by isoclinal folding (Plates I, II). Contacts with the enveloping schists are sharp and everywhere concordant. In most localities, lenses of amphibolite crop out adjacent to sandy marble layers. These rocks, composed of horn-blende, quartz, calcite, and epidote attain a maximum thickness of 2 metres. Minor layers of calcareous gneiss, composed of alternating layers of hornblende, biotite, K-feldspar, and quartz crop out both adjacent to amphibolite lenses and more randomly throughout the carbonate schists. Internally, all calcareous schists and gneisses are thinly laminated with individual laminae ranging from 5 to 60 mm in thickness.

Calcareous schist proximal to the Antler-Snowshoe boundary shows evidence of strong mylonitization and annealing. Deformation textures become gradationally less mylonitic approximately 1.5 kilometres away from this boundary and throughout the remainder of this calcareous zone, carbonate units appear strongly folded with mylonites restricted to narrow zones which are subparallel to axial plane orientations of various fold geometries.



Figure 2-4. Photograph of complexly folded calcareous metapelite of the upper Snowshoe. Compositional layers are outlined by numerous quartz and calcite layers.

Micaceous Quartzites

Lithologies containing 70-90 percent quartz with minor phases of biotite, muscovite, plagioclase, and garnet crop out in layers throughout all levels of the Snowshoe Group (Fig. 2-5). The frequency and thickness of the layers increase up-section, with respect to the North-east study area boundary, where sequences in excess of 35 metres are exposed near the structural top of the Snowshoe. Layers below this structural level range in thickness from 0.5 to 20 metres. Deformation textures are often poorly preserved in the quartzites due to strong polygonization within quartz grains. Several samples of quartzite mylonite from the antiform core zone contain quartz ribbon grains showing elongation ratios in excess of 50:1. It is uncertain as to the nature and degree of transposition that has taken place in these units.

Amphibole-Bearing Schist

Schists containing porphyroblasts of amphibole, garnet, and biotite crop out as lenses within the upper 100 metres of the Snowshoe Group. Mineral phases within the groundmass include quartz, calcite, biotite, epidote, and muscovite. Textures are generally coarse with hornblende crudely aligned parallel with northwest-southeast trending fold axes. Post-kinematic biotite porphyroblasts are randomly oriented and often transverse to the foliation.



Figure 2-5. Photograph of Snowshoe micaceous quartzite. Compositional layers are parallel to the regional metamorphic foliation. Light colored layers are composed of approximately 80% recrystallized quartz.

Alkalic Feldspar Augen Gneiss Mylonite

Light grey, rodded augen gneiss containing muscovite, quartz, and alkali feldspar represents the upper-most unit within the exposed Snowshoe Group. The gneiss is in sharp tectonic contact and regionally discordant with lowermost amphibolites of the overlying Antler Formation. Structural thicknesses within this medium grained gneiss range from 50 to 180 metres in a southeasterly trend toward the hinge zone of the Eureka Synform. Texturally, the rock type varies irregularly in outcrop from a layered augen gneiss to schistose mylonite.

Within the mylonitic layers, deformed alkali feldspar and quartz augen appear flattened and elongate within the foliation, thereby giving the gneiss a homogeneous leucocratic outcrop appearance. This textural variability is most likely due to internal anisotropy and differential flattening active within the gneiss during deformation. Quartz grains within the matrix have been polygonized, which indicates that metamorphic recrystallization (annealing) outlasted deformation in this region. A strong pervasive northwest-southeast trending mineral lineation contained within the foliation has produced a rodded texture throughout the study area.

Anhedral microcline, K-feldspar, and quartz augen, relict deformed porphyroclasts, range in diameter from 3 mm at the upper contact with Antler amphibolites to 15 mm at the lower contact zone with calcareous

Snowshoe metapelites. This lower contact can best be described as a zone as the contact is diffuse and often appears as a homogeneous mixture of gneiss and metapelite. The nature and significance of this gradational contact along with protolith considerations will be discussed in later sections.

Quartzo-Feldspathic Gneiss

Within the exposed Snowshoe Group, quartzo-feldspathic gneiss forms a continuous marker horizon which outlines the doubly plunging nature of the Perseus antiform (Plate I). Gneiss contained within the overturned limb of the antiform crops out approximately 2200 metres below the upper contact of the Snowshoe and maintains a structural thickness of about 500 metres. Thickness within the upright limb remains constant at approximately 200 metres.

Textures within this unit vary from fine-grained leucocratic feldspathic gneiss confined principally within the limbs of the antiform, to a coarse grained mafic-rich gneiss exposed primarily within the antiform core zone. Compositional layers composed of hornblende, epidote, biotite, muscovite, microcline, quartz, sphene, and local garnet are oriented subparallel to the earliest recognized metamorphic foliation. Individual layer thickness range from 1 to 10 mm.

Contacts between the gneiss and enclosing metapelite schists often

appear gradational over several metres and highly sheared but remain concordant with respect to the gneissic layer-parallel foliation. Several localities adjacent to these contacts display annealed textures characterized by randomly oriented hornblende and biotite porphyroblasts. In most other areas, both hornblende and biotite show preferred orientation in the form of a strong pervasive northwest trending mineral lineation. Samples taken from within the antiform core zone contain quartz grains which have been completely polygonized. This evidence of annealing and recrystallization is most strongly developed adjacent to the schist-gneiss contact within the antiform core zone and in rocks proximal to the Antler-Snowshoe contact. Throughout the rest of the field area, recrystallized textures and mylonites are confined to zones subparallel to axial plane orientations of various fold geometries.

In the region immediately southeast of the Mount Perseus summit, both gneiss and metapelitic schist are complexly interfolded. This area is characterized by interslicing of both rock types in which minerals appear elongate and flattened within a mylonitic foliation. This zone of shearing and flattening provides evidence for and in part documents the existence of early deformation geometries related to macroscopic folding. This and other factors concerning deformation will be discussed in the following chapter.

Several localities within the gneiss contain abundant xenoliths of melanocratic, fine grained amphibolite (Fig. 2-6). Xenolith diameters

range from 5 to 30 cm and do not deflect the metamorphic foliation present within the host rock though most display a moderately developed cleavage oriented parallel to the gneissic foliation.

Granitoid Pegmatite

Irregular, scattered bodies of mildly to intensely deformed coarse and fine grained granitoid pegmatite intrude all rock types within the Snowshoe Group exposed in the study area. Intrusives display both concordant and discordant contact relations. Concordant pegmatites crop out mainly in deep structural levels within the core zone of the Perseus Antiform. Pegmatites with discordant contacts intrude shallower structural levels and within the limbs of the antiform.

Within the deepest exposed levels of the antiform, pegmatites intrude along the metamorphic foliation present within schists and gneisses. These intrusives are generally fine-grained and are often complexly folded along with the host rock. Subhedral microcline, K-feldspar, quartz, epidote, muscovite, and biotite comprise the mineralogy and are often aligned parallel to the foliation within the host rock. In several localities, gneissic host rock and fine grained pegmatite display a migmatite texture in which gneiss and intrusive appear homogeneously mixed.

Pegmatites which crop out within shallower structural levels of the core zone and within the limb regions of the antiform structure are



Figure 2-6. Photographs of the Mt. Perseus gneiss. Xenoliths of altered amphibolite are contained within the foliation.

mostly coarse grained and discordant with respect to foliations present in the host rock, are seldom involved in folding and display a very crudely defined foliation oriented subparallel to cleavages produced by late stage fold geometries within host rocks. Mineral phases include 4-5 cm subhedral phenocrysts of biotite and muscovite and anhedral masses of K-feldspar, quartz, epidote, and garnet. Abundant xenoliths of host rocks are visible throughout the intrusives (Fig. 2-7).

From the above description, one can infer that intrusives deep within the antiform core zone behaved plastically and were involved in folding along with the host rocks. Outcrops of migmatite may suggest that the intrusives were in part generated from in-situ partial melting of host rock during peak metamorphism or that intrusion from another source caused partial melting within host rocks. As deformation continued, intrusives penetrated shallower structural levels (antiform limbs), became increasingly contaminated by Snowshoe rocks, and suffered less intense deformation than structurally deeper intrusives.

Antler Formation (Slide Mountain Group)

Sutherland-Brown (1957, 1963) examined the Slide Mountain Group and divided it into two formations: the basal Guyet Formation and the overlying Antler Formation. The type section is loosely designated at Slide Mountain (Sutherland-Brown, 1963), located in the northern Cariboo Mountains approximately 125 miles north of the Mt. Perseus area. Slide Mountain lithologies dominantly comprise basic volcanic

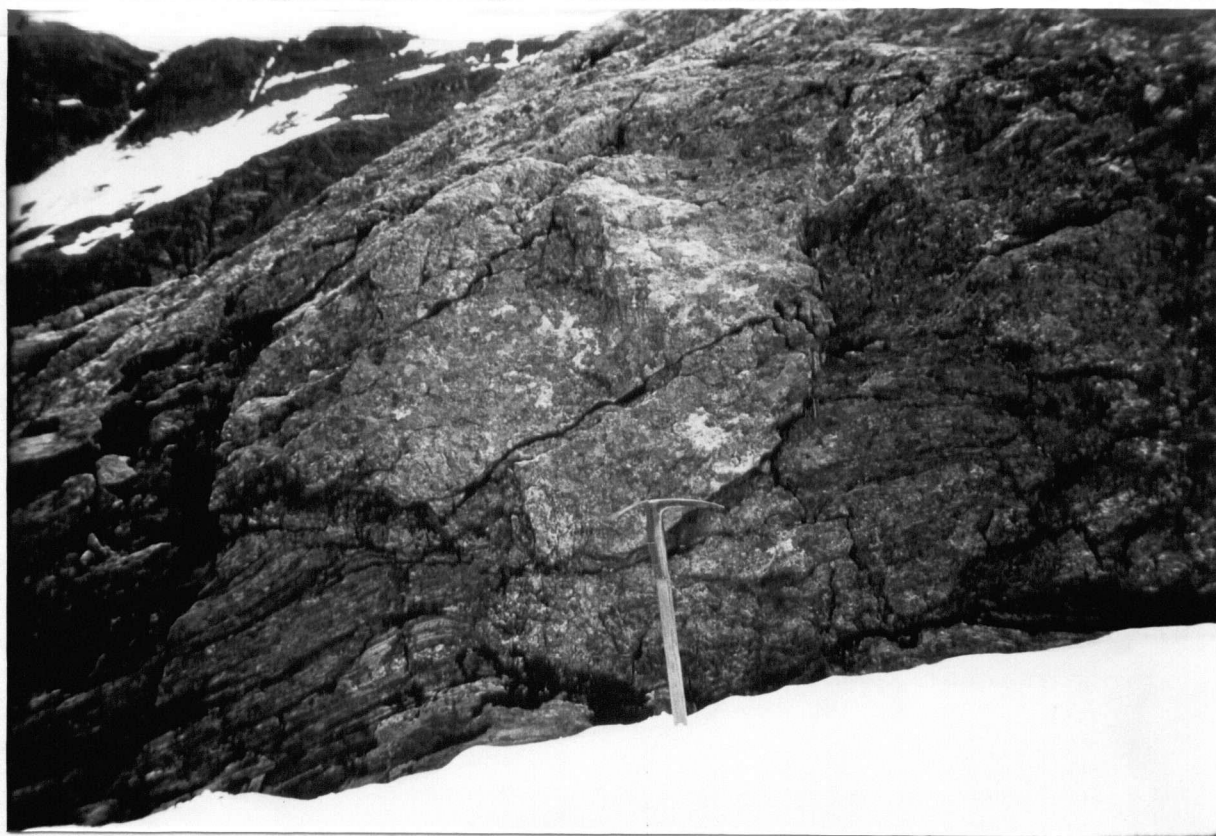


Figure 2-7. Photographs of an outcrop of coarse pegmatite containing xenoliths of highly foliated garnet-biotite schist.

rocks, ribbon chert, argillite, pillow basalts, aphanitic greenstone, limestone, fine grained tuffs, and coarse volcanic breccia (Sutherland-Brown, 1957).

The Guyet Formation contains scant fossil evidence which has been dated as Early Mississippian and currently represents the lower age limit for the Slide Mountain Group (Sutherland-Brown, 1957). The base of the Antler Formation conformably overlies the Greenberry Limestone member of the Guyet Formation. Fossil evidence has not been found in the Antler, hence its upper age limit can only be inferred from the presence of Upper Triassic (?) graphitic phyllites which conformably overlie the Antler Formation. Thus the age of the Antler is bracketed between the Early Mississippian and the Late Triassic (Campbell et. al., 1973).

More recently, Campbell (1971), Montgomery (1978), and Rees (1981, 1983) have examined the Antler Formation at several locations along its trend. The Antler Formation in these areas often contains extensive outcrops of meta-ultramafic and mafic assemblages.

Within the Dunford Lake area, Montgomery (1978) describes the Black Riders mafic-ultramafic complex as one of a series of alpine-type ultramafics which crop out adjacent to the Omineca - Quesnellia tectonic boundary. The complex tectonically truncates underlying Snowshoe rocks and is conformably overlain by greenstones, believed to be of Antler affinity. The assemblage is composed of dunite,

peridotite, gabbro and amphibole-bearing schists, all containing preserved cumulate structures. Similar outcrops have been found in Upper Triassic metavolcanics in the Spanish Lakes area (Ross, personal communication, 1984). Rees (1981, 1983) describes Antler lithologies north of Quesnel Lake as being composed of banded greenstone and talc-antigorite bearing meta-ultramafic schist. Within the Mt. Perseus area, several trace outcrops and abundant talus of highly altered serpentinized dunites and talc-actinolite schists were found adjacent to the Antler-Snowshoe contact.

Mafic-ultramafic rocks are thus recorded as being restricted mainly to the Antler-Snowshoe contact together with minor outcrops structurally contained within the overlying Upper Triassic metavolcanics. From the above information, it is evident that ultramafic slices appear in both Antler rocks as well as in Upper Triassic assemblages; and thus, little can be said concerning the exact age of these rocks. It is possible that these slices are only associated with the Antler Formation but it seems more plausible that they may represent successive oceanic floor rocks of both the Antler and Upper Triassic assemblages.

Monger and Price (1979) attribute the regional presence of Mississippian-Permian cherts, argillites, and mafic-ultramafic volcanics to profound subsidence of miogeoclinal terrane in the Devonian, during which subsidence was followed by deposition of deep water sediments and mafic volcanics. This subsidence is inferred to

have taken place in a back-arc or marginal basin situated behind a volcanic arc in southern B.C. Later, in the Mesozoic, this assemblage is interpreted as having been thrust eastwards onto cratonic sediments.

The Antler Formation within the Mt. Perseus area consists of discontinuous layered assemblages of coarse amphibole-talc-chlorite schist, chlorite-hornblende schist, chlorite schist, sericite schist, and discontinuous lensoid outcrops of aphanitic pillowed greenstone and minor outcrops of grey micaceous quartzites. Mississippian-Permian (?) Antler rocks are of upper greenschist metamorphic grade and tectonically overlie late Proterozoic (Hedrynian?) Snowshoe Group units. Graphitic phyllites and argillites of an unnamed Upper Triassic formation conformably and probably tectonically overlie Antler rocks. Contacts between the three formations (on outcrop scale) are often complexly interfolded and generally not well exposed. The tectonic thickness of the Antler Formation fluctuates along strike and compositional layering is internally discontinuous. Thicknesses of the Antler vary from a maximum of 800 metres to a minimum of approximately 150 metres. Discontinuities may be indicative of the paleo-environment of deposition or may be a function of post-depositional tectonics of both.

Within the Antler, internal layering represents transposed original compositional layering. All units contain a layer parallel foliation that becomes progressively mylonitic and annealed adjacent to the contact with the Snowshoe Group. In general, metamorphism and porphyroblast size increase toward the Antler-Snowshoe contact.

Actinolite-Tremolite-Talc Schist

The lowermost units of the Antler Formation within the study area are composed of coarse grained magnesian schists containing assemblages of actinolite-tremolite, talc, chlorite, antigorite, and albitic plagioclase. The structurally lowest layers, in contact with augen gneiss mylonite of the Snowshoe Group, display a garbenschiefer texture in which large crystals of pale green actinolite-tremolite are randomly oriented in a fine grained annealed groundmass composed dominantly of talc, chlorite, and calcite. A poorly developed metamorphic foliation becomes recognizable approximately 75 metres structurally above the lower contact. Adjacent to the Snowshoe Group-Antler Formation contact, small pods and lenses of extremely coarse grained antigorite-bearing actinolite-tremolite-talc schist crop out randomly within the lowermost layer. Amphibole phases often occur as massive radiating splays with individual crystals attaining lengths of up to 24 cm.

The above stratigraphy is often discontinuous along strike and range in thickness from 50 to 100 metres in a southeasterly trend toward the hinge zone of the Eureka Synform.

Amphibole-Chlorite Schist

Dark and light green, medium to fine grained foliated actinolite-hornblende chlorite schist structurally overlies the lowermost

magnesian schists "garbenschiefer". This unit is recognized by a well developed light colored amphibole lineation contained within the metamorphic foliation; the preferred orientation of which often gives the rock a strong rodded appearance. Texturally, porphyroblasts of actinolite-hornblende are contained within a foliated groundmass of annealed plagioclase, epidote, calcite, and quartz. Thicknesses range from 10 to 180 metres along strike.

Chlorite - Hornblende Schist

Dark green chlorite-hornblende schist structurally (and probably stratigraphically) overlies basal amphibole schists of the Antler Formation. Within this fine grained unit, the well developed mylonitic foliation is parallel to compositional layering. Tectonic thicknesses range from 20 metres to 40 metres in a southeasterly trend along strike. Contact relations with underlying mafic amphibolites are sharp and well defined whereas contacts with overlying metavolcanic rocks are gradational over several metres and generally not well exposed. Hornblende and chlorite porphyroblasts are elongate and flattened within the mylonitic foliation and show preferred orientation in a northwest-southeastern trend.

Muscovite-Sericite Schist, Micaceous Quartzite, Aphanitic Greenstone, Pillowed Greenstone

The remaining local Antler strata are composed of discontinuous layers of muscovite schist and lenses of micaceous quartzite, aphanitic

greenstone, and meta-pillow basalts. Within the field area, no lateral continuity was found to exist in the above strata.

Coarse grained schist containing approximately 70% muscovite-sericite occurs throughout this succession in layers up to 4 metres thick. Minor mineral phases include quartz, chlorite and biotite. This rock type has a well developed micaceous foliation parallel to compositional layering and is typically somewhat mottled in appearance.

Grey micaceous quartzites form discontinuous lensoid units within Antler stratigraphy. Compositionally, these rocks contain 80% quartz with more minor phases of muscovite and chlorite. Quartz appears as flattened stringers and ovoid porphyroclasts within the foliation.

Aphanitic greenstone displaying relict primary igneous pillow structure crops out adjacent to the contact between Upper Triassic graphitic phyllites and Antler rocks. Greenstone units are extremely fine grained and show evidence of intermittent compositional layering with a layer parallel foliation outlined predominantly by chlorite. Pillow structures are ovoid and flattened within the foliation and have semi-major ellipse axes ranging from 6 to 15 inches in length.

Outcrops of poorly exposed argillite, chlorite schist, and coarse amphibolite were found throughout the area. In general, Antler rocks become more fine-grained, micaceous, and less amphibole rich near to the contact with Upper Triassic assemblages and coarse annealed, and amphibole-rich at the Snowshoe-Antler contact.

Upper Triassic Graphitic Phyllites and Argillites

Within the Crooked Lake area, unnamed black graphitic phyllites, pelitic shists and argillites unconformably overlie the Antler Formation and are conformably overlain by Upper Triassic - Lower Jurassic metavolcanics and volcaniclastics (Campbell, 1971). North of Quesnel Lake, similar graphitic assemblages are overlain by early Jurassic marine sediments and volcaniclastics (Tipper, 1960; Rees, 1981, 1983). South of the Crooked Lake area, Campbell and Tipper (1970) mapped black phyllitic rocks they thought to be stratigraphically equivalent to the Slide Mountain Group. Scant fossil evidence found in these equivalent marine strata was dated to the early Jurassic. Therefore, the Upper Triassic age of this formation remains very tentative at this time.

Within the Mount Perseus area, black graphite-bearing phyllitic assemblages, graphitic schist, and argillite structurally overlie the Antler Formation. The contact between graphitic phyllites and overlying Takla Group volcaniclastics is exposed to the southwest, outside of the map area, and will therefore not be discussed. Structural thicknesses are estimated to be in excess of 1500 metres. Black graphitic phyllite and schist comprise approximately 80 percent of the outcrop within this formation with the remaining strata composed mostly of one metre layers of chlorite schist, micaceous quartzite, and horizons of black calcareous schist. The Upper Triassic unit is divided into three sub-units based upon differences in rock type. The

sub-units are termed Lower, Middle and Upper based upon the order of structural position. Contacts between basal rocks of the Upper Triassic Lower Unit and the Antler Formation are poorly exposed. In areas where folding has not obscured the contacts, they appear sharp and locally conformable.

Lower Unit

The lower unit represents a structurally complex zone which separates the Antler from Upper Triassic strata. Layers of well foliated basal micaceous quartzite, dark grey to black argillite, chlorite schist, and quartz sericite schist comprise the rock types within a 60 to 220 metre wide zone.

Grey to tan micaceous quartzite mylonite forms the lowest exposed unit within the Upper Triassic assemblage, which, when exposed is in conformable tectonic contact with hornblende-chlorite schist of the underlying Antler Formation. Tectonic thickness of this unit varies from 20 to 150 metres. Muscovite outlines the earliest foliation which is parallel to compositional layering/bedding. This unit is classified as a mylonite due to the presence of highly elongate, flattened quartz porphyroclasts contained within the foliation. Remaining lower unit strata consist of complexly folded discontinuous layers and lenses of grey-black argillite, chlorite schist, and quartz sericite schist. Foliation within individual layers is often discordant with respect to foliation attitudes within underlying micaceous quartzite and overlying

black phyllites. This discordancy is believed to be the result of local anisotropy within this unit as a whole during deformational shearing.

Middle Unit

The middle unit is characterized by grey to black lustrous phyllite with minor intercalations of limestone. Lenses, pods and irregular veins of translucent to milky white quartz outline the foliation in the phyllite. Porphyroblast phases of pyrite, magnetite and hematite occur infrequently. A prominent horizon exists within this middle unit that is dominated by boudinaged layers of siderite. Flattening effects have produced a "knotted" appearance in which individual "knots" are composed of soft, limonitic carbonate (calcite) and quartz.

Upper Unit

The upper unit, which consists of well foliated black phyllite, chlorite schist and lenses of aphanitic greenstone probably forms a transition zone between the middle phyllite unit and overlying mixed phyllite/volcaniclastic assemblages of the Takla Group. No lateral continuity of this sub-unit was found within the study area.

The above sub units, as with most of the metavolcanic assemblages in the Mt. Perseus area, are often laterally discontinuous in both

composition and outcrop appearance. This discontinuous nature reflects the environment of deposition as well as post-depositional tectonics.

STRUCTURE

All pre-Tertiary rocks within the Mt. Perseus area have been complexly deformed throughout the mid-Paleozoic to the late-Mesozoic. Early within the deformational history, two terranes of principally different origin and affinity, termed the Intermontane zone (Quesnellia) and Omineca Crystalline Belt, were tectonically juxtaposed via low angle, east-directed thrusting (Monger and Price, 1979).

Regional deformation associated with this convergence resulted in the formation of a ductile shear zone and large scale east-verging folds with associated amphibolite grade metamorphism. Protracted regional tectonism superposed upon earlier folds produced nearly coaxial large scale southwest verging ductile folds which deform the convergent boundary and control the present map configuration within the Crooked Lake area (Fig. 3-1). Strain associated with this deformation was accommodated in part along the regional shear zone and in part in the formation of localized subsidiary zones related to fold geometry. Successive superposed folding about similar axes and reactivation of high strain zones characterizes the present geometry within the Mt. Perseus area.

The various structural elements associated with folding were distinguished in the field on the basis of their geometry and orientation. These elements with their nomenclature are listed in

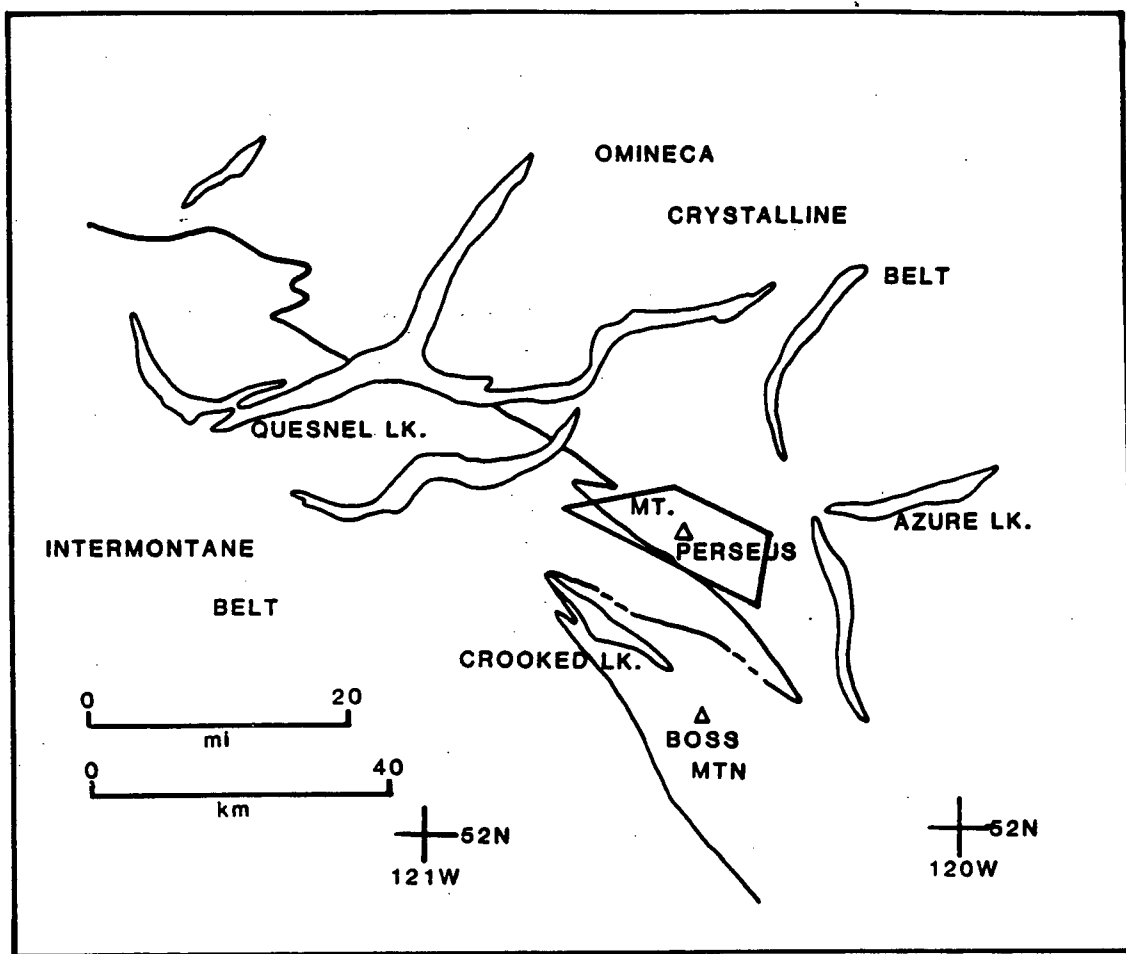


Figure 3-1. Map of the Quesnel Lake region showing the present configuration of Quesnellia-Omineca terrane boundary (modified from Campbell, 1978).

Table 3-1. Relative ages of the different phases of folding were established primarily from parallel or cross-cutting relationships between cleavages and fold axial surfaces and from refolding of earlier cleavages and related linear structures. Slight differences in fold style of successive phases may also be distinguished but are much complicated by the varied response of different lithologies during any particular phase of folding.

A sequence of six deformational phases has been established within the Snowshoe Formation of which only five are common to the overlying Antler and Upper-Triassic Formations. These overlying formations lack evidence of an early fold phase only observed within the Snowshoe Group (Table 3-1).

TABLE 3-1

CHARACTERISTIC DEFORMATIONAL FABRICS
ASSOCIATED WITH THE PROPOSED DEFORMATION SEQUENCE

<u>EVENT</u>	<u>DESCRIPTION</u>	<u>NOMENCLATURE</u>
D ₆	- open fracture set	F ₆
D ₅	- symmetric vertical open buckle folds - locally developed fracture and crenulation cleavage; some kink banding	F ₅ S ₅
D ₄	- open to tight NE-verging recumbent folds - well developed SW-dipping crenulation cleavage - poorly developed mica-edge lineations, shallow NW plunge	F ₄ S ₄ L ₄
D ₃	- disharmonic upright SW verging shear folds with associated high strain zones; production of Perseus Antiform and control of regional map pattern; NW-SE trend - strongly developed crenulation cleavage and localized axial planar shear zones - amphibole and mica-edge lineations, shallow NW plunge	F ₃ S ₃ L ₃
D ₂	- mesoscopic recumbent tight to isoclinal east verging folds; very appressed with sharp hinges and planar limbs; production of east-verging large scale folds and associated high strain zones - well developed axial planar foliation associated with formation of regional ductile zone of convergence and subsidiary zones - shallow plunging amphibole, quartz, flattened K-feldspar augen mineral lineation in gneiss; mica-edge lineation in pelitic schist; variable NW-SE trend.	F ₂ S ₂ L ₂
D ₁	- mesocopic intrafolial isoclinal folds outlined by S ₀ , flattened, appressed, with sharp hinges and planar limbs; evidence of east-vergence - primary schistosity/foliation parallel to transposed compositional layering; development prior to formation of Quesnellia-Omineca convergent boundary - mica-edge lineation	F ₁ S ₁ L ₁
D ₀	- compositional layering	S ₀

D₁

The earliest recognized structures within the field area are only developed within the Snowshoe Group. These structures, designated phase 1, are rootless isoclinal intrafolial folds (Table 3-1). Mesoscopic F_1 folds deform and transpose S_0 compositional layering and have a well developed axial plane foliation (Fig. 3-2 a,b). This foliation, the earliest surface which outlines any recognizable structure, is subparallel in orientation to S_0 and is hence considered to be transpositional in nature. Mica-edge lineations, L_1 , associated with F_1 folds plunge variably and shallowly to the northwest and southeast. Lower hemisphere stereographic projections of phase 1 fold elements are presented in Figure 3-3. These diagrams illustrate the present geometry as deformed by successive deformation phases. Little can be inferred concerning the scope and original geometry of these folds due to the effects of superposed folding and metamorphism. As yet, these folds and their associated transposed foliation have not been related to any large scale regional structure(s).

D₂

The earliest phase of deformation common to all formations within the study area is phase 2 folding. This deformation is easterly verging, recognizable on all scales, and is associated with widespread ductile behaviour in all rock types. Associated with this folding is a

NE

SW



Figure 3-2a. Snowshoe garnet-biotite schist containing mesoscopic F_1 intrafolial isoclinal folds.

SW

NE



Figure 3-2b. Snowshoe Group micaceous quartzite containing flattened mesoscopic F_1 isoclinal folds.

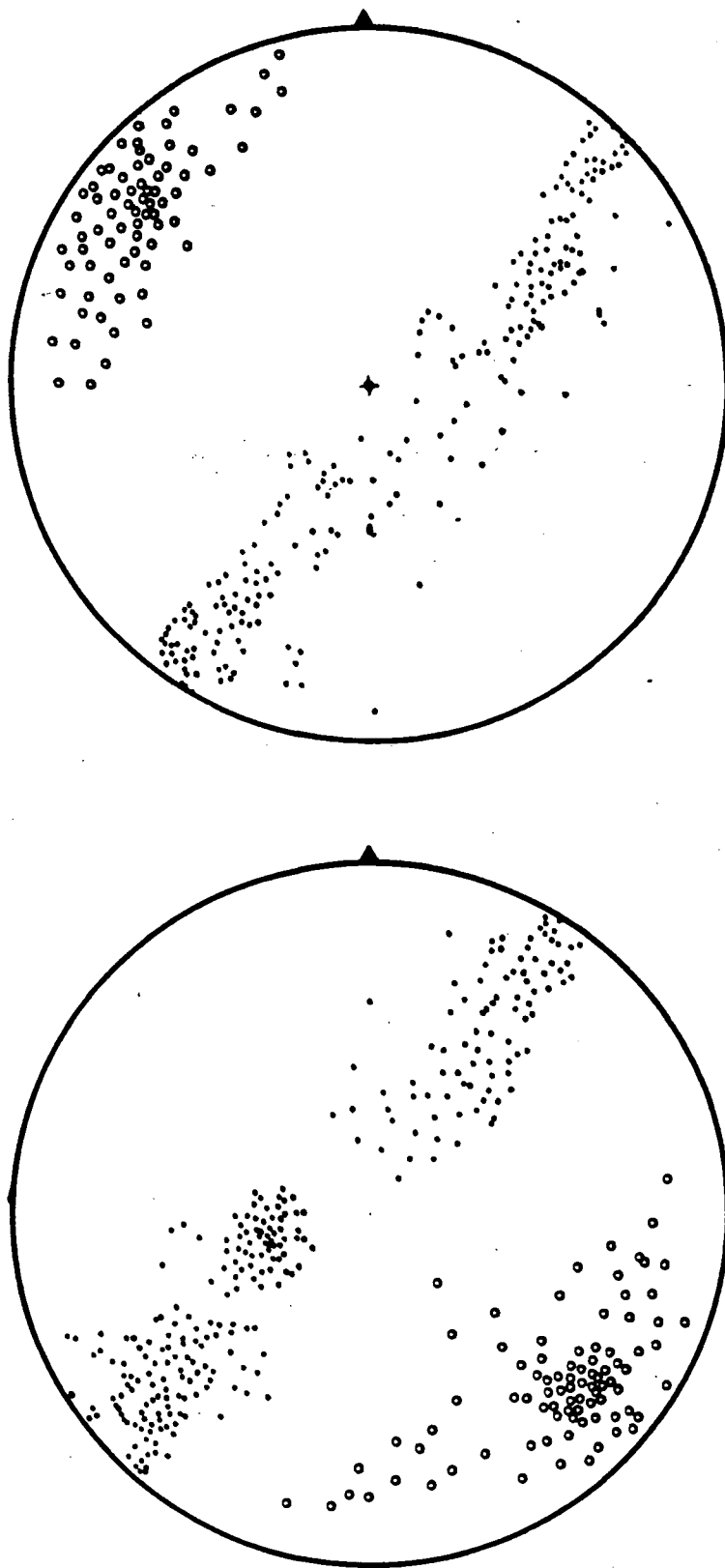


Figure 3-3. Lower hemisphere stereo projections of the present geometry of phase 1 deformation structures as deformed by phase 2 and phase 3 folding. Solid dots = poles to S_1 foliation; circles = L_1 lineations. a) 215 poles and 73 lineations taken from the northwestern region of the antiform. b) 178 poles and 87 lineations taken from the southeastern portion of the map area. L_1 lineations are deformed along great circles and show girdle distribution around later fold axes.

well developed foliation that is axial planar to both mesoscopic and larger fold structure. Mineral lineations within the Perseus gneiss shows strong preferred orientation parallel to L_2 fold axes which plunge variably to the northwest and southeast. Phase 2 represents the main penetrative phase of deformation within the area and is accompanied by synkinematic metamorphism within the lower amphibolite facies. Micro-textures and mineral assemblages indicate that metamorphism outlasted this deformation and began to wane with the third deformation phase. Second phase deformation involves all rock types but does not deform the tectonic boundary separating them, and from this, it can be inferred that D_2 is associated with the formation of this convergent zone. Hence, this geometry most likely describes the nature of convergence between Intermontane and Omineca rocks. Further discussion of this topic is presented in the conclusion chapter.

Minor folds within the Snowshoe (Table 3-1) show consistent vergence which outlines a large scale second phase structure that closes to the southwest (Fig. 3-4). The original geometry of this structure, best outlined by the Perseus Gneiss, has been obscured and refolded by the nearly coaxial phase 3 Perseus antiform (Plates II, III, IV). A composite diagram illustrating the geometry and sense of rotation of F_2 minor folds (as they relate to the larger polydeformed second phase structure) at various structural positions around this phase 3 antiform is presented in figure 3-5. From this diagram, it is apparent that minor folds and their associated foliation within both

NE

SW



Figure 3-4a. Mesoscopic F_2 isoclinal folds within the Perseus gneiss outlined by S_1 transpositional foliation.

SW

NE



Figure 3-4b. Mesoscopic F_2 isoclinal folds, contained within gneiss in the overturned limb of the Perseus antiform (area IX, Fig. 3-5).

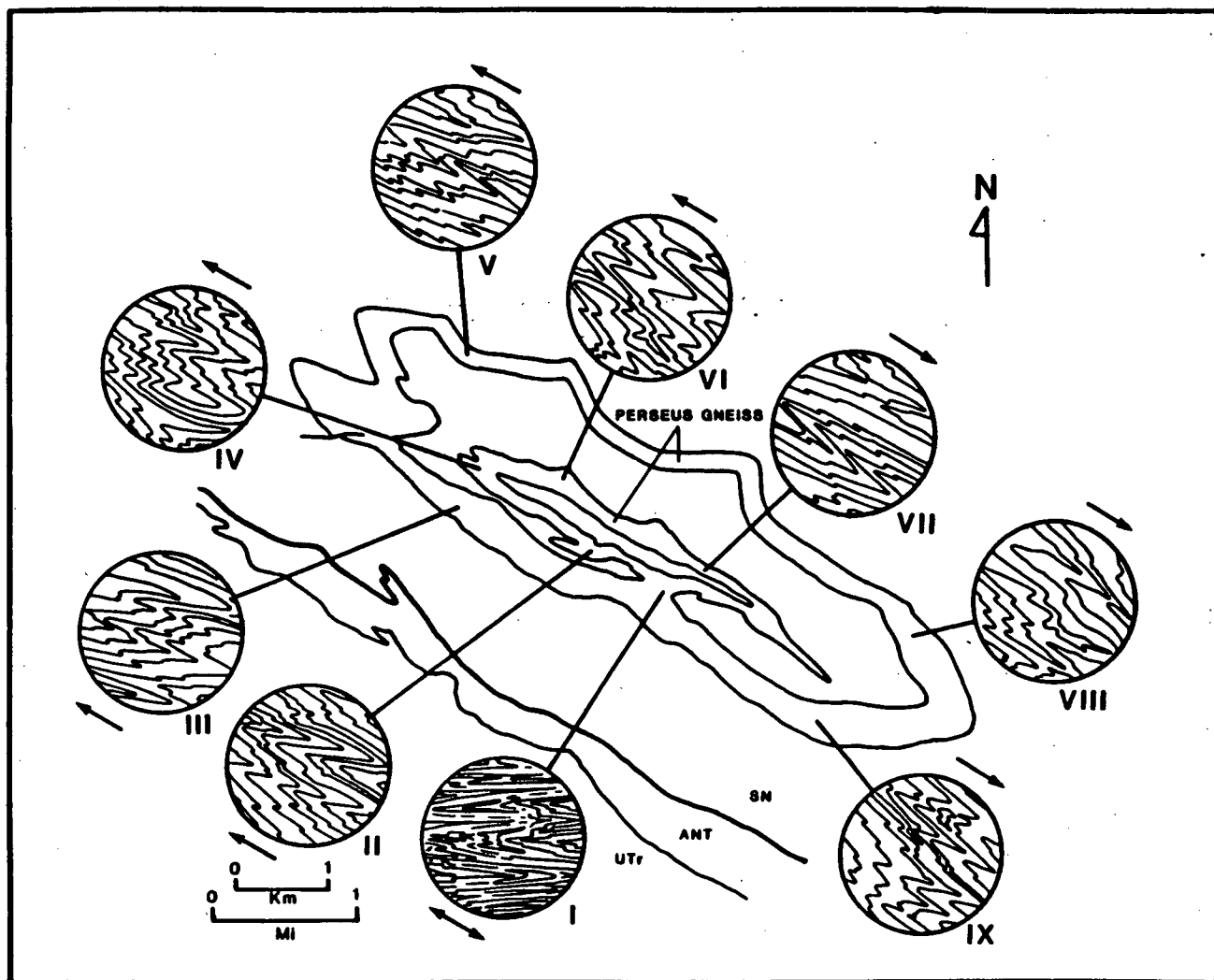


Figure 3-5. Map view of Perseus Gneiss within the Snowshoe Group. Circles represent close-up views of small cross-sections which illustrate the sense of rotation of F_2 minor folds around the Perseus Antiform (arrows indicate plunge). F_2 folds within both limbs of the antiform have similar vergence whereas F_2 folds contained within the antiform core zone display an opposite sense of vergence. These opposing vergence senses outline the deformed limbs of a large phase 2 synform. See text for further explanation. Refer to Plate II for additional nomenclature.

limb regions of the Perseus antiform share similar vergence and hence indicate closure to the southwest. Folds within the antiform core zone (in both schist and gneiss) display a consistent yet opposite sense of rotation with respect to minor folds contained within the limb regions. Therefore, from changing orientations of S_2 around the antiform and from variations in minor fold vergence, it can be inferred that F_2 folds within both limb regions of the Perseus antiform outline the continuous deformed limb structure of an earlier second phase fold. Minor folds within the phase 3 antiform core zone outline the folded complementary limb structure (Fig. 3-6). The convergence of these deformed limbs culminates in a relict hinge zone (outlined by the Perseus Gneiss) located within the vicinity of the southeastern flank of Mt. Perseus (Plate I, III, IV).

F_2 minor folds within this region show little or no sense of rotation and are mostly isoclinal due to localized high flattening strains (Fig. 3-7). Based upon the geometry of minor folds (Figures 3-8,9,10,11,12) and the pattern of lithologic contacts, a possible orientation of the F_2 structure prior to refolding can be approximated. By removing the effects of the third phase antiform, the phase 2 structure appears east-verging, synformal, and southeast plunging (Fig. 3-13). Phase 3 westerly verging folds refold pre-existing easterly verging phase 2 geometry and it is this near coaxial superposition that gives rise to the curvilinear nature of phase 2 axial structures and results in regional elongate domes having the phase 2 trend. Axial

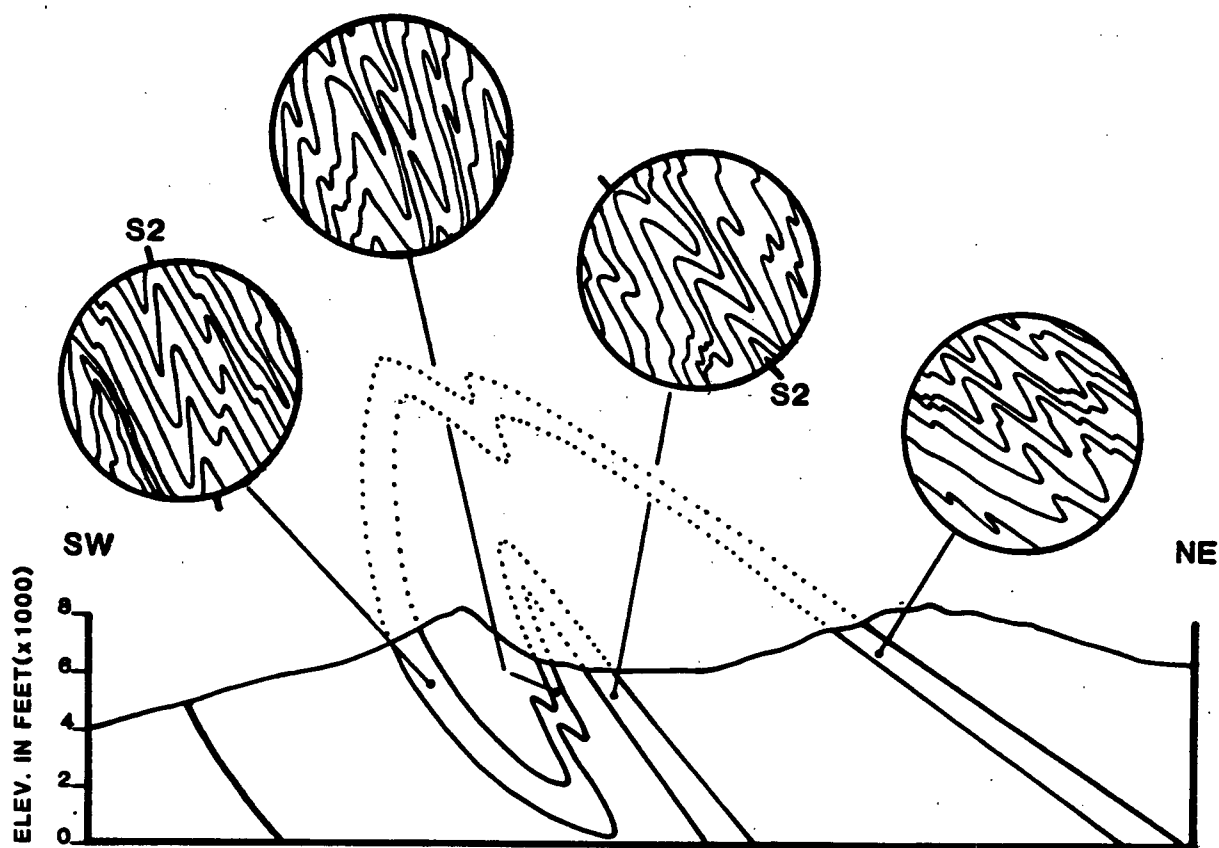


Figure 3-6. Schematic cross-section through the phase 3 Perseus Antiform (outlined by gneiss) which illustrates the refolded nature of a large phase 2 fold. Circles represent close-up views of small cross-sections of F_2 minor folds observed at various structural positions within the folded Perseus Gneiss. F_2 fold vergence is used to outline the limb regions of the larger deformed phase 2 fold.

SW

NE

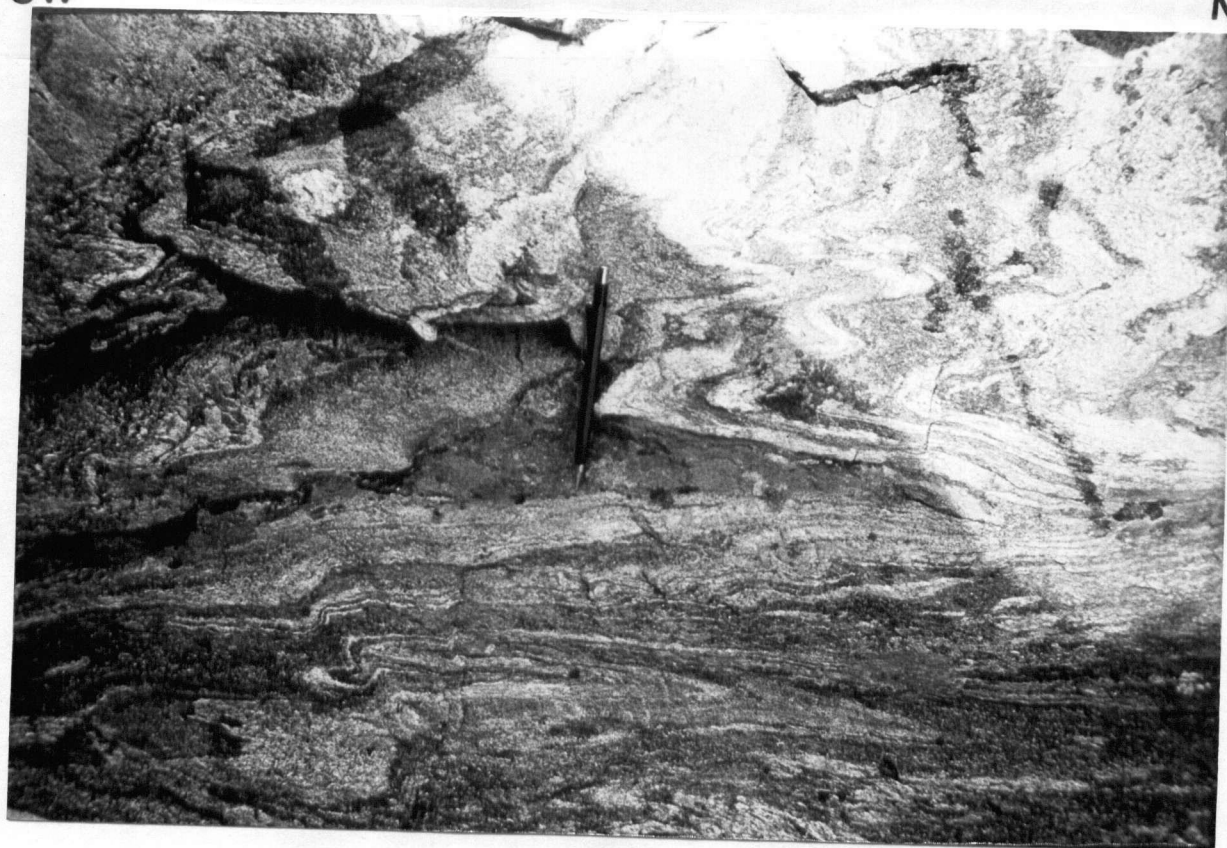


Figure 3-7a. Mesoscopic flattened F_2 isoclinal folds within the Perseus Gneiss. Location corresponds to area I, Figure 3-5.

SW

NE



Figure 3-7b. Mesoscopic F_2 isoclinal fold within Snowshoe garnet-biotite schist. Location corresponds to area I, Figure 3-5.

NE

SW



Figure 3-8. Mesoscopic open F_3 fold in gneiss refolding an F_2 isocline (lower left limb of F_3 structure).

NE

SW



Figure 3-9. Tight mesoscopic F_2 fold contained within the hinge region of the Perseus Antiform (between areas II and VI, Figure 3-5) in which Snowshoe metapelites occupy the core zones of folds within the Perseus Gneiss.

NE

SW

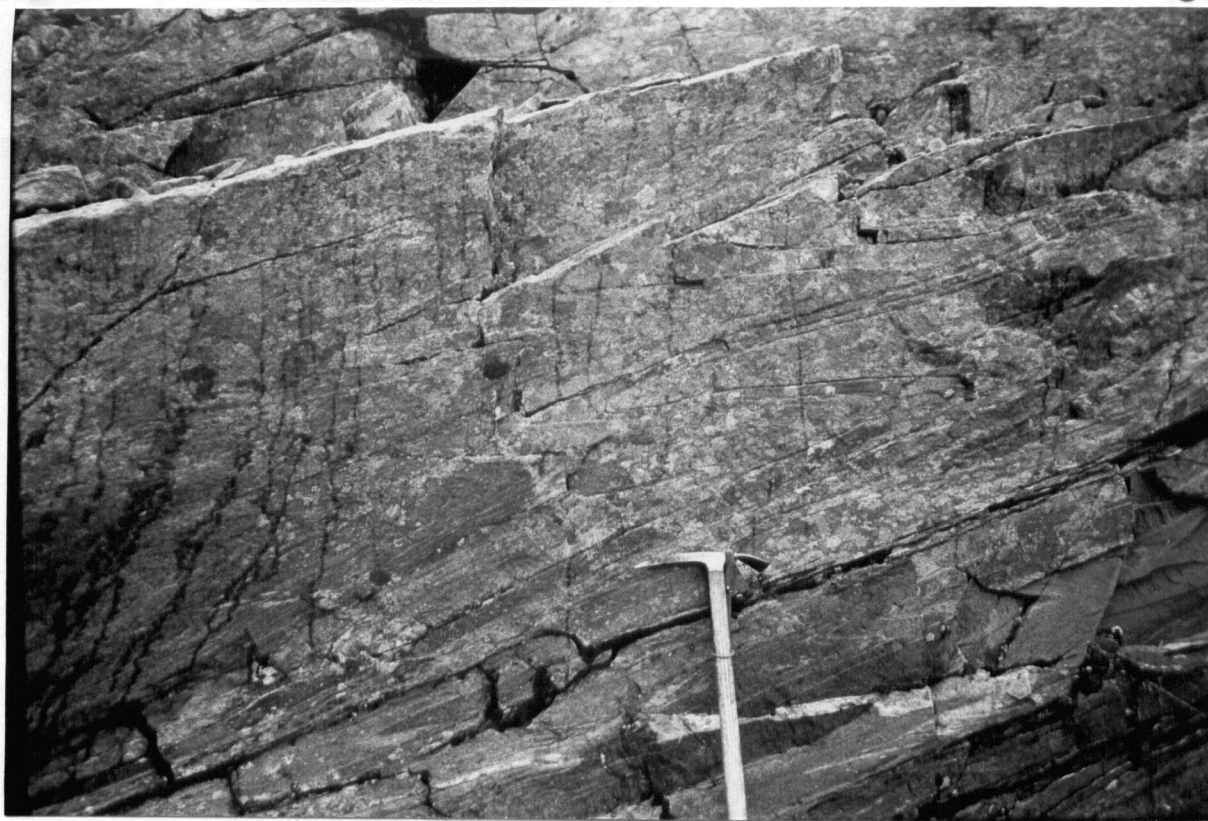


Figure 3-10. Mesoscopic F_2 tight to isoclinal folds contained within the Perseus Gneiss. After the removal of later deformational effects, folds appear east-verging (location corresponds to area VI, Figure 3-5).

NE

SW



Figure 3-11 Large mesoscopic east-verging F_2 folds within shallowing dipping Snowshoe metapelite in the southeastern portion of the Perseus Antiform hinge zone (southeast plunging). Location corresponds to an area between areas VIII and IX, Figure 3-5.

SW

NE



Figure 3-12. Steeply inclined F_2 isoclinal folds overprinted by shallowing dipping open F_4 folds. Compositional layers in this garnet schist are outlined by layers of quartz. Location corresponds to area II, Figure 3-5.

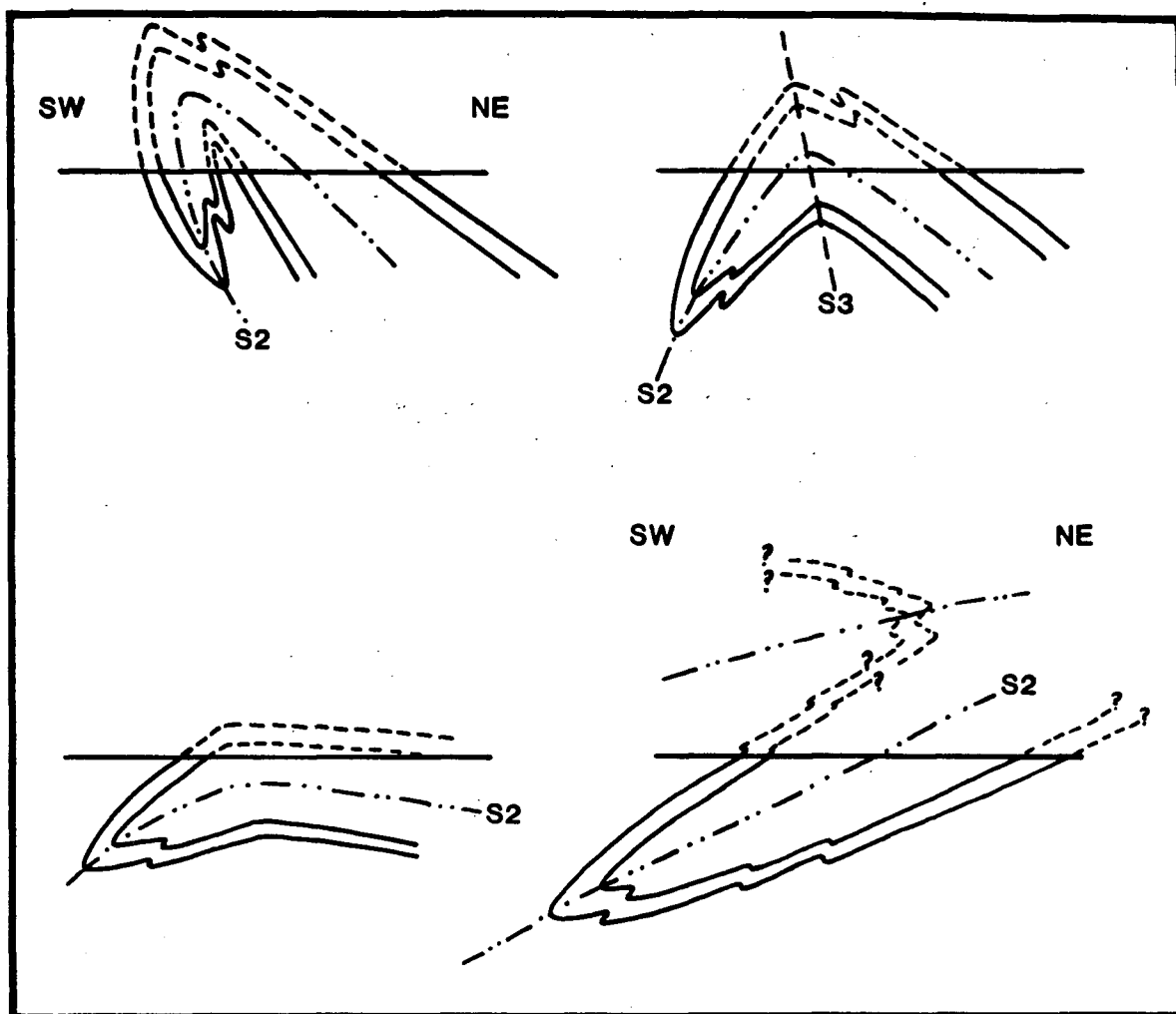


Figure 3-13. Schematic illustrating the unfolding of the superposed phase 3 Perseus Antiform. By unfolding the phase 3 limbs such that their dip equals the plunge of the phase 3 fold axis, the resultant phase 2 geometry appears synformal and east-verging.

traces of the deformed F_2 synform are presented in Figure 3-14.

Phase-two minor fold structures within Antler and Upper-Triassic Formations are mostly isoclinal and intrafolial within the S_2 foliation (Fig. 3-15). S_2 fabrics within these rocks deform S_0 compositional layering and thus can be considered transpositional and similar in nature to S_1 within the Snowshoe. Minor folds display a sense of rotation that is consistent with F_2 geometry in the Snowshoe within the overturned limb of the Perseus antiform. The flattened and often transposed nature of these folds is confined to a zone containing mylonites which attains a maximum width of approximately 1 kilometre on either side of the Snowshoe-Antler contact. Geometry within this zone is most likely the result of concentrated high flattening strain associated with regional deformation of the Intermontane-Omineca boundary. Transposition of early fold structures is more easily accommodated in Antler and overlying rocks due to the strong ductility contrast present between them and the Snowshoe. Hence, only Snowshoe rocks immediately adjacent to this tectonic boundary have been subject to widespread mylonitization and transposition. Lower hemisphere stereographic projections of second phase structures are presented in Figure 3-16.

D₃

Third phase geometry, unlike phase 2, is southwest-verging and is associated with a well developed moderately to steeply northeast

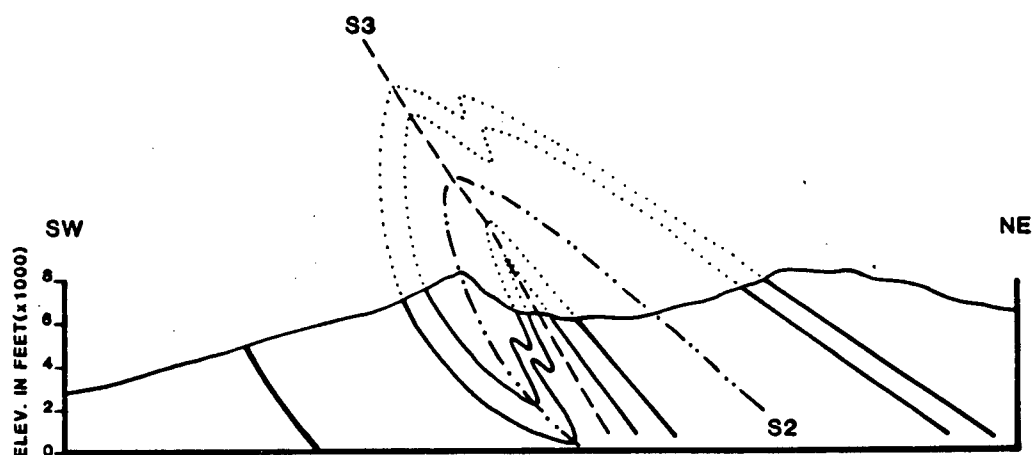
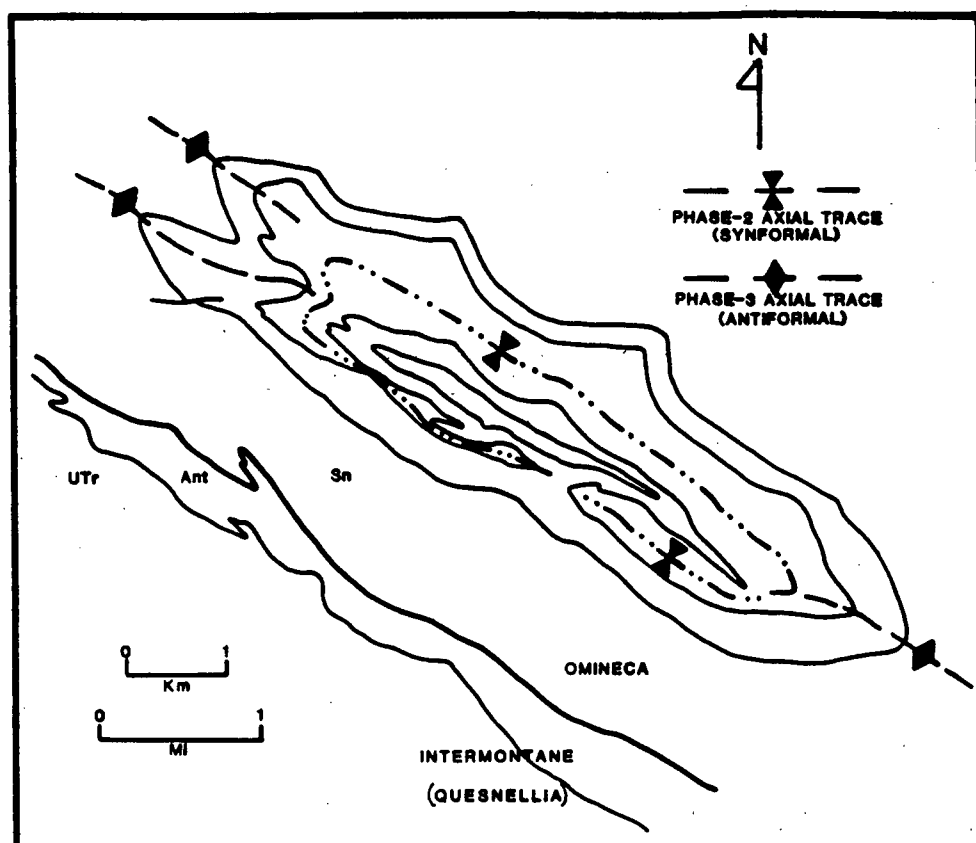


Figure 3-14. Map and schematic cross-section through the Perseus Antiform showing the nature and orientation of phase 2 and phase 3 axial surfaces and axial traces.



Figure 3-15. Photograph of a small phase 2 isoclinal fold within a chlorite schist of the Antler Formation.

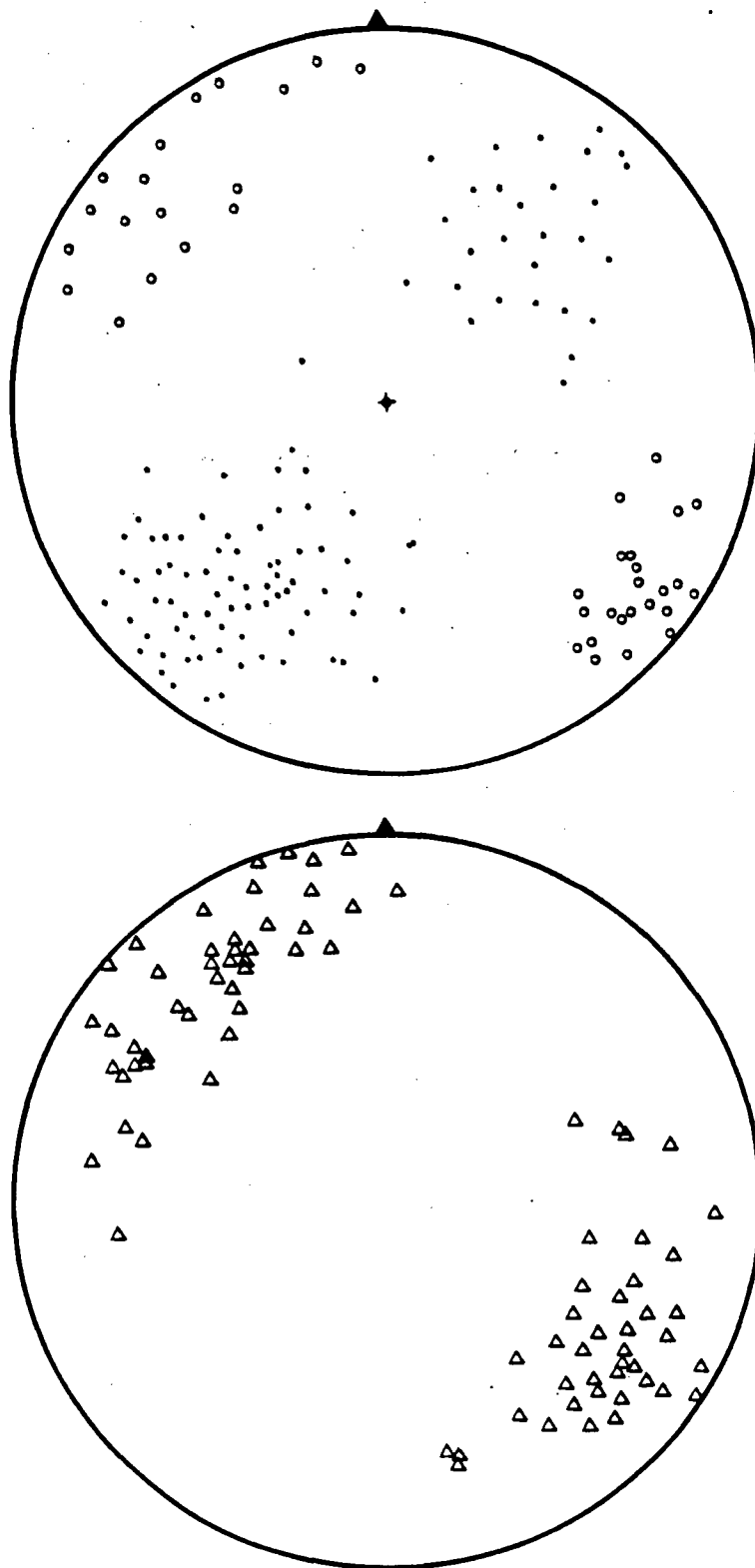


Figure 3-16. Lower hemisphere stereo projections of 101 poles to F_2 minor fold axial planes (solid dots), 41 L_2 mineral lineations (circles), and 83 F_2 minor fold axes (triangles). Distributions outline the doubly plunging nature of the phase 3 antiform. Girdle distributions of deformed linear structures lie along great circles.

dipping axial planar foliation. Mineral assemblages and micro-textures indicate that metamorphism associated with phase 3 was within the middle greenschist facies and represents a reduction in metamorphic grade from the peak lower amphibolite facies active during second phase deformation.

Adjacent to the Intermontane-Omineca boundary, phase 3 geometry is characterized by large northwest plunging, upright antiformal closures in the Snowshoe, separated by highly attenuated synforms. These synforms become transposed parallel to their axial surfaces into small shear zones which extend down into the Snowshoe and are often cored by small sheared bodies of Antler amphibolites. Larger scale northwest plunging third phase folds define and control the present configuration of the Intermontane-Omineca convergent boundary within the Crooked Lake area.

The Perseus antiform, one example of these larger fold structures, is dome-like in outcrop with northwest trending fold axial traces and fold axes (Figure 3-14; Plates I, III, IV). Geometry is classified as moderately tight and overturned to the northwest with a variable interlimb angle averaging 50 degrees. Axial planar foliation is well developed throughout the structure within Snowshoe and Antler rocks. Upper Triassic rocks characteristically contain a spaced cleavage and buckle-folds associated with phase 3 rather than penetrative foliation.

Third phase minor folds appear everywhere parasitic to the larger

antiform and change in both style and nature across the antiform as a function of lithology and proximity to the Snowshoe-Antler tectonic boundary. (Fig. 3-17).

Within the northeast limb of the antiform, minor folds vary as a function of lithology from moderately open structures with interlimb angles averaging 50 to 60 degrees in gneissic rocks to tight folds and associated small scale crenulations in metapelites (Fig. 3-18). Well developed mica-edge lineations oriented parallel to fold axes plunge shallowly to the northwest and southeast.

Phase 3 structures within the core-zone of the antiform display little sense of rotation and vary in style from tight folds with 30-40° interlimb angles to near isoclinal geometry (Figs. 3-19, 20, 21, 22). The more open structures show a characteristic progressive gradation into isoclinal form over the course of several metres. In several localities isoclinal folds become further flattened within small transposition (mylonite) zones oriented parallel to their respective axial planes (Fig. 3-17). Large volumes of metamorphic quartz "sweats" occupy the core zones within isoclinal folds and associated shear zones. These regions of high strain most likely served as conduits for fluid transport during metamorphism. Disharmonic folding is observed within both gneiss and metapelite and increases in frequency toward the Intermontane- Omineca boundary.

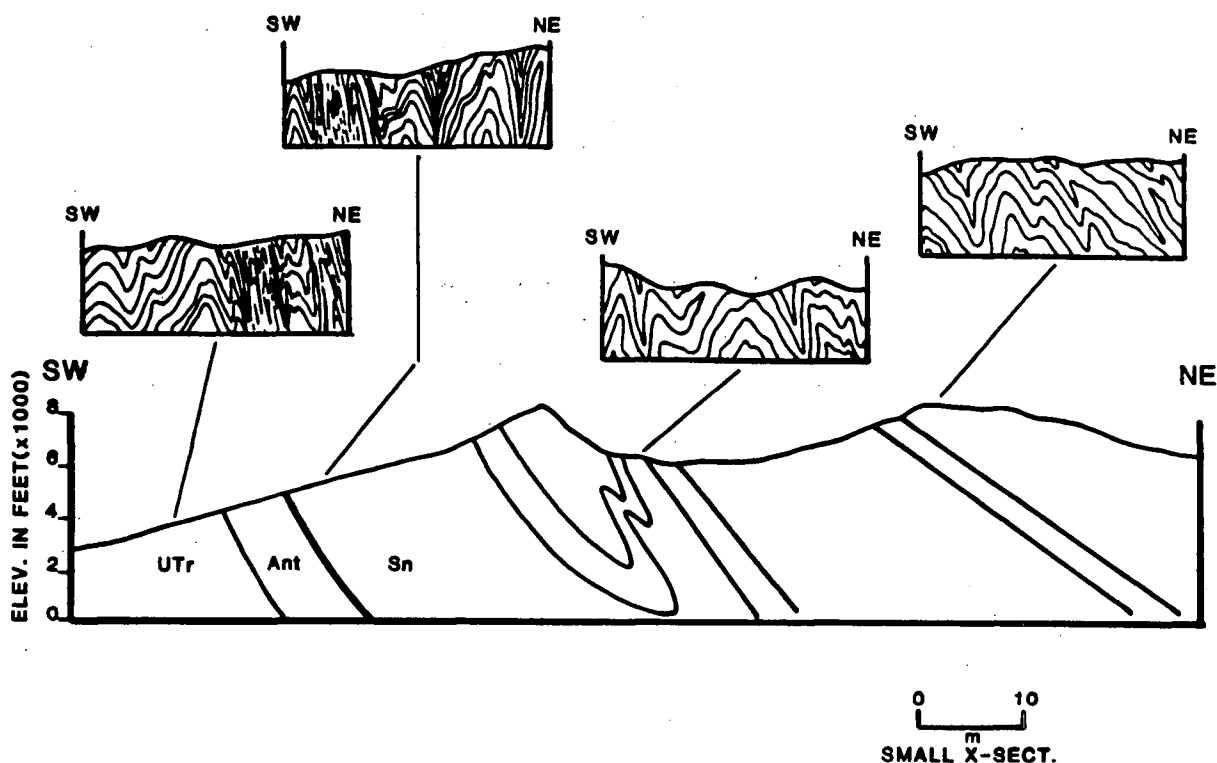


Figure 3-17. Schematic cross-section through the Mt. Perseus area showing contacts between Upper Triassic, Antler, and Snowshoe rocks. Small cross-sections, based upon field sketches, illustrate the changing style of F_2 folds across the antiform. Folds become progressively more flattened and sheared as the Quesnellia-Omineca boundary is approached. Rocks adjacent to this boundary are penetrated by narrow longitudinal shear zones related to fold geometry.

NE

SW



Figure 3-18a. Mesoscopic F_2 folds in Snowshoe micaceous quartzite. The sense of rotation is directed to the southwest (southeast plunge) and is thus parasitic to the larger Perseus Antiform.

NE

SW



Figure 3-18b. Phase 3 mesoscopic folds contained within the upright limb of the Perseus Antiform.

NE

SW



Figure 3-19. Outcrop of garnet-biotite schist exposing the superposition of an upright phase 3 fold onto a phase 2 isoclinal fold (F_2 hinge zone located at lower left of photo).

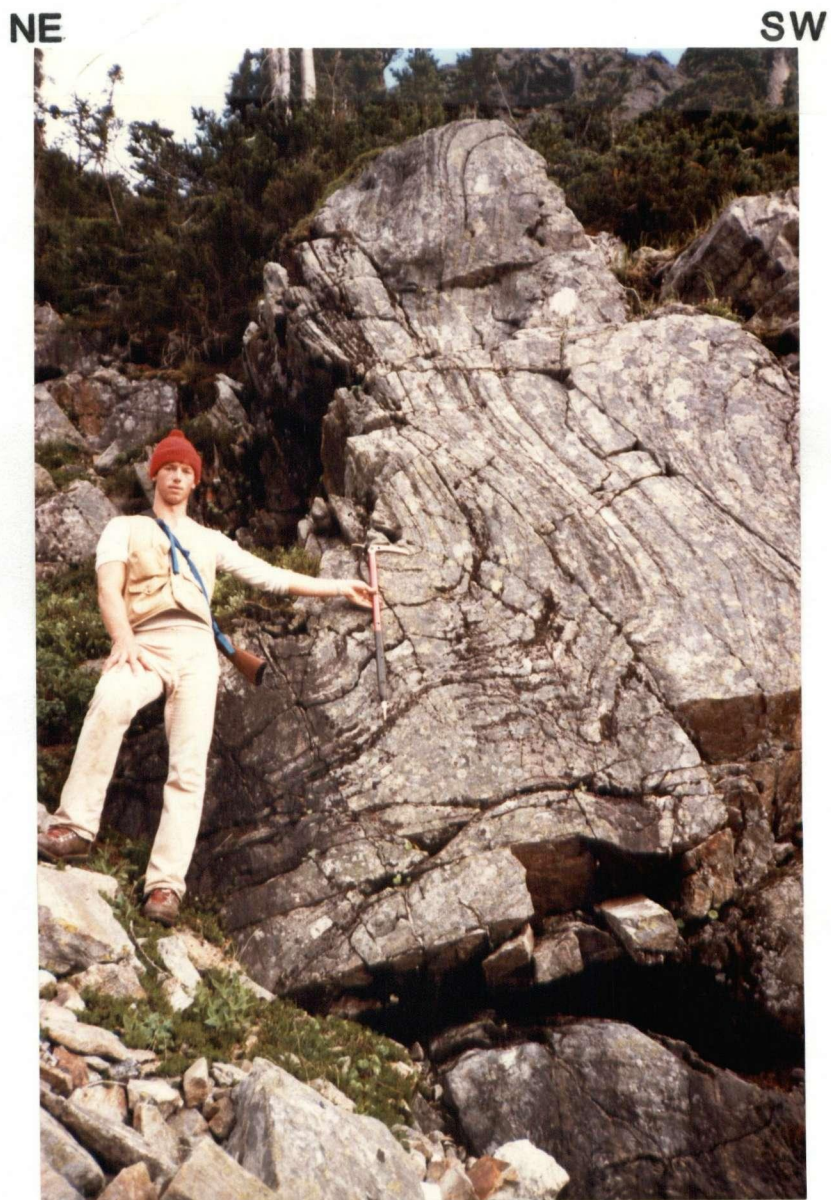


Figure 3-20. Open style upright F_3 folds in metapelite contained within the antiform core zone. Most folds in this zone show little or no sense of rotation. Compositional layers are composed of quartz and muscovite.

SW

NE



Figure 3-21. Upright moderately tight F_3 fold in calcareous metapelite adjacent to the hinge area of the Perseus Antiform.

NE

SW



Figure 3-22. Outcrop of micaceous quartzite containing an F_2 isocline refolded by phase 3 minor folds. Location is within the antiform hinge zone and compositional layering is therefore shallowly inclined and is intersected at a high angle by S_3 .

NE

SW



Figure 3-23. Outcrop of calcareous garnet-bearing metapelite which contains small scale disharmonic F_3 folds. Structural location corresponds to an area within the overturned limb of the Perseus Antiform in the southwestern portion of the field area.

NE

SW



Figure 3-24. Close-up view of calcareous metapelite in which an F_2 isocline (outlined by quartz) is refolded at a high angle by open to tight F_3 folds. Location is adjacent to Figure 3-23.

Within the deformed axial regions of the large scale phase 2 structure (Fig. 3-14), third phase minor folds are characteristically flattened and transposed within their foliation due to the convergence in orientation of second and third phase axial surfaces (Fig. 3-25). Strain associated with phase 3 in these regions was more easily accommodated through slip reactivation along the pre-existing S_2 fabric.

Sequences of disharmonic folding accompanied by increased frequency of transposition (shear) zones characterize third phase minor structures within the southwest overturned limb region, and in particular, adjacent to the convergent boundary (Figs. 3-26,27,28).

The tectonic contact zone or zone of convergence, contained within the southwest limb of the antiform, is characterized by a pronounced mylonite belt in which nearly all structures (phase 2 and phase 3) are highly sheared and often transposed and flattened within their respective nearly coplanar foliations. Third phase minor folds within the Antler are mostly isoclinal and often sheared and transposed with zones along their respective axial planes. Phase 3 folds within the Upper Triassic units are flattened and sheared within their respective foliation immediately adjacent to their lower contact with Antler rocks. Approximately 100 metres structurally higher within the phyllites, F_3 folding is confined to zones averaging 3 to 5 metres in width. Third phase structures in the remainder of the formation are characterized by buckle folds associated with a well developed spaced

NE

SW



Figure 3-25. Mesoscopic phase 2 isocline (hinge at bottom right of photo) flattened and refolded by phase 3 folding. Location corresponds to areas I and II, Figure 3-5, within the deformed phase 2 axial region.

SW

NE



Figure 3-26. Phase 3 disharmonic folds in garnet-biotite schist adjacent to a small localized shear zone (far left of photo). Fold geometry becomes more flattened as the zone is approached and again more open further from the zone. Location corresponds to an area within the overturned phase 3 limb in the vicinity of Mt. Perseus.

NE

SW



Figure 3-27. Mesoscopic phase 3 isoclinal fold adjacent to a small shear zone (left of photo) in which F_3 geometry becomes transposed parallel to S_3 axial surfaces. These zones often contain large volumes of metamorphic quartz veins.

SW

NE



Figure 3-28a. Mesoscopic phase 3 antiform in Snowshoe micaceous quartzite immediately adjacent to the Quesnellia-Omineca boundary. This fold is one in a sequence of disharmonic fold sets that flank numerous ductile shear zones in this structural region. Microtextures indicate that rocks in these structures have undergone extensive mylonitization and recrystallization.

SW

NE



Figure 3-28b. Phase 3 antiform situated immediately adjacent to photo (a). Fold geometry is becoming progressively tightened as a small shear zone is approached (left side of photo). Note large volumes of quartz concentrated along the axial surface and limb of the fold.

SW

NE



Figure 3-28c. Mesoscopic F_3 antiform immediately adjacent to the previous photo (b). The intervening synform (far right of photo) has been nearly completely transposed within the foliation and is generally unrecognizable. As a shear zone is approached (left of photo), fold geometry becomes isoclinal and rapidly transposed within the shear zone.

SW

NE

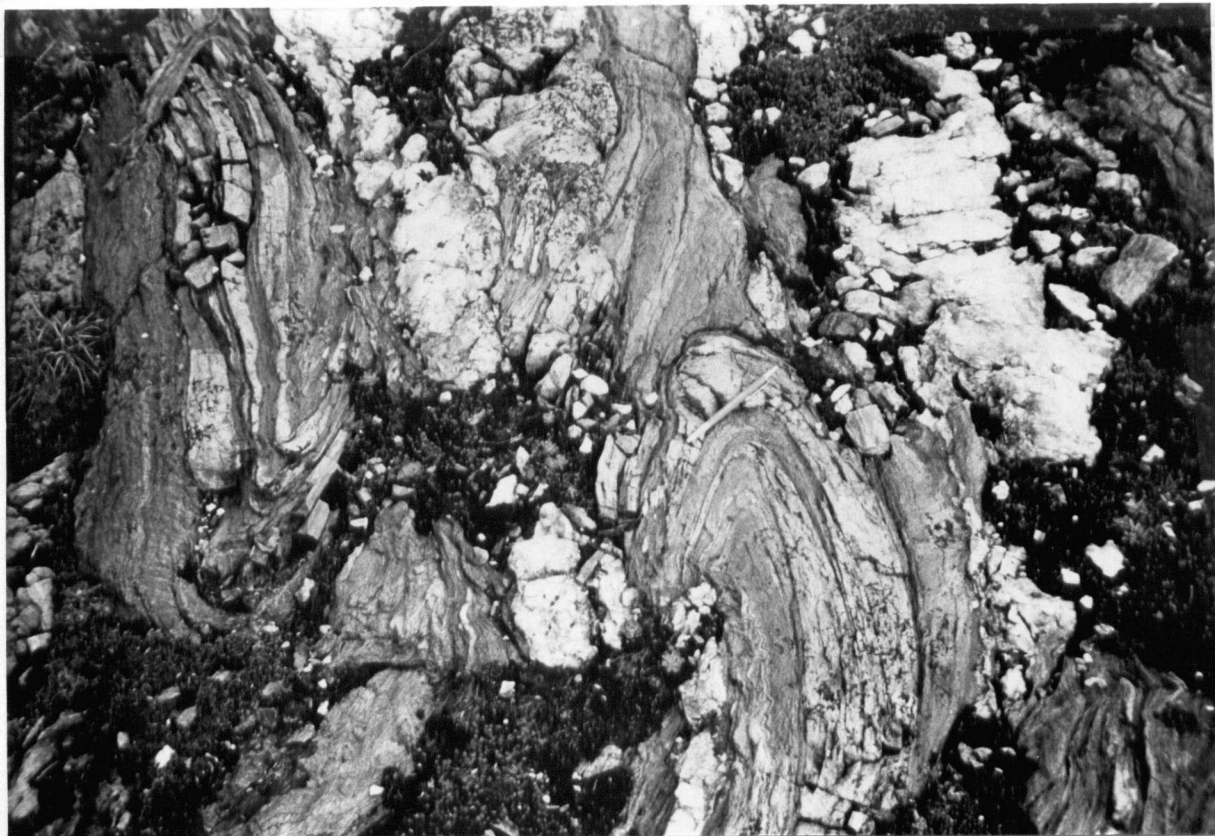


Figure 3-28d. Mesoscopic isoclinal fold adjacent to the far left of photo (c). These phase 3 folds are flattened and partially transposed parallel to their axial surfaces and often have a rootless form. The remainder of the shear zone is characterized by abundant rootless isoclinal folds, mylonites, and large volumes of quartz veins.

crenulation cleavage. Hence the wave length amplitude of F_3 folds increases away from the contact. Folds within Snowshoe rocks however, are nearly all transposed and where flattening strain was less intense near isoclinal geometry is cored by large volumes of metamorphic quartz "sweats" (Figs. 3-28b,c,d).

Northwest plunging mineral lineations, most prominently developed within Antler amphibolites and Snowshoe augen gneiss, are strongly elongate with the mylonitic foliation parallel to L_3 fold axes. This geometry extends for approximately 1 kilometre on either side of the Snowshoe-Antler boundary. Mesoscopic fold structures within the Snowshoe outside of this 2 kilometre wide mylonitic zone are only transposed within isolated localized zones of high flattening strain averaging 5 to 10 metres in width.

Adjacent to the tectonic boundary, south of Cayuse Creek, isolated elongate bodies of highly sheared Antler amphibolite, averaging 100 metres in length and 2 metres in width are structurally infolded within Snowshoe metapelites (Plate I). These infolds represent remnant, sheared out core zones of large scale attenuated phase 3 synforms developed within the Antler Formation that have been drawn-down and structurally isolated within the Snowshoe (Fig. 3-29). Large scale complimentary antiforms within the Snowshoe, adjacent to these sheared-out synforms are typically more open and less attenuated. From this geometry, it can be inferred that the phase 3 structural style within the contact zone is characterized by large tight antiforms in

the Snowshoe separated by amphibolite-cored shear zones which represent attenuated synformal extensions of Antler rocks into the Snowshoe (Fig. 3-30). Smaller scale phase 3 shear zones throughout other portions of the Snowshoe most likely represent structurally deeper extensions of these attenuated synformal closures. Lower hemisphere stereographic projections of phase 3 geometry are presented in Figure 3-31.

D₄

Phase-4 deformation is characterized by non-penetrative east-verging folds. Axial cleavages which dip shallowly to the southwest, crenulate all pre-existing surfaces, and are associated with minor growth of biotite. Most often F_4 folds produce open recumbent warps within steeply inclined portions of the Snowshoe (Figs. 3-32, 33, 34) and are generally less well developed within Antler and Black Phyllite Formations. Fold styles vary from open to tight as a function of varied lithologies. Lower hemisphere stereographic projection are presented in Figure 3-35.

D₅

Phase-5 deformation is represented by non-penetrative small scale vertical buckle folds accompanied by local crenulations and kink-banding (Fig. 3-36). Folds are typically symmetrical and open and are rarely associated with a measureable cleavage. Folding of this style is prominent within all units in the study area.

SW

NE



Figure 3-29. Talus blocks containing interfolded Antler amphibolite and Snowshoe garnet metapelite. Location is adjacent to a narrow lense of isolated Antler rock in the Snowshoe Group approximately 200 metres structurally below the Antler-Snowshoe contact in the vicinity of Cayuse Creek.

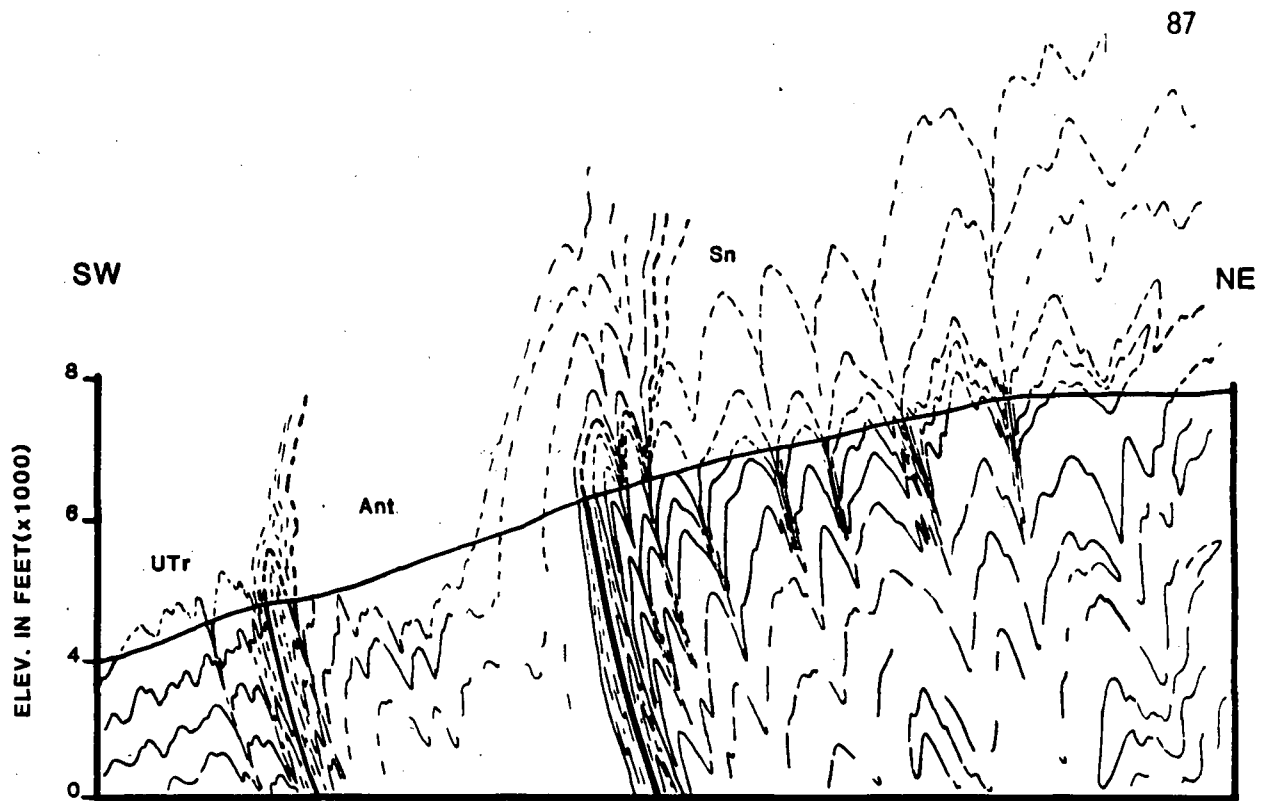


Figure 3-30. Schematic cross-section of phase 3 folding throughout the contact zone between the Black Phyllite and Antler Formations and the Snowshoe Group. F_3 synforms within the Snowshoe are locally cored by Antler amphibolites which are manifest as shear zones at greater structural depths within the Snowshoe.

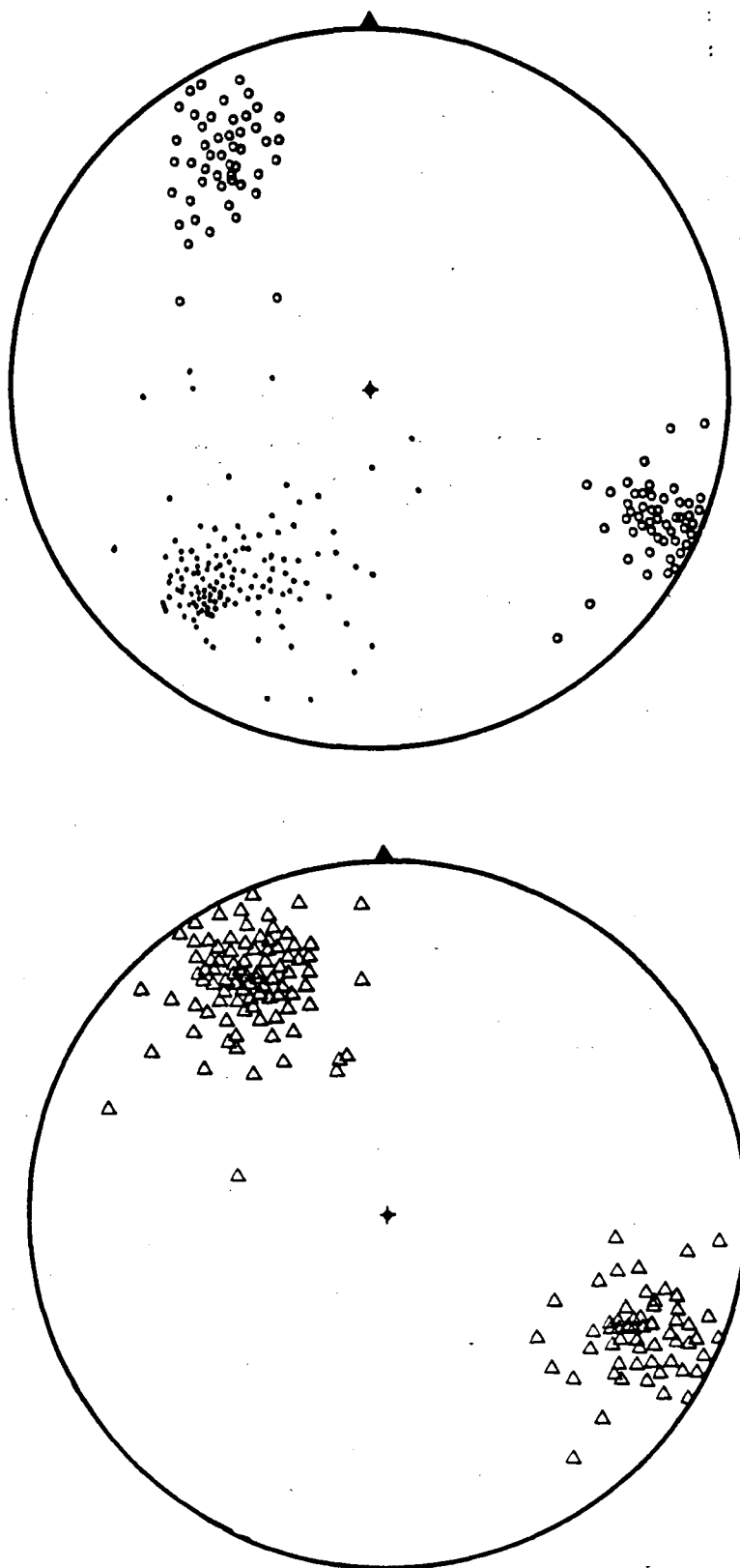


Figure 3-31. Lower hemisphere stereo projections of 130 poles to F_3 minor fold axial planes (solid dots), 96 L_3 lineations (circles), and 134 minor fold axes (triangles). Poles to minor fold axial planes outline the larger Perseus Antiform whose axial surface averages 125/54 NE. Linear structures appear doubly plunging due to their superposition on variably oriented earlier geometry. The majority of phase 3 linear structures plunge to the northwest and have an average orientation of 23/330.

SW

NE



Figure 3-32. Phase 4 recumbent open folds refolding steeply inclined phase 2 isoclinal folds (outlined by compositional layers). Photo location is within the phase 3 antiform core zone, adjacent to Mt. Perseus.

SW

NE

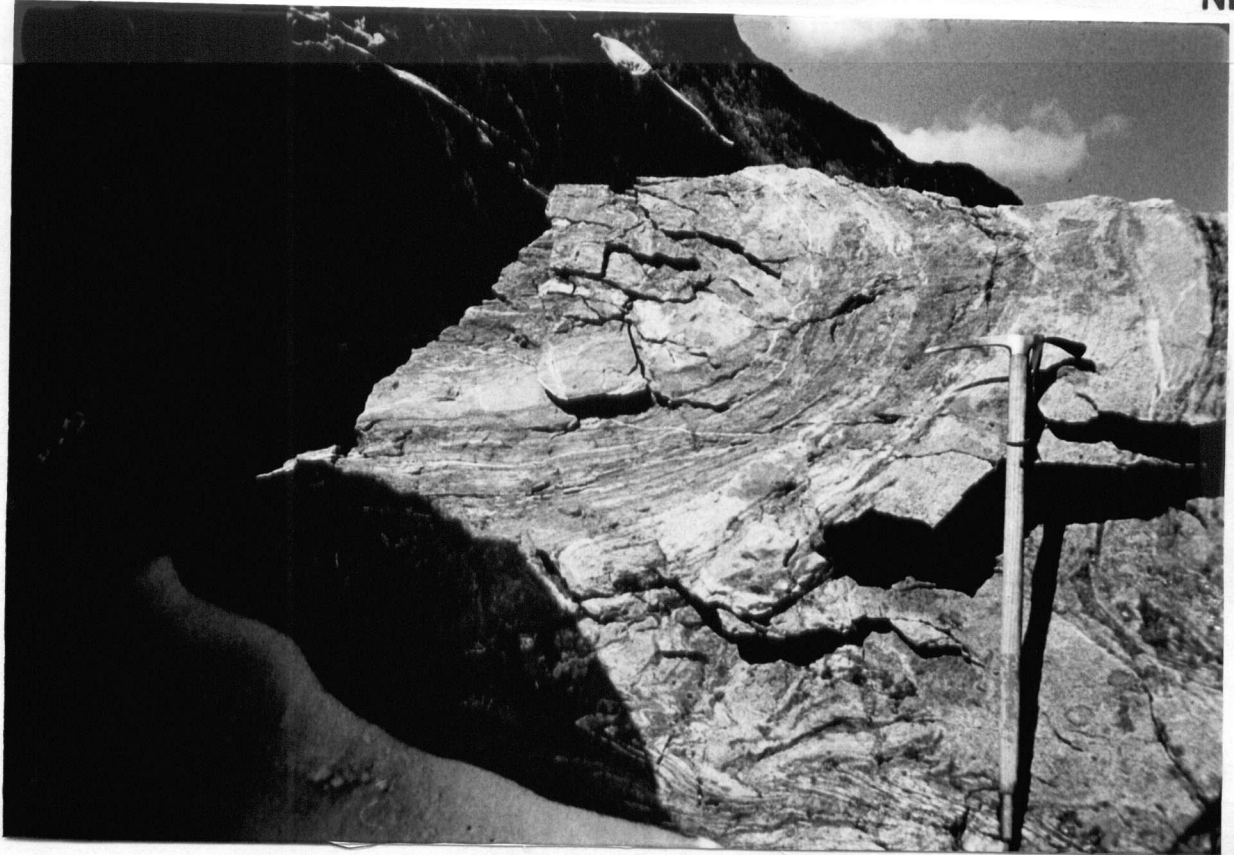


Figure 3-33. Nearly recumbent phase 4 fold deforming phase 2 isoclinal folds contained within the Perseus Gneiss on the eastern flank of Mt. Perseus.

SW

NE



Figure 3-34. Gently dipping phase 4 folds deforming S_0/S_1 layering within Snowshoe garnet-biotite schist. Location is within the southeast flank of Mt. Perseus.

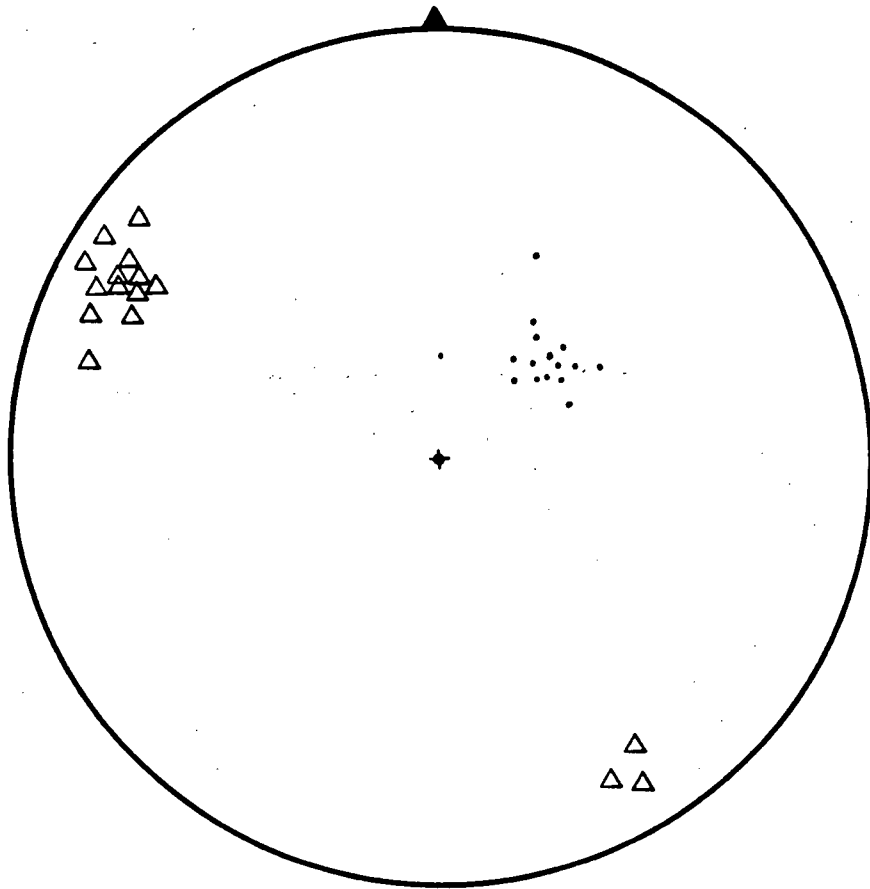


Figure 3-35. Lower hemisphere stereo projection of phase 4 fold geometry. Solid dots indicate poles to axial planes and triangles represent minor fold axes.

NE

SW

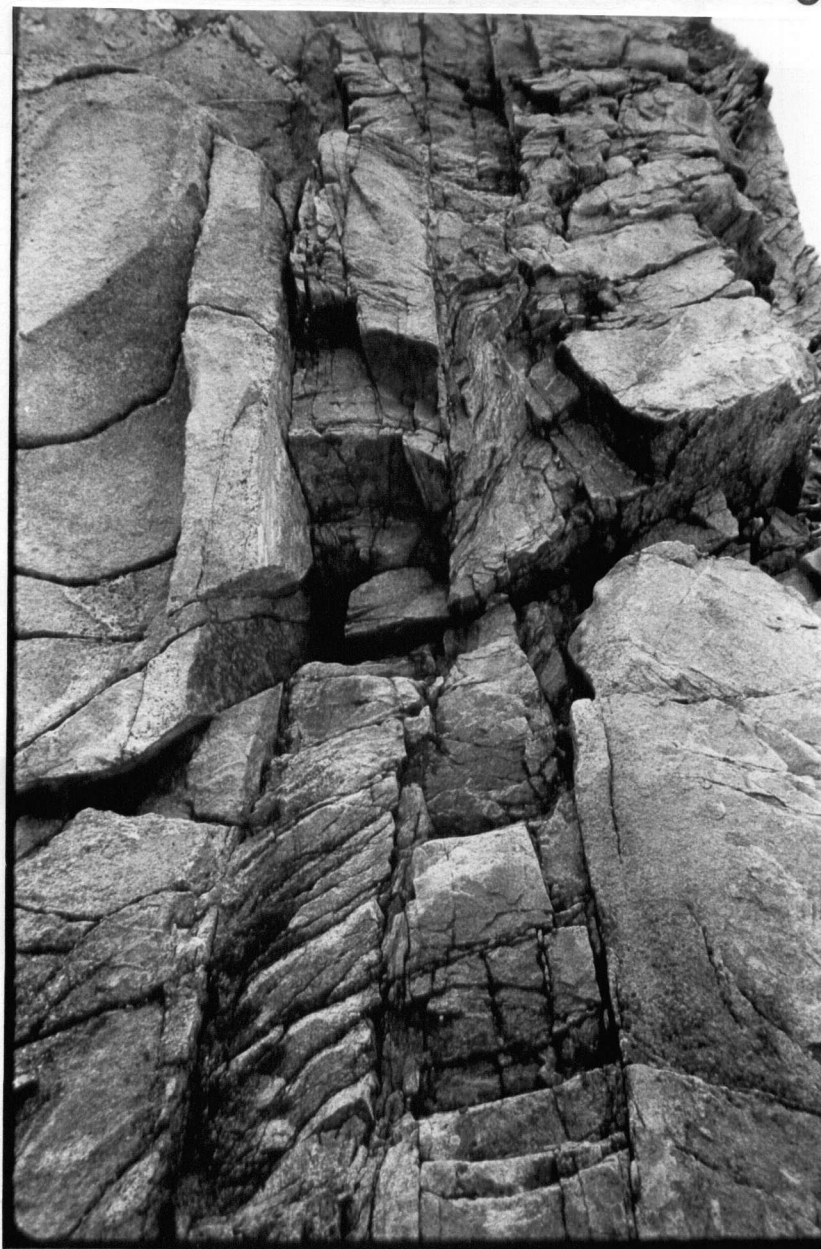


Figure 3-36. Large kink-band structure within the Perseus Gneiss. This deformation overprints all earlier geometry (except joints) and is probably associated with phase 5 deformation.

D₆

The final phase of deformation consists of a pervasive open fracture set common within all rock units. Most fractures and joints have a common orientation of 032/81NW, and most likely represent relaxation features associated with waning regional deformation.

MICROTEXTURES

The metamorphic character of rocks within the Mt. Perseus area has been described by Campbell (1971) who distinguished a Barrovian metamorphic sequence ranging from middle greenschist to the middle amphibolite facies. Isograds delineating biotite, garnet, and kyanite/staurolite zones were mapped on the basis of first appearance of the respective phases.

In this study, characteristic textural and mineralogical features of relevant stratigraphy are described and related to deformational phases. Mineral assemblages within the study area describe a Barrovian sequence which increases in grade to the northeast from the middle greenschist facies in Upper Triassic phyllites to lower amphibolite (garnet grade) within portions of the Antler and in Hadrynian Snowshoe Group rocks. The peak metamorphic activity appears synkinematic to phase-two (D_2) deformation with a reduction to middle greenschist during the third deformational phase (D_3). No evidence of kyanite/staurolite zones were located. Post deformational annealing is strongly developed adjacent to the Snowshoe-Antler boundary and within narrow longitudinal subsidiary shear zones throughout the Snowshoe.

A summary of the relevant stratigraphy, metamorphic rock types and typical mineral constituents is presented in Table 4-1.

	STRATIGRAPHIC UNIT	TYPICAL MINERALOGY*	PROTOLITH ROCK TYPE
S N O W S H O E G R O U P	Alkali-Feldspar Augen Gneiss (Mylonite)	Microcline + Quartz + Muscovite + Plag + Biotite (An 8-27)	Feldspathic Sandstone, Arkose (?) or Granitic sheetlike intrusive (Quartz Monzonite?)
	Garnet-Biotite Schist	Biotite + Quartz + Muscovite ± Garnet ± Plagioclase (An 10-23) ± Hornblende	Mixed assemblage of Sandstones, Mudstone and Greywacke
	Micaceous Quartzite	Quartz + Muscovite ± Garnet ± Plagioclase (An 15-27)	Greywacke, Sandstone
	Calcareous Garnet - Biotite Schist	Quartz + Calcite + Dolomite + Biotite ± Muscovite ± K-Spar ± Plagioclase (An 13-23) ± Garnet	Impure calcareous Psammite, Greywacke
	Sandy Marble	Quartz + Calcite + Dolomite + Muscovite	Impure Limestone, Calcareous Psammite
	Quartzo - Feldspathic Gneiss	Biotite + Muscovite + Quartz + Perthitic microcline + Hornblende + Plagioclase (An 14-30) ± Garnet ± Epidote ± Sphene	Sill-like Quartz - Dioritic Intrusives

* Common Accessory Minerals Include: Tourmaline, Apatite, Zircon, and Opaque Dust

TABLE 4-1

SNOWSHOE GROUP

Mineral assemblages within the Snowshoe indicate that all rock types (with the exception of late stage pegmatites) have undergone peak metamorphism within the lower amphibolite facies (garnet grade) which gradually wained to middle greenschist grade. Micro-textures within coexisting garnet and biotite relate peak metamorphism to D_2 . Strong post-deformational annealing throughout the Snowshoe has rendered many early textures obscure and as yet, no evidence, either mineralogical or textural, was found to substantiate any metamorphism associated with D_1 .

METAPELITIC-PSAMMITIC ROCKS

Garnet-Biotite Schist

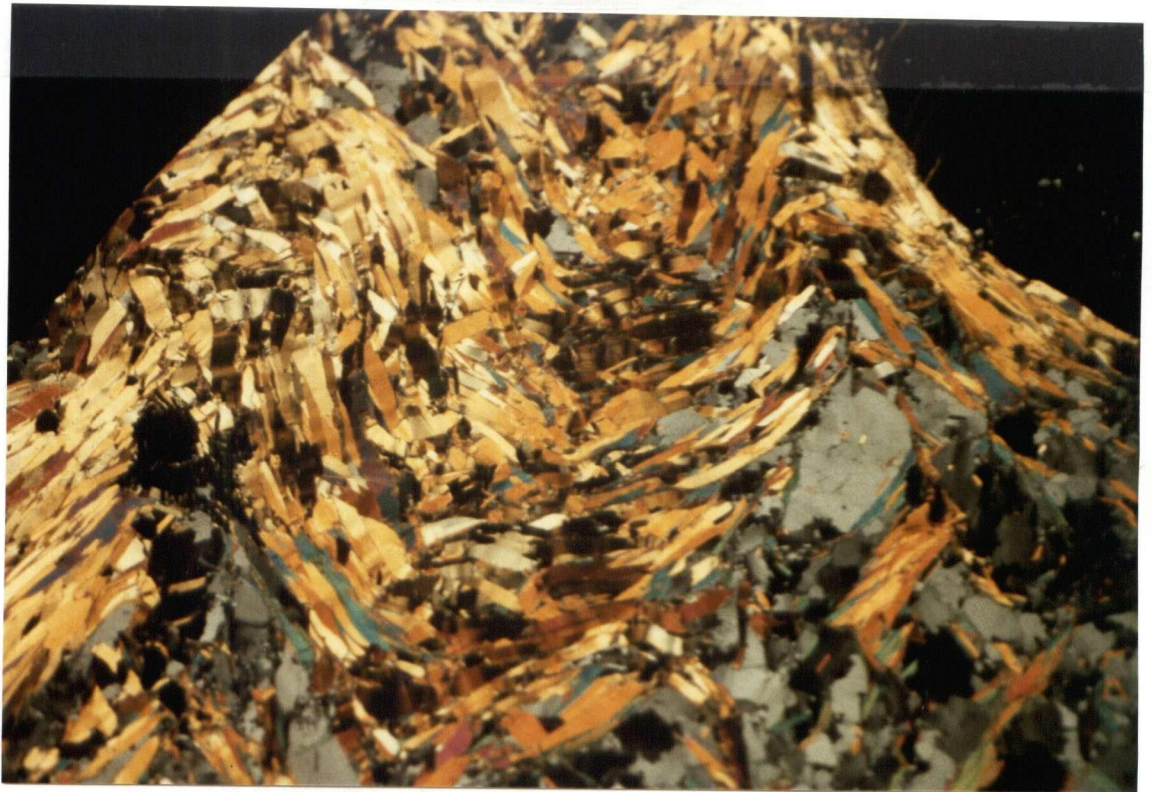
Pelitic schists containing coexisting garnet and biotite comprise the dominant lithology within the Snowshoe. The following text describes the mineral phases present within this rock type and their relation to the proposed deformation (refer to Table 4-1).

Chlorite

Chlorite occurs in small amounts throughout the Snowshoe as fine laths and together with muscovite often defines the S_1/S_2 foliation. Chlorite is present as a retrogressive phase having formed from biotite and garnet. This retrogressive metamorphism was presumably associated with phase 3 and later deformation.

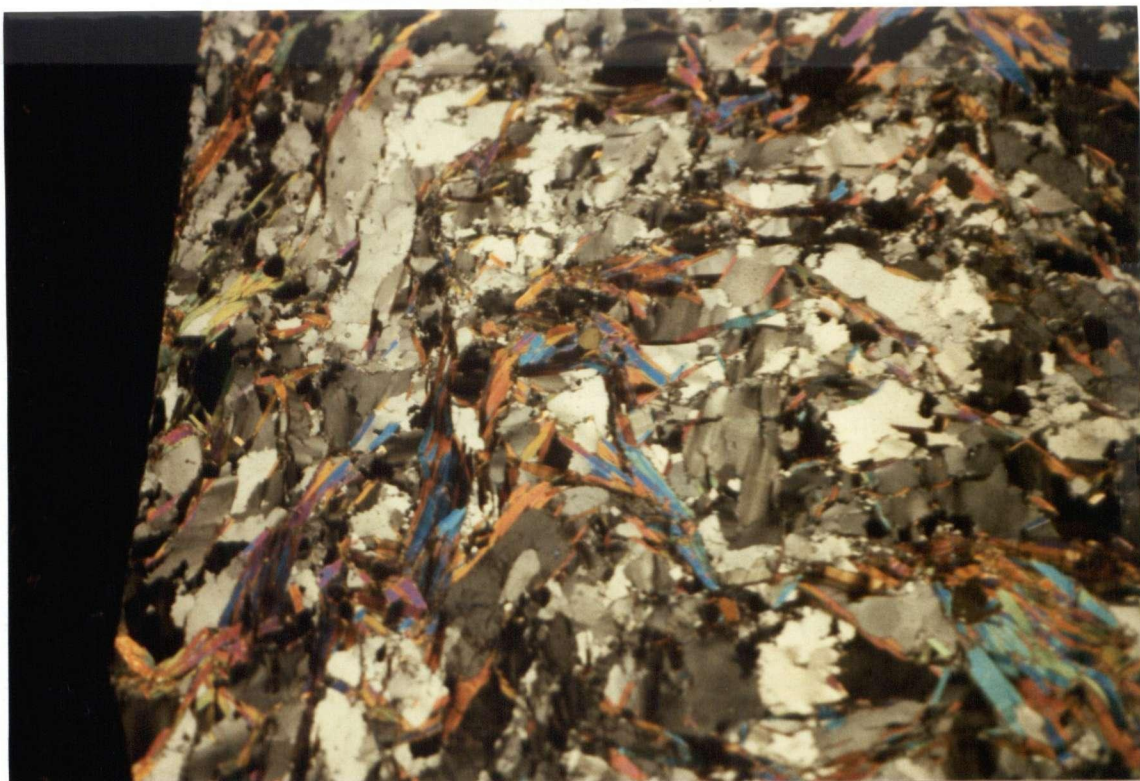
Biotite:

Porphyroblastic brown biotite occurs throughout the Snowshoe and is most commonly recognized as small plates and laths within the matrix. Porphyroblastic phases crystallized at random throughout these rocks and are commonly associated with post-deformational annealing. Several samples yielded porphyroblasts which contain relict internal schistosity which has been rotated relative to the external S_1/S_2 foliation. Biotite of this type most likely formed during D_1 and underwent rotational and flattening strain during D_2 and D_3 which caused the foliation to rotate with respect to the growing porphyroblast and hence "trap" earlier foliation orientations. The matrix biotites formed before and after D_2 , and define, together with muscovite the schistosity (partially transposed foliation) associated with F_2 folds.



1 mm

Figure 4-1. Photomicrograph (x-nicols) of a Snowshoe Group quartz-muscovite schist. Muscovite laths outline S_2 and are deformed at a high angle by F_3 crenulations.



1 mm

Figure 4-2. Photomicrograph (x-nicols) of a Snowshoe micaceous quartzite. Muscovite and biotite laths are aligned parallel to S_2 and are folded by F_3 crenulations. Note subgrain development at the grain boundaries of larger quartz grains.

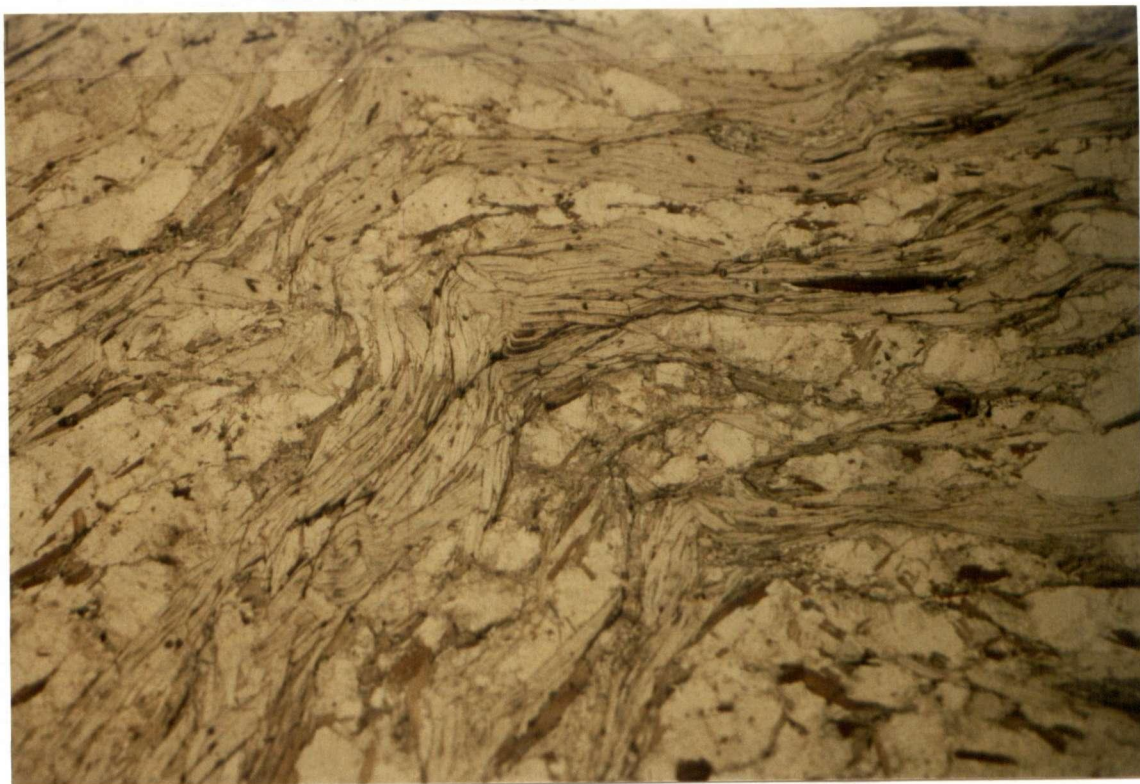
Muscovite

Muscovite occurs as small laths oriented parallel to the S_1/S_2 foliation and along S_3 cleavage planes (Fig. 4-1,2,3). Polygonal arcs defining F_2 and F_3 microfolds are seen throughout the Snowshoe (Fig. 4-4) except in the area adjacent to the Omineca-Intermontane boundary, where any polygonal arcs have been largely flattened and transposed.

Garnet:

Garnet (presumably almandine) development within the Snowshoe Group is largely dependent upon composition and hence is often confined to local layers. Two stages of prophyroblastic garnet growth are present within metapelitic and gneissic rocks. The first generation is characterized by large (up to 4 cm) xenoblasts which contain numerous inclusions that are generally recognizable as relict S_2 schistosity (Fig. 4-5). These inclusions are predominantly quartz with minor biotite and muscovite. Substantial flattening has occurred around these garnets which has resulted in the formation of extensive quartz pressure shadows (Fig. 4-5).

Helicitic internal structures vary as a function of structural position within the Perseus antiform. Figure 4-6 presents a schematic interpretation of the timing of garnet growth.



1 mm

Figure 4-3. Photomicrograph (plane-light) of a Snowshoe Group garnet-muscovite-biotite schist. Muscovite and biotite outline $S_0/S_1/S_2$. Phase 3 crenulations are seen to deform mica laths.

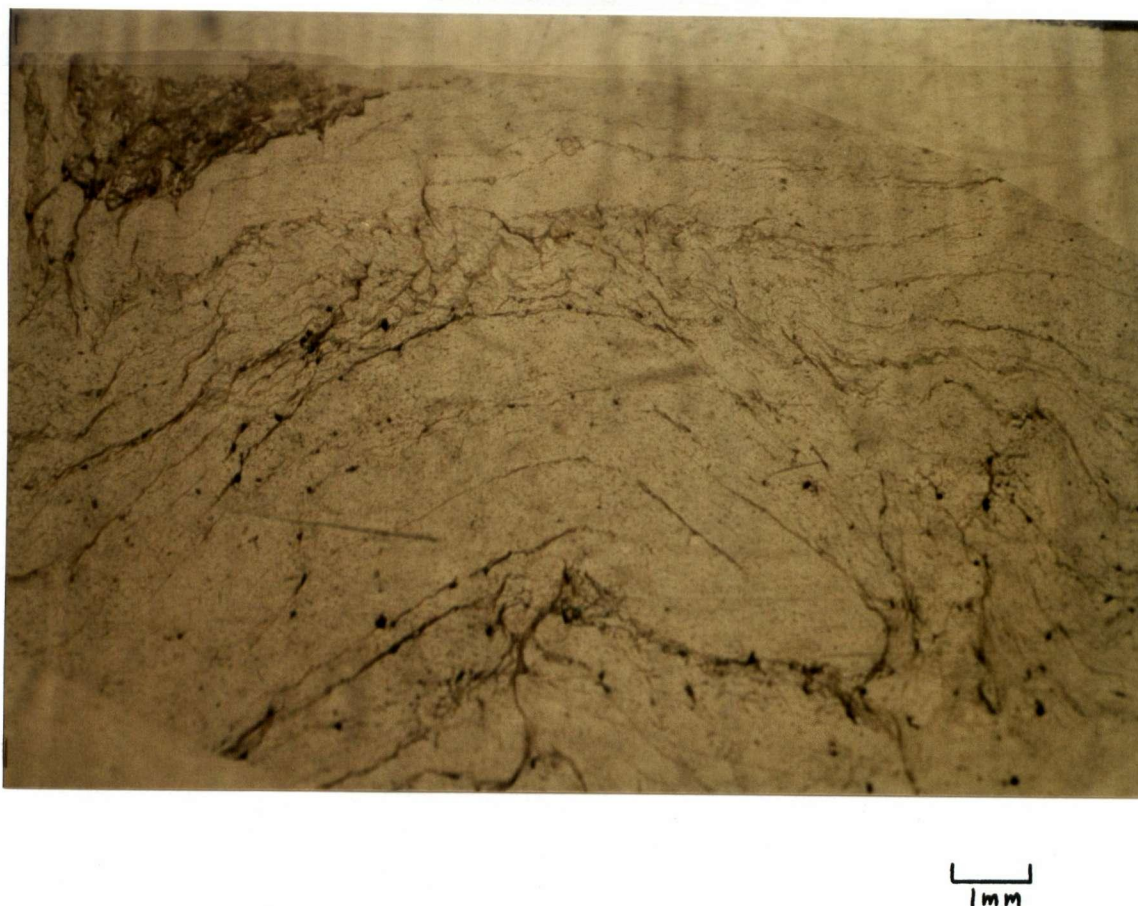
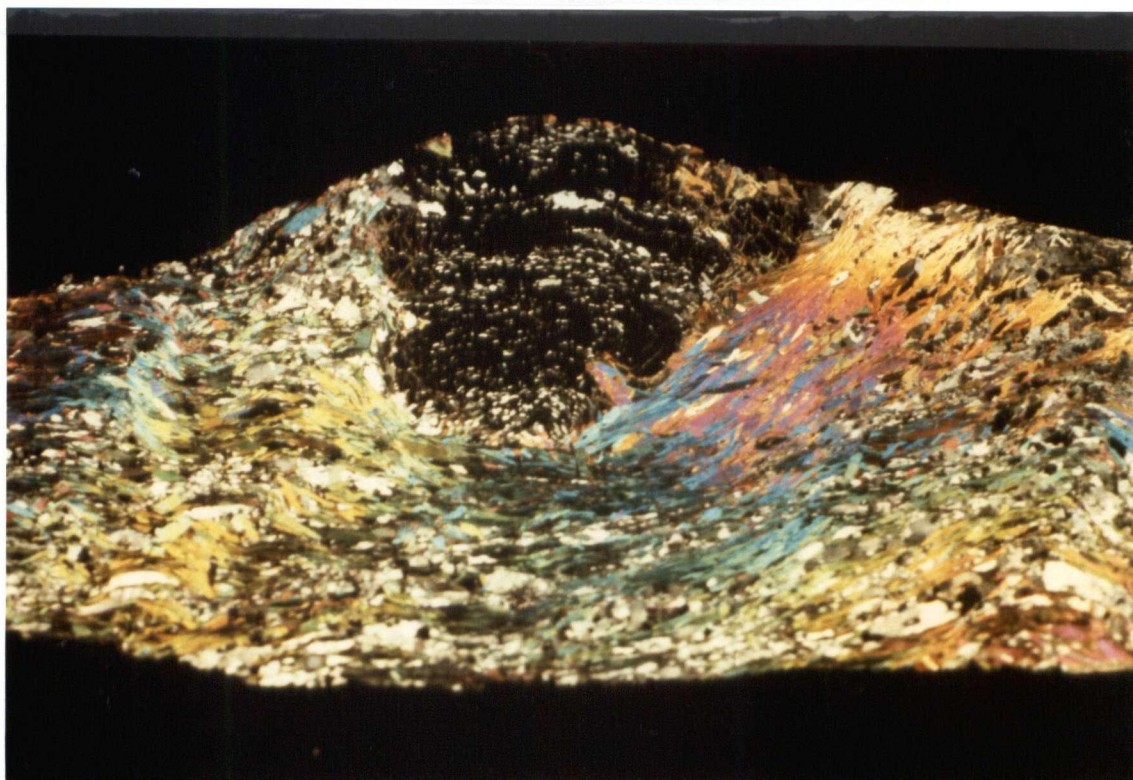


Figure 4-4. Photomicrograph (plane-light) of a phase 2 microfold outlined by fine grained muscovite and quartz (S_0/S_1) in a Snowshoe micaceous quartzite (hinge is located in lower right corner area of photo). The metamorphic growth of muscovite initiated early within D_2 and continued throughout D_3 .



1 mm

Figure 4-5. Photomicrograph (x-nicols) of a helicitic phase 1 type garnet in a Snowshoe garnet-muscovite-biotite schist. Rotated inclusion trails of quartz, muscovite, and biotite outline S_2 and have been rotated relative to the external S_2 schistosity through flattening processes active during D_3 .

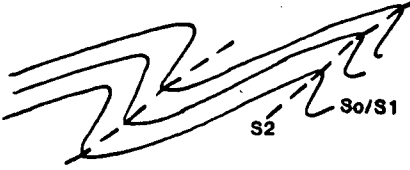

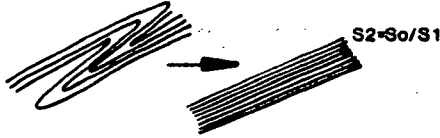
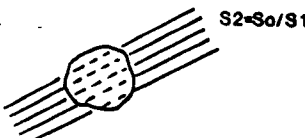


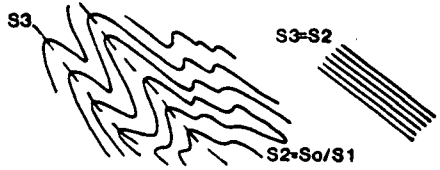
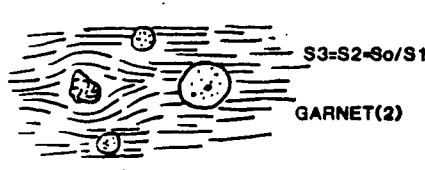
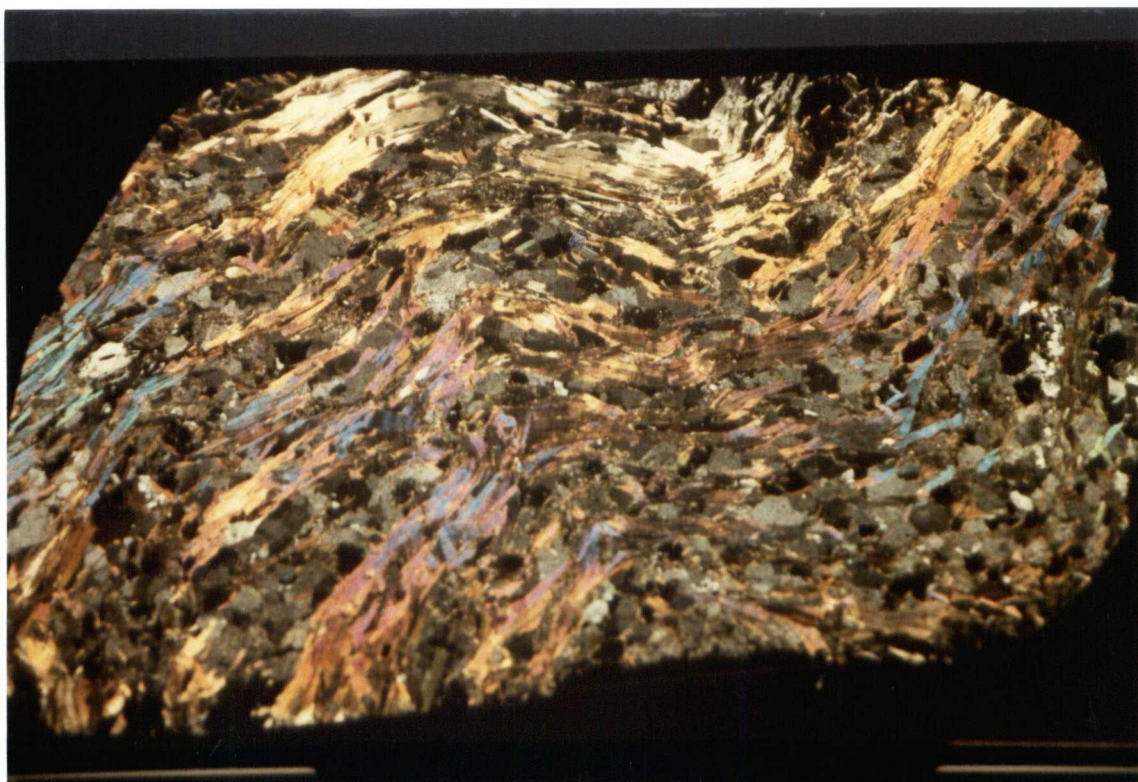
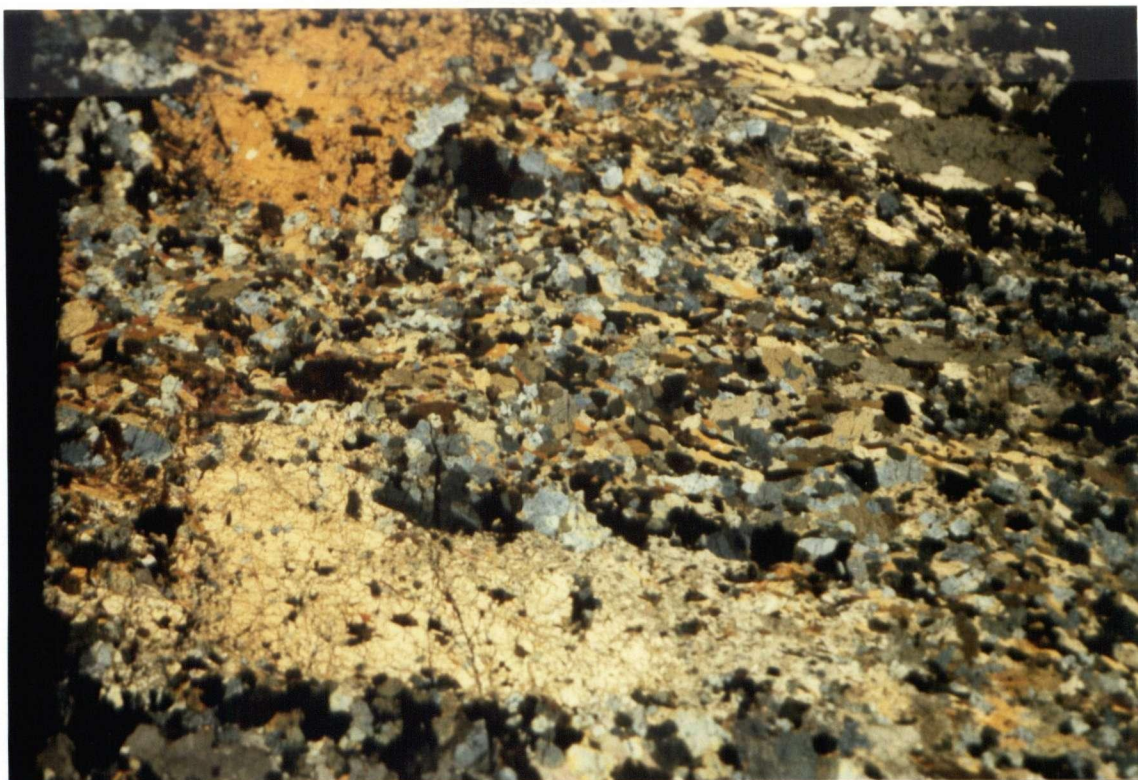
EVENT	DEFORMATION STYLE	MINERAL GROWTH
SYN		
D2		
POST		
SYN		
D3		
POST		

Figure 4-6. Schematic illustration of the timing of garnet growth with respect to deformation episodes and styles in the Snowshoe Group.



┌
└ mm

Figure 4-7. Photomicrograph (x-nicols) of small idioblastic phase 2 type garnets in a Snowshoe Group garnet-biotite muscovite schist. Mica laths outline the S_1/S_2 foliation which is deformed by F_3 crenulations. Phase 2 garnets grew during the latter stages of D_2 and during D_3 .



| mm

Figure 4-8. Photomicrograph (x-nicols) of hornblende crystals which have been altered to epidote and clinozoisite in this calcareous Snowshoe amphibolite. Lenses of these rocks occur extensively throughout calc-silicate metapelites.

The second stage of garnet growth occurred after D_2 . Second generation garnets are characterized by their small size, idioblastic form, low content of random inclusions, and general lack of pressure shadows (Fig. 4-7). These garnets are most commonly found in metapelites adjacent to the Snowshoe-Antler contact and within gneisses in the antiform core zone.

Hornblende:

The crystallization of dark green hornblende as a metamorphic phase in metapelites is generally restricted to small irregular pods situated adjacent to highly calcareous units in the Upper Snowshoe group. Hornblende shows preferred orientation within the S_2 fabric and is deformed by S_3 crenulation cleavages (Fig. 4-8). Hence this phase is considered synkinematic to D_2 deformation.

Table 4-2 presents the relationship between the proposed deformation sequence and mineral paragenesis for Snowshoe Group pelitic rock types.

The following metamorphic reactions most likely account for the formation of prominent phases observed in lower amphibolite-upper greenschist grade Snowshoe Group metapelites.

BIOTITE:*

- (1) stilpnomelane + phengite \rightarrow biotite + chlorite + quartz + H_2O
- (2) stilpnomelane + phengite + actinolite \rightarrow biotite + chlorite + epidote + H_2O

BIOTITE-MUSCOVITE:†

- (3) microcline + chlorite + muscovite (phengitic) \rightarrow biotite + muscovite (less phengitic) + quartz
- (4) muscovite (phengitic) + chlorite \rightarrow biotite + muscovite (less phengitic)
- (5) muscovite + stilpnomelane \rightarrow biotite (Fe-rich) + epidote

GARNET: (almandine)†

- (6) chlorite + biotite + quartz \rightarrow garnet + biotite + H_2O
- (7) chlorite + muscovite + quartz \rightarrow garnet + biotite + H_2O

* Winkler, 1979

† Turner, 1981

MINERAL PHASES		SYN ^{D₁} POST	SYN ^{D₂} POST	SYN ^{D₃} POST	SYN ^{D₄} POST
S N O W S H O E	BIOTITE				
	MUSCOVITE				
	GARNET		_____	-----	
	PLAGIOCLASE		_____	-----	
	HORNBLENDE		_____		

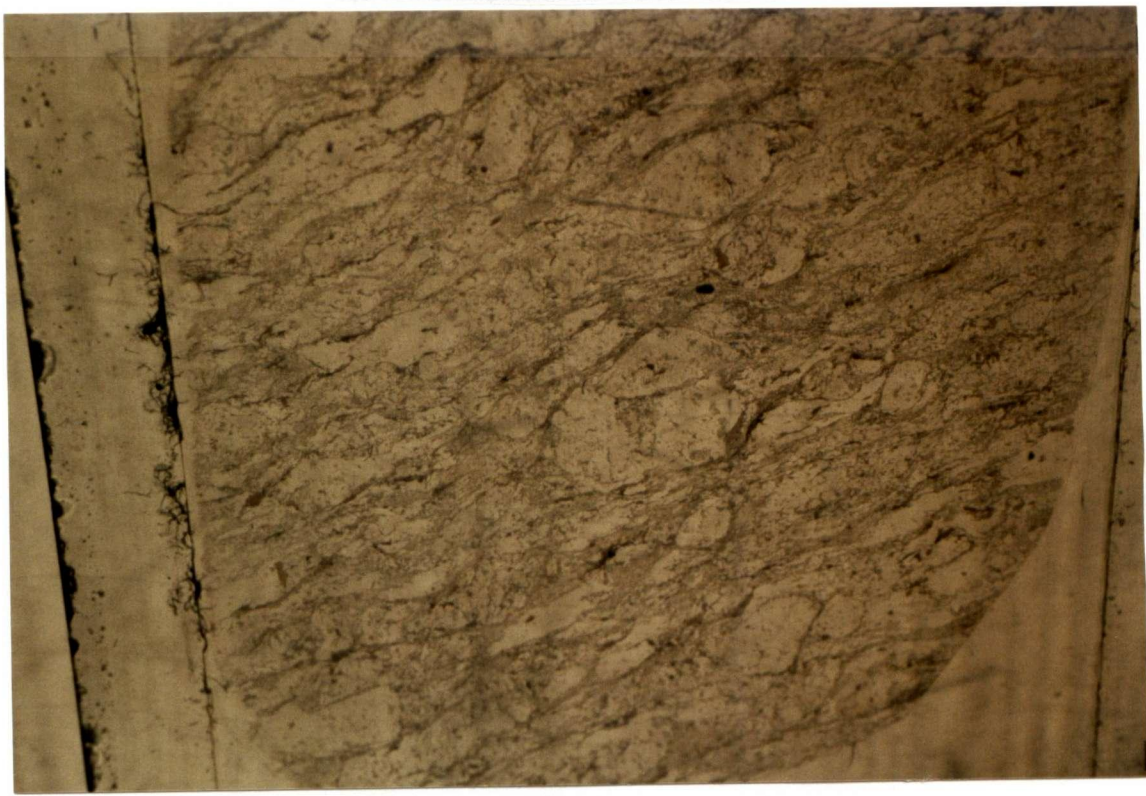
TABLE 4-2

Relation of mineral growth to proposed deformation scheme
in Snowshoe metapelites, Mt. Perseus area, Crooked Lake, B.C

NON-PELITIC ROCK TYPES:Alkali-Feldspar Augen Gneiss

Silicious augen gneiss containing porphyroblasts of anhedral microcline and quartz defines a narrow layer which separates Antler and Snowshoe lithologies. Small laths of muscovite together with quartz and plagioclase (An - 8-27) outline the well developed S_1/S_2 foliation. Quartz is generally strained such that larger grains display distinct dimensional preferred orientation, strongly undulose extinction, subgrain development and serrate grain boundaries. These larger grains occur commonly as flattened augen or porphyroclasts in a matrix of polygonal quartz (Fig. 4-9) of finer grain size (and plagioclase (An $_{10-13}$)). Hence the term mylonite is used. The term porphyroclast is used in describing the augen as these "clasts" appear to have undergone dynamic grain size reduction through shear and flattening processes while in a ductile environment (mylonitization) rather than metamorphic nucleation and growth within the foliation. Flattening features are manifest in the formation of quartz pressure shadows around the augen (Fig. 4-9,10). Rotation of these porphyroclasts is generally small (less than 30°) and is most likely associated with flattening and shear synkinematic to D_2 which continued well into and throughout D_3 .

Textural and mineralogical features within the augen gneiss



1 mm

Figure 4-9. Photograph (plane-light) of a thin section of Snowshoe augen gneiss. Augen are mainly composed of K-feldspar, microcline, and quartz and represent deformed relict porphyroclasts of an early granitic intrusive.

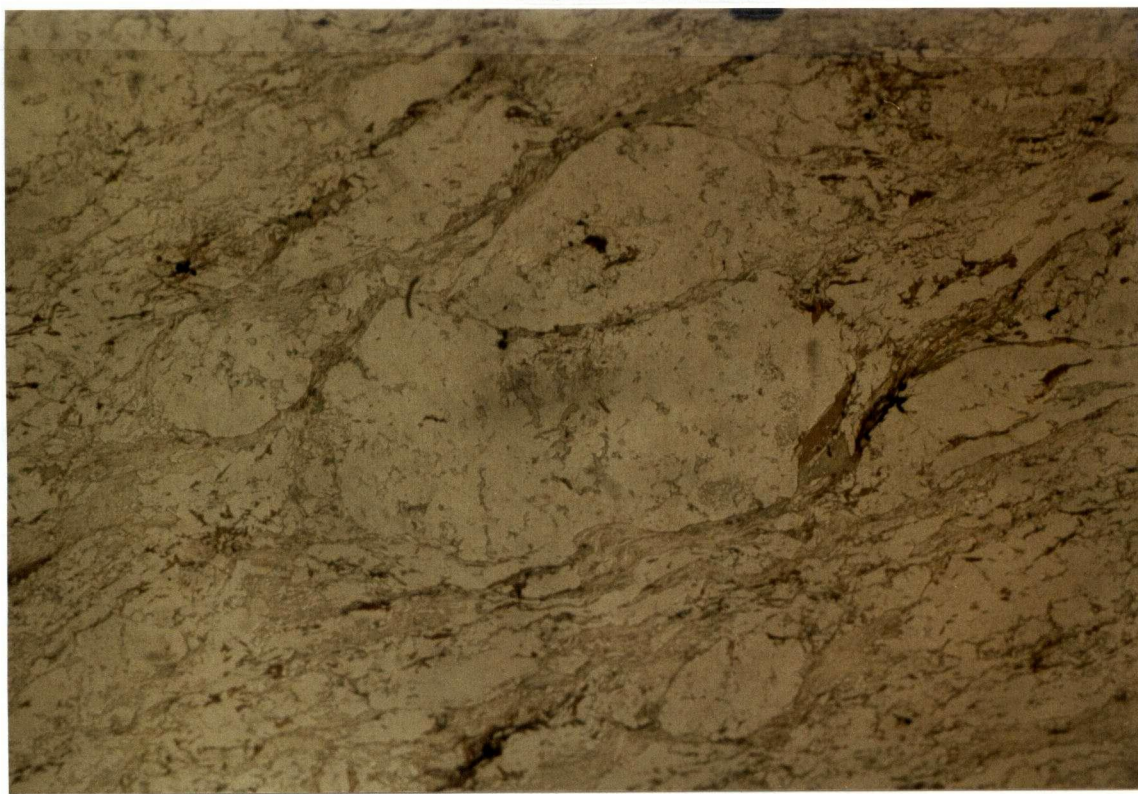
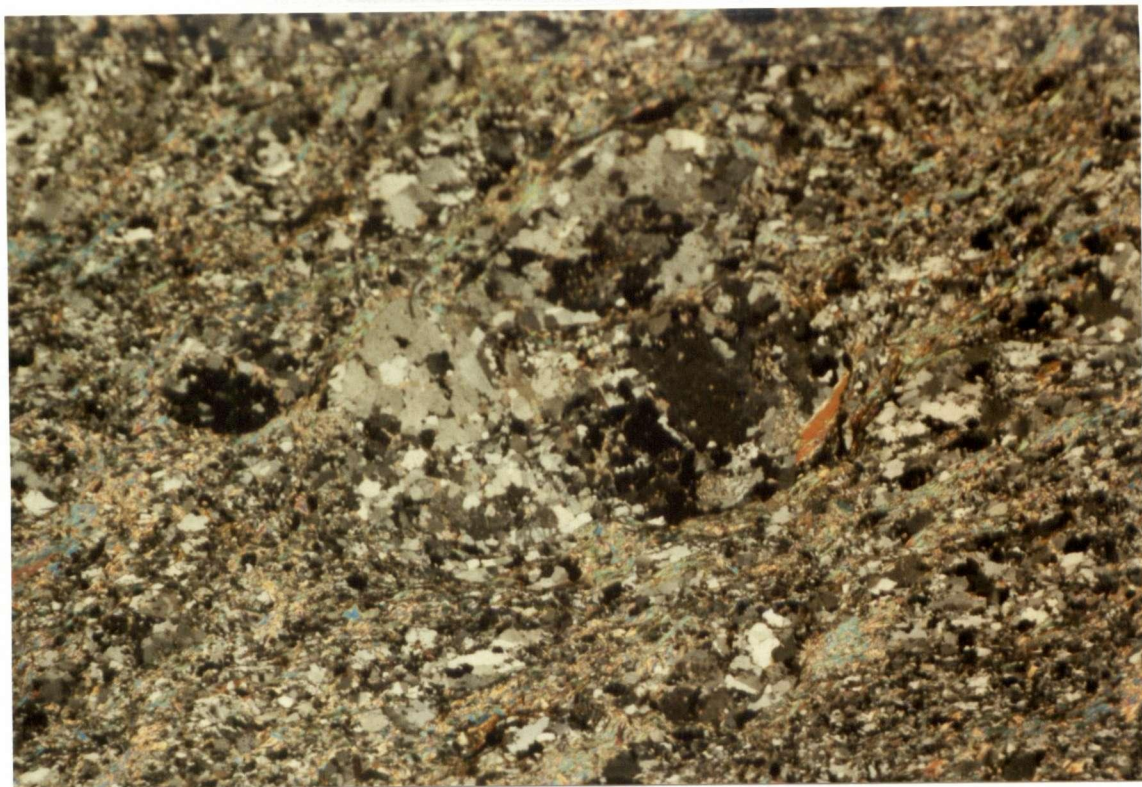


Figure 4-10a. Photomicrograph (plane-light) of figure 4-9 centered on a K-feldspar-quartz augen. The S_2 foliation is flattened around the various porphyroclasts. Quartz grains throughout this rock type have undergone significant dynamic grain size reduction, as shown in figure 4-10b.



1 mm

Figure 4-10b. Cross-nicols view of figure 4-10a which illustrates the highly recrystallized nature of quartz. This sample was subject to mylonitization (dynamic grain size reduction) during D_2 and recrystallization during and after D_3 . Fine grained muscovite (sericite) and quartz outline the S_1/S_2 foliation.

present several possibilities for protolith rock types. From the high abundance of alkali feldspar and quartz one could infer a sedimentary origin with protoliths of feldspathic sandstone or arkosic wacke. Most, if any, stratigraphic indicators have been multiply transposed in the zone of convergence. A possible exception to this may exist in that augen or porphyroclast diameters range in diameter from 3 mm to 15 mm away from the Antler contact. This variance may be interpreted as relict graded bedding which would indicate that protolithic rocks were stratigraphically deposited onto calcareous pelitic rocks of the Upper Snowshoe Group. Problems within this assumption lie in the fact that, firstly, material from presumably underlying calcareous sediments has not been incorporated within the augen gneiss protolith and secondly, one would have to account for a rapid change in the depositional mechanism and source rock to obtain coarse feldspar rich clastics. Similar assumptions would be required to account for carbonate deposition on top of pre-existing feldspathic sandstones. The contact between augen gneiss and calcareous metapelites may also represent a disconformity in which one or the other rock types were deposited at a much later time.

Textural and mineralogical indicators may also support the possibility of an igneous protolith of quartz monzonitic composition which prior to the D_2 deformational event, penetrated Snowshoe Group meta-sediments as a sheet or sill-like intrusive. Mylonitization and recrystallization processes have largely destroyed any evidence of igneous texture. Quartz and alkali feldspar porphyroclasts may

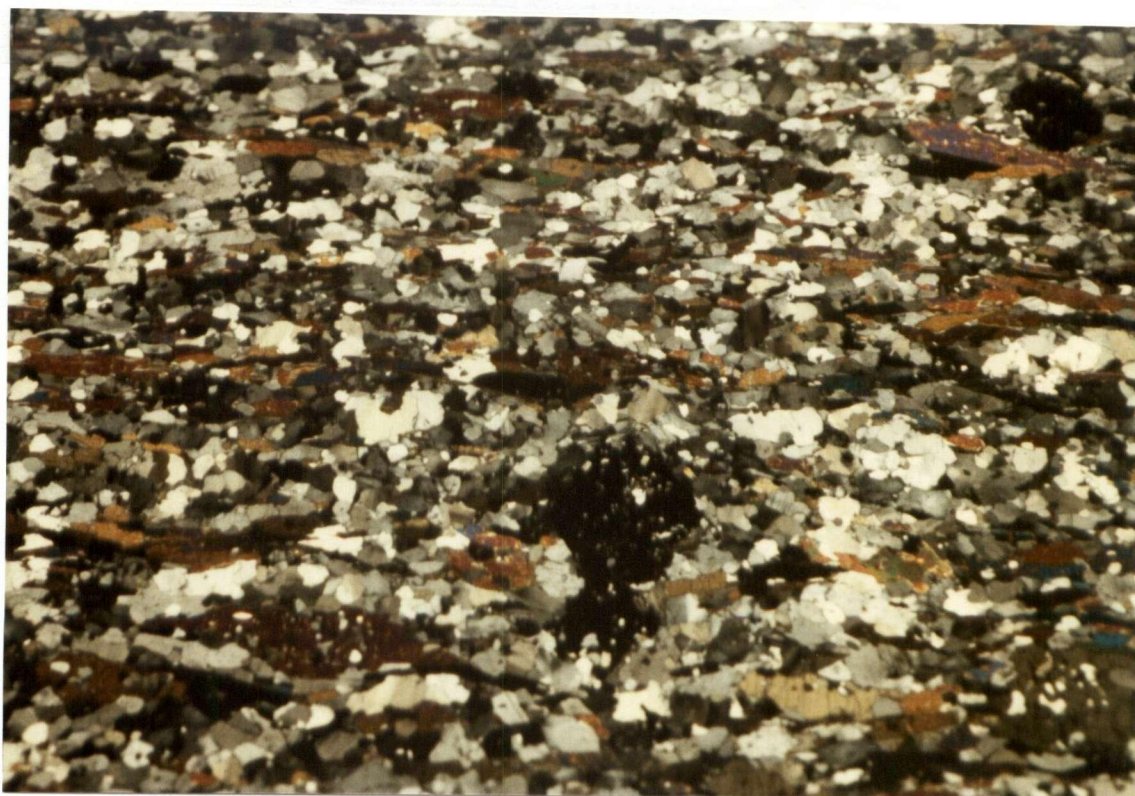
represent relict igneous porphyritic phenocrysts which have been subsequently altered and reduced in grain size through mylonitization. Concordant contact relations with Upper Snowshoe Group meta-pelites may indicate that the proposed intrusive was sill-like in structure as no evidence of discordant relations was found. The contact between the gneiss and underlying metapelites is best described as a zone in which gneiss is ductily intertwined with calcareous garnet-biotite schist. This mixing may well represent simple tectonic intercalation of the two rock types or may be indicative of relict migmatite texture. This type of contact is not seen to exist with Antler amphibolites and is hence interpreted as having possibly resulted from original igneous emplacement. Less deformed rocks of nearly identical composition and texture have been examined to the north of Quesnel Lake, in a similar structural stratigraphic setting adjacent to the Antler Formation. These rocks, interpreted as part of the Quesnel Lake Gneiss (Rees, 1983; Struik, 1984; Montgomery, 1985) have been designated as orthogneiss based upon relict igneous textures and detailed geochemical analysis. Observations within the Mt. Perseus area coupled with the above data most likely support an igneous origin for the alkali-feldspar augen gneiss.

Quartzo-Feldspathic Gneiss

Layered gneiss containing porphyroblasts of garnet and hornblende and porphyroclasts of microcline and quartz defines a poly-deformed layer within the Snowshoe Group. This quartzo-feldspathic rock is

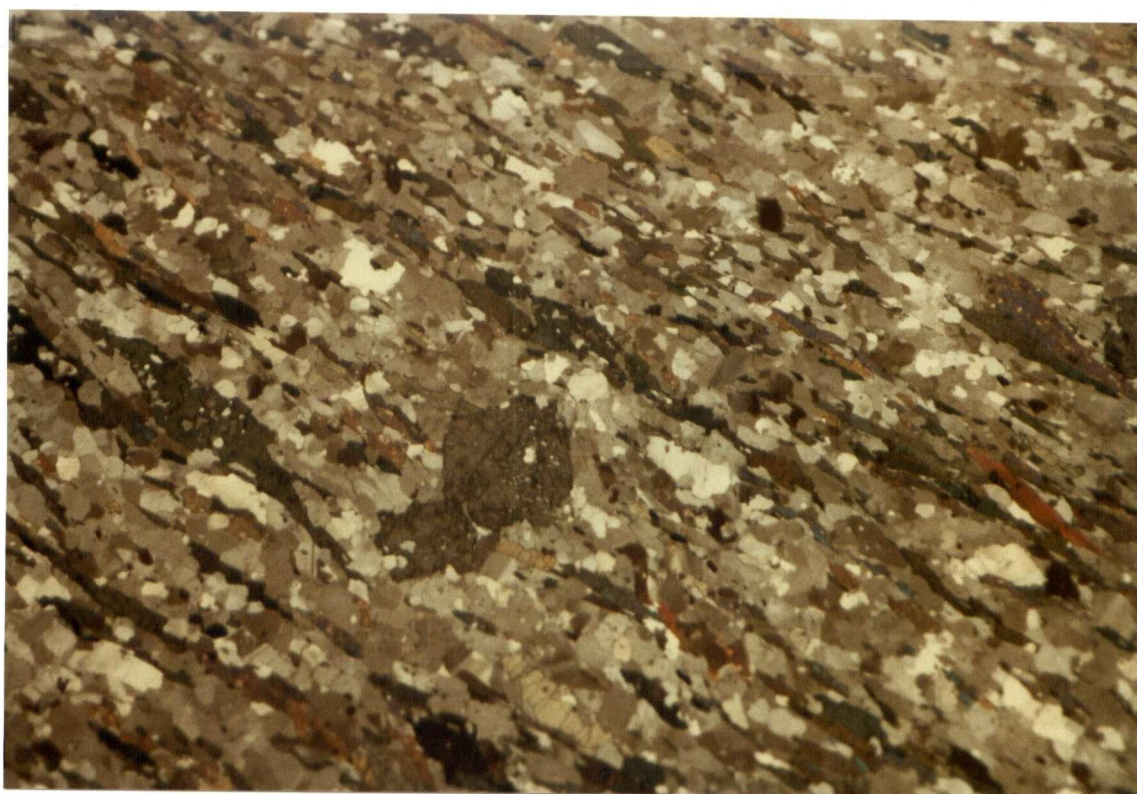
characterized by a granoblastic aggregate of quartz, microcline, plagioclase (An 15-23), hornblende, muscovite, biotite, epidote, chlorite, and sphene which are aligned along and define the S_1/S_2 tectonic fabric (Fig. 4-11). Microcline and quartz porphyroclasts both show signs of recrystallization through grain size reduction of originally larger single grains. Plagioclase porphyroclasts occur as small aggregates within the groundmass and may represent recrystallized remnants of once larger feldspar crystals. Quartz within the matrix is generally strained and exhibits subgrain development with sutured grain boundaries. Many show preferred orientation and optical continuity indicating that they were once part of larger grains. Larger quartz porphyroclasts are strained, show preferred orientation parallel to S_2 , and have serrate grain boundaries. All evidence indicates that microcline, quartz, and plagioclase represent porphyroclasts that have been deformed and recrystallized in a ductile state into smaller grain aggregates.

Porphyroblastic garnets are generally small (less than 1 mm in diameter), idioblastic and contain random inclusions of quartz and biotite (Fig. 4-11). Foliation around these garnets is mildly displaced by signs of flattening. Poorly developed quartz pressure shadows aligned with S_2 flank some garnets though most of the quartz has been highly recrystallized and now obscure most early textures. Crystallization most likely started during the later stages of D_2 and continued during D_3 .



1 mm

Figure 4-11a. Photomicrograph (x-nicols) of the Perseus Gneiss. Location is within the hinge zone of a large phase 2 synform. The groundmass is composed of an equigranular aggregate of strained quartz and feldspar. Larger porphyroblast phases include green hornblende and idioblastic garnet. Hornblende blasts show a preferred orientation within the S_1/S_2 foliation of 30/330.



1 mm

Figure 4-11b. Partially cross-nicols view of figure 4-11a showing detail of the idioblastic garnet form and hornblende alignment along S_1/S_2 .

Hornblende occurs as porphyroblastic laths aligned within the S_1/S_2 foliation (Fig. 4-11,12). Some aggregates show signs of optical continuity through uniform extinction under cross-polarization and are hence interpreted as representing finer grained pseudomorphs after originally larger hornblende crystals associated with the protolith rock type.

Porphyroclastic textures combined with the relatively equigranular nature of this gneiss generate two main protolith possibilities.

Compositionally, the rock could be classified as either a coarse arkosic clastic or as a grano or quartz diorite intrusive. Problems associated with a sedimentary protolith involve source rock origin as the Snowshoe Group is largely composed of pelitic and psammo-pelitic rocks. Rapid changes in sedimentation environment and source material would be required to account for this unique layer of feldspathic presumably arkosic rock. The presence of numerous hornblende porphyroclasts in an arkosic-type sediment are also difficult to explain. Hence, the igneous alternative seems more plausible in this area.

Contact relations with the enveloping metapelites are mostly concordant but in several areas, contacts appear gradational and ambiguous possibly representing relict migmatite texture, since

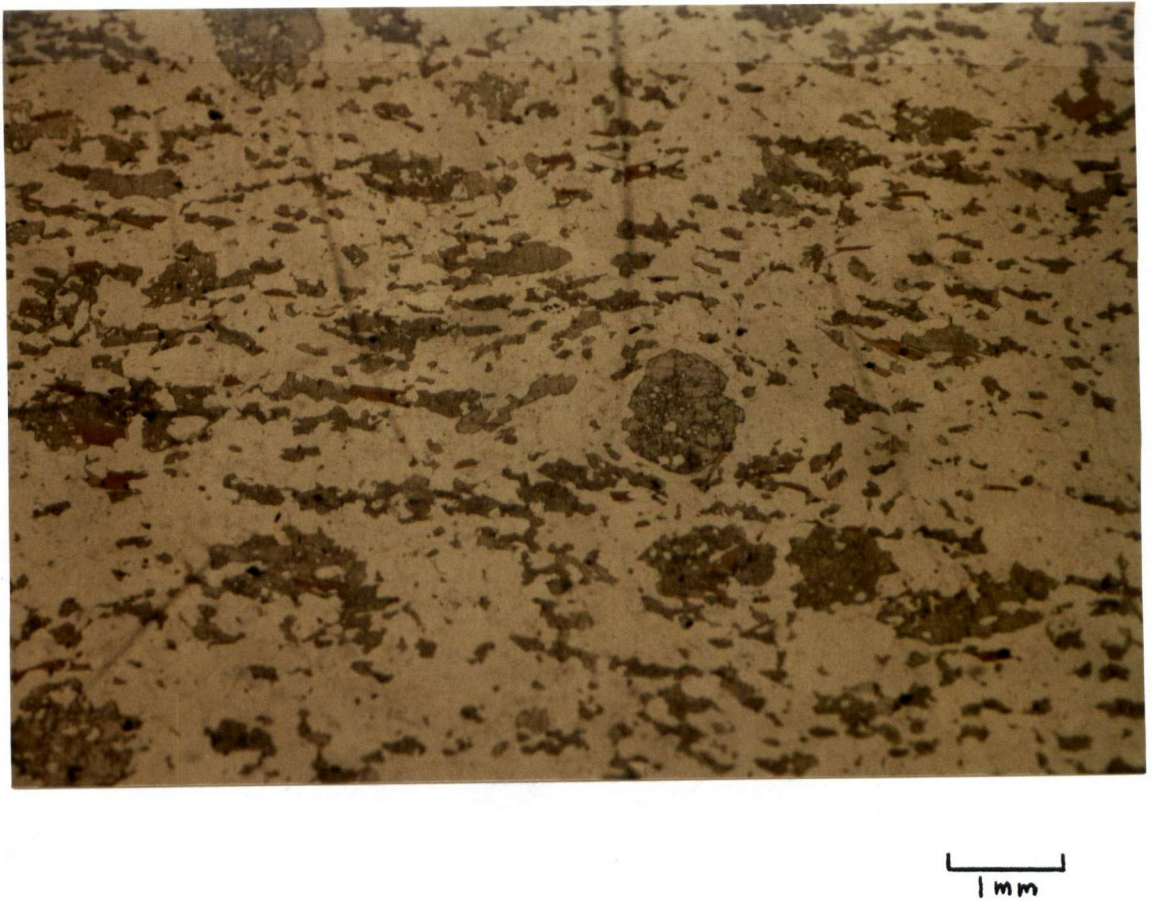


Figure 4-12a. Photomicrograph (plane-light) of the Perseus Gneiss. Garnet porphyroblasts are small, idioblastic, and contain random inclusions. The S_1/S_2 foliation is outlined by green hornblende and biotite and appears displaced around garnets.



1 mm

Figure 4-12b. Photograph (plane-light) of the thin section appearing in figure 4-12a. The photo illustrates the nature of the S_1/S_2 foliation.

subjected to high degrees of shear and flattening. Xenoliths of highly altered country rock have been located in the gneiss adjacent to contact with meta-pelitic rocks.

Composition and texture within the Perseus gneiss is nearly identical to features found in a large adjacent regional gneiss body termed the Quesnel Lake Gneiss (Montgomery, 1985). Structural and geochemical investigations (including trace-element studies) conducted on the Quesnel Lake Gneiss have concluded that the rock is orthogneissic and of grano-dioritic composition. (Rees, 1983; Montgomery, 1985). The Perseus gneiss, apparently located only several thousand feet structurally lower than the Quesnel Lake Gneiss (with respect to the Antler-Snowshoe contact), may represent a relict sill-like off-shoot of this larger quartz-diorite intrusion that has since been structurally isolated through intense shear and flattening processes. The time of emplacement of the Perseus orthogneiss would have been prior to D_1 deformation.

Antler Formation

Mineral assemblages within Antler rocks are indicative of the transition between the middle and upper-greenschist and lower amphibolite metamorphic facies. The contact area between Snowshoe Group and Antler Formations is characterized by strong post deformational annealing and alteration which has rendered ambiguous textures within basal Antler rocks. A majority of the Antler stratigraphy is dominated by lower temperature mineral assemblages than in adjacent underlying Snowshoe metapelites. Pelitic layers within the Antler show no evidence of garnet growth though, chlorite porphyroblasts within these layers may indicate retrograde metamorphic activity. Based upon the difference in phase assemblages between Antler and Snowshoe rocks of pelitic composition and upon the diagnostic greenschist minerals within a majority of the Antler, it seems likely that an isograd separating upper-greenschist and lower amphibolite facies is present in the lower stratigraphy of the Antler. The existence of this isograd is based primarily upon the first appearance of respective mineral phases rather than on a particular metamorphic reaction (i.e. tie line flip). A summary of relevant stratigraphy, metamorphic rock types and typical mineral constituents are presented in Table 4-3.

	STRATIGRAPHIC UNIT	TYPICAL MINERALOGY	PROTOLITH ROCK TYPE
A N T L E R	actinolite-hornblende chlorite schist	actinolite-hornblende + chlorite + albite + sericite + quartz ± biotite ± magnetite ± calcite ± sphene	diabase, basalt (tholeiite) (sills?)
	chlorite-biotite schist	chlorite + biotite + muscovite-sericite + quartz	diabase, basalt (tholeiite) (sills?)
	----- micaceous quartzite	----- quartz + muscovite-sericite + chlorite ± albite ± sphene	----- silicious sub- greywacke
F O R M A T I O N	actinolite-hornblende- chlorite-albite- epidote-schist	actinolite-hornblende + chlorite + albite + epidote + calcite ± quartz ± magnetite ± clinozoicite	diabase, basalt (tholeiite) (sills?)
	actinolite-talc schist	actinolite-tremolite + talc + chlorite + calcite + albitic plagioclase + epidote ± hornblende	gabbro
	actinolite-tremolite- antigorite-talc schist	actinolite-tremolite + talc - antigorite + chlorite + epidote ± hornblende	ultramafic peridotite (?)

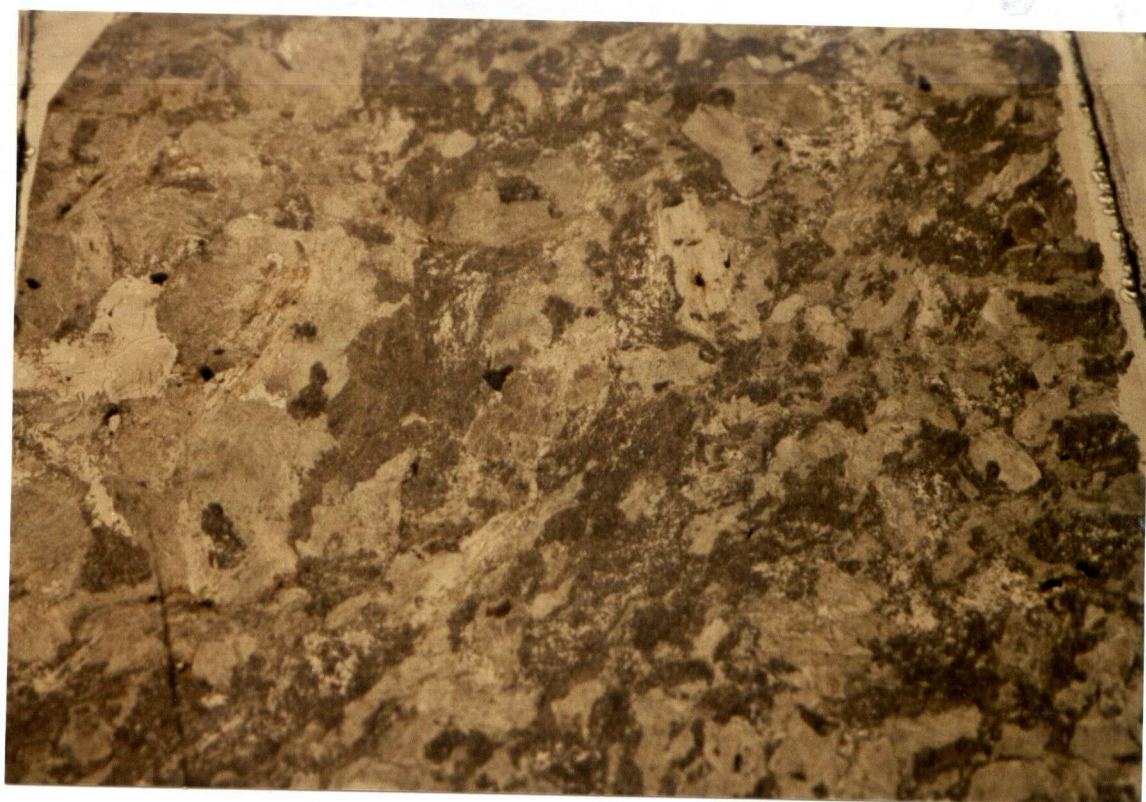
TABLE 4-3

A general lithologic progression exists within the Antler Formation from coarse grained amphibole schists at the Snowshoe Group contact to finer grained chlorite schists and phyllitic rocks adjacent to Upper-Triassic lithologies. The coarse nature and magnesian composition of basal Antler units are interpreted as having resulted from post deformational annealing within the upper-greenschist facies and hydrothermal alteration of mafic-ultramafic igneous assemblages. The remaining Antler stratigraphy is composed of greenschist grade derivatives of calc-alkaline diabase, tholeiitic basalts, and minor intercalations of psammitic rocks.

Basal Actinolite - Tremolite - Talc Schist

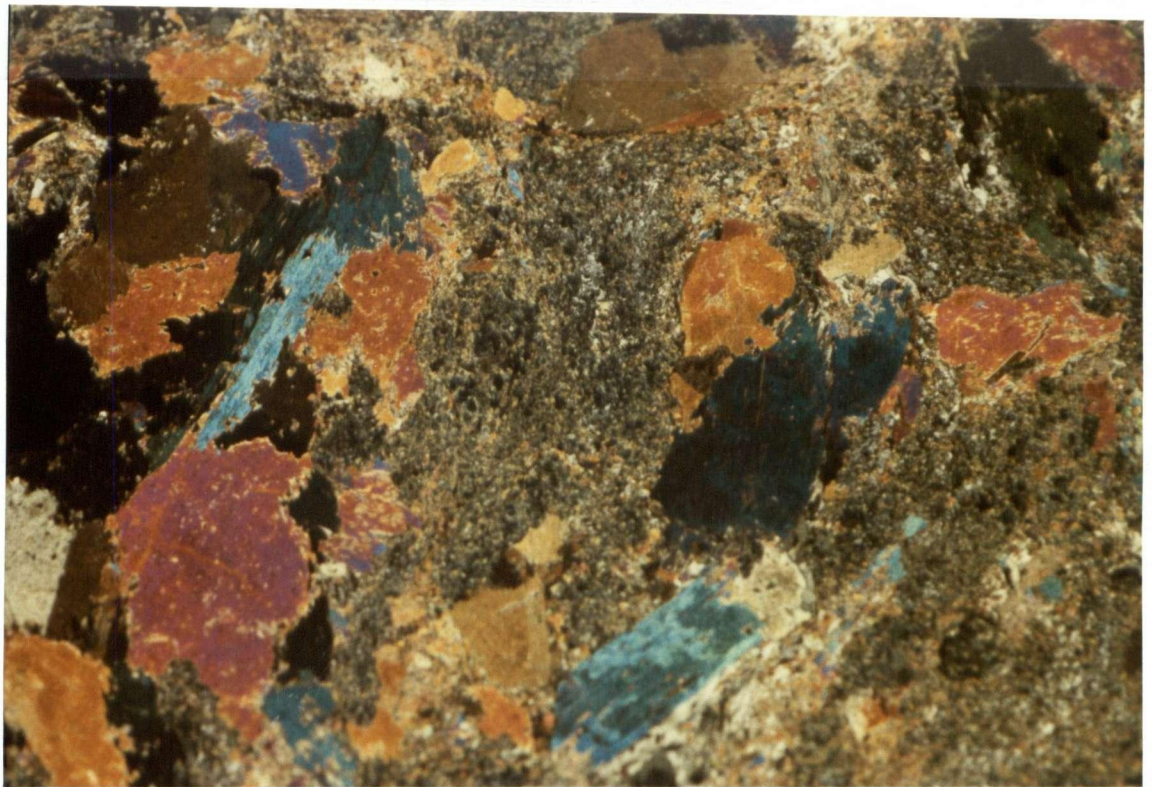
Basal or lowermost units of the Antler Formation within the Mt. Perseus area are composed of coarse-grained schists (almost gneissic) containing assemblages of actinolite-tremolite, talc, chlorite, calcite, antigorite, and albitic plagioclase.

The lowermost layer of the Antler, in tectonic contact with Snowshoe Group mylonites, consists of coarse schist containing large porphyroclasts of pale green actinolite-tremolite randomly oriented in a groundmass of talc, chlorite, albite, calcite, sphene, quartz, and magnetite (Fig. 4-13). Externally this rock is best described as having garbenschiefer texture. Internally, post-deformational recrystallization (annealing) has resulted in an ambiguous texture



1 mm

Figure 4-13a. Photomicrograph (plane-light) of basal Antler Formation actinolite-tremolite schist. Tremolite, actinolite, and talc are coarse and randomly oriented throughout this unit.

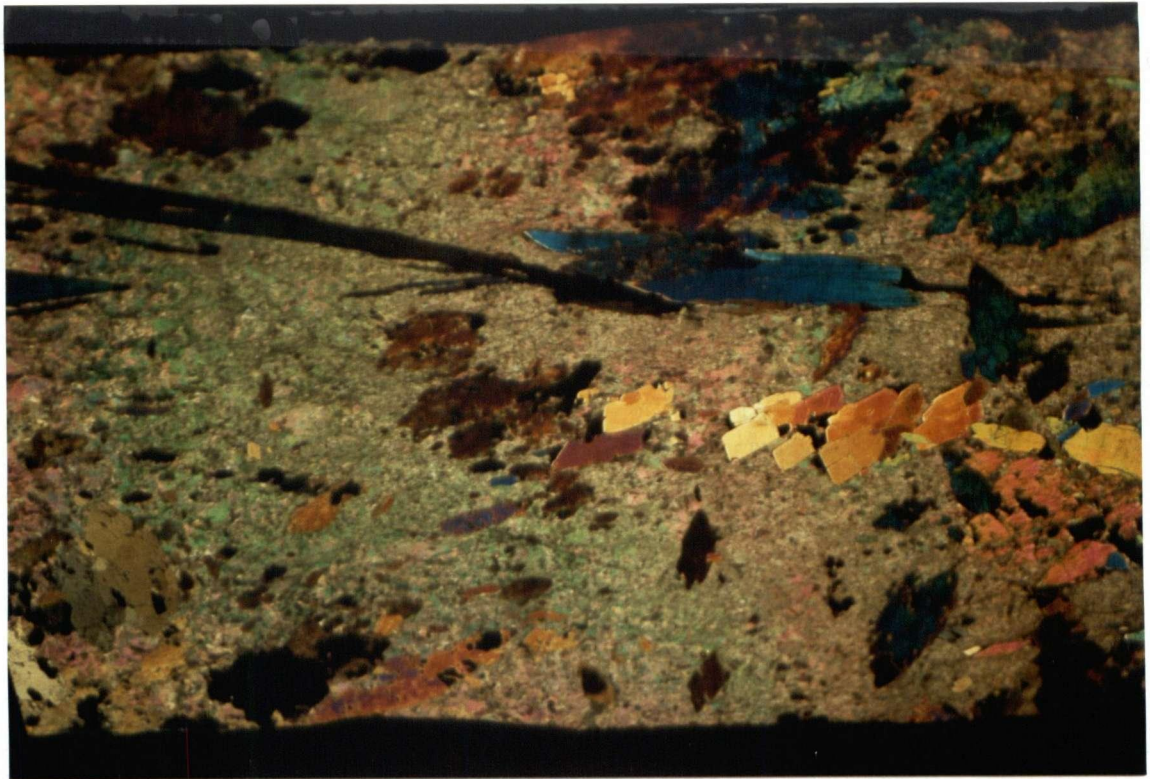


1 mm

Figure 4-13b. Photomicrograph (x-nicols) of Figure 4-13a. "Garbenschiefer" texture is the result of mylonitization and epidote-amphibolite metamorphism during the latter stages of D_2 and shear reactivation, recrystallization, and metasomatism during and after D_3 . Recrystallization outlasted deformation.

showing little or no preferred orientation of mineral constituents. Adjacent to the contact between this unit and Snowshoe Group augen gneiss, small minor pods of extremely coarse grained actinolite-tremolite-antigorite-talc schists crop out randomly (Fig. 4-14). Compositionally, these rocks are similar to the enveloping schist with the exception of the presence of antigorite, a metamorphic derivative of original olivine. The amphibole phase occurs often as massive radiating splays with individual actinolite-tremolite crystals attaining lengths of up to 24 centimeters.

Both rock types display magnesian compositions derived by metamorphism and hydrothermal alteration (carbon dioxide metasomatism) of mafic-ultramafic rocks with gabbroic-peridotitic compositions. Assemblages observed within these lowermost Antler units are indicative of metasomatic transformation involving large volumes of carbon dioxide (Turner, 1981). This would have most likely occurred indirectly as a result of metamorphic dehydration of overlying Snowshoe carbonate metapelites in which carbonate-rich fluids may have been present in large quantities adjacent to lower Antler stratigraphy. During subsequent metamorphism these fluids would have been involved in Antler metamorphic activity. Amphibole phases are most likely pseudomorphic after clinopyroxene and the presence of chlorite (prochlorite) and actinolite is probably controlled by the reaction:



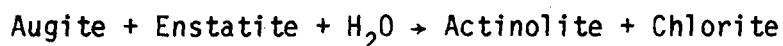
┌
└ 1mm

Figure 4-14a. Photomicrograph (x-nicols) of actinolite-tremolite-antigorite-talc schist of the lowermost Antler unit. The groundmass is composed almost exclusively of talc and calcite and contains larger randomly oriented porphyroblasts of tremolitic and actinolitic amphibole. Antigorite phases are less pronounced and constitute a small percentage. The "garbenschiefer" texture resulted from post-deformational annealing and alteration.



1 mm

Figure 4-14b. Magnified view of Figure 4-14a which shows an interesting "en-echelon" growth of tremolite twins within the talc-carbonate groundmass. The present configuration of these twins is most likely the result of flattening during the latter stages of metamorphism, which permitted twin gliding along their respective twin planes. Subsequent recrystallization and annealing has destroyed any earlier textures.



The presence of calcite-dolomite probably resulted from the breakdown of calcic plagioclase components in the protolith. Metamorphic reactions (simplified) in the following table list other possible assemblage combinations resulting from greenschist grade metamorphism of ultramafic minerals.

REACTIONS*	RESULTING ASSEMBLAGE
1) olivine + SiO_2 + H_2O \rightarrow antigorite (-MgO)	antigorite
2) antigorite + SiO_2 \rightarrow talc (-MgO)	antigorite-talc
3) olivine + SiO_2 + CO_2 + H_2O \rightarrow antigorite + talc + magnesite (-MgO)	antigorite-talc-carbonate
4) antigorite + CO_2 \rightarrow talc + magnesite (- H_2O)	
5) antigorite + CaO + CO_2 \rightarrow talc + domomite (-MgO)	talc-carbonate
6) talc + CO_2 \rightarrow magnesite + quartz (- SiO_2)	
7) talc + CaO + CO_2 \rightarrow dolomite (-MgO - SiO_2)	quartz-carbonate
8) antigorite + CO_2 \rightarrow magnesite + quartz (- SiO_2)	

* Williams, Turner and Gilbert, 1954

Actinolite - Hornblende - Chlorite - Albite - Epidote - Calcite Schist

Green medium to fine grained foliated actinolite-hornblende chlorite schist overlies lowermost actinolite-talc garbenschiefer of the Antler Formation. In outcrop, the schist is recognized by a well developed light colored mineral lineation outlined by chlorite and albite contained within the flattened S_2 metamorphic foliation. Mineral assemblages consist of porphyroblastic actinolite-hornblende contained within a well developed S_2 foliation outlined by chlorite, xenoblastic albitic plagioclase, epidote, xenoblastic calcite, and quartz. Accessory minerals include sphene and magnetite. Actinolite porphyroblasts, flanked by chlorite-quartz-albite pressure shadows, show rotation within the flattened foliation of up to 45 degrees. Small oriented laths of epidote occur throughout the foliation and often appear concentrated around actinolite-hornblende crystals. Quartz is mostly confined to small discontinuous layers and is generally strained displaying only moderate subgrain development. In thin sections oriented perpendicular to the foliation and dominant mineral lineation, S_2 is folded and crenulated by S_3 microfolds with minor chlorite crystallization along its cleavage trace. In several localities, L_3 intersection lineations overprint the main penetrative mineral lineation. This would indicate that the mineral lineation was developed parallel to F_2 fold hinges, though no evidence of relict folds were seen within thin section.

Compositionally, the typical mineral assemblage within this rock

type is most likely the product of metamorphism of basic igneous rocks. Actinolite-hornblende are probably pseudomorphic after pyroxene and calcite from relict calcium feldspars.

Reactions controlling the formation of actinolite and hornblende are governed by the following (Winkler, 1976):

ACTINOLITE:

- (1) augite + enstatite + H_2O \rightarrow actinolite + chlorite
- (2) pumpellyite + chlorite + quartz \rightarrow clinozoicite + actinolite

HORNBLENDE:

- (3) actinolite + clinozoicite + chlorite + quartz \rightarrow hornblende

The presence of coexisting actinolite-hornblende, epidote and calcite place this rock with the upper-greenschist facies and possibly within a zone of transition between the lower amphibolite and upper-greenschist facies (Turner, 1981; Mason, 1978). Composition may infer protoliths such as oversaturated calc-alkaline diabase and basalt, spillitic diabase, gabbro, and possibly a tholeiite derivative. The stratigraphic association with the underlying magnesian meta-ultramafic

indicates that this lower portion of the Antler is dominated by extremely mafic igneous stratigraphy similar to alpine-type ophiolite complexes such as those described within the Antler Formation further to the south adjacent to Dunford Lake (Montgomery, 1978).

The remainder of the Antler Formation consists of irregular layers and lenses of chlorite schist, sericite-muscovite schist, hornblende-actinolite-chlorite schist, chlorite biotite schist, micaceous quartzite, meta-pillow basalt (now greenstone), and argillite.

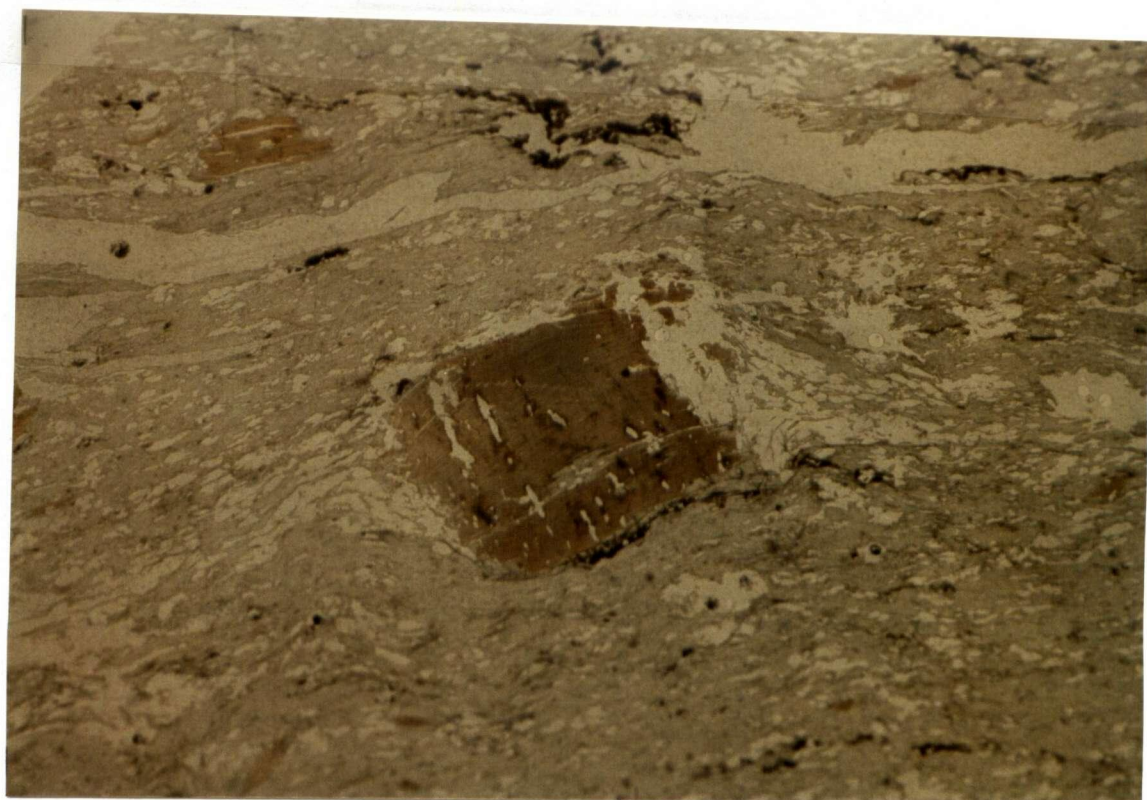
Typical hornblende-actinolite-chlorite schists are fine grained and composed of porphyroblastic hornblende-actinolite aligned in a matrix of chlorite, albitic plagioclase (untwinned), sericite, quartz, biotite, magnetite, calcite and sphene. Amphibole, chlorite and sericite are aligned and define the main S_2 foliation. Intense flattening effects have displaced the fabric around amphiboles and some larger chlorite porphyroblasts. Quartz occurs as small strained polygonal grains in pressure shadows flanking both amphibole and chlorite porphyroblasts and in small discontinuous layers parallel to S_2 . No optical continuity was observed in these grains. Microfabrics associated with F_3 folding are characterized by small warps and crenulations of the existing S_2 foliation. Small laths of muscovite define S_3 though most often, little mineral growth was observed along the S_3 plane. Rocks of the above composition most likely represent middle greenschist facies equivalents of oversaturated calc-alkaline diabase and/or basalt. Amphibole phases are most likely pseudomorphic

after pyroxene while chlorites represent pseudomorphs and alteration products after original amphibole and/or mica.

Chlorite-biotite schist is characterized by porphyroblasts of brown biotite set in a fine grained assemblage of chlorite and muscovite-sericite which together with small layers of strained quartz, outline the prominent S_2 transpositional foliation. Accessory minerals include magnetite and sphene. Rocks of this composition within the central portion of the Antler contain chlorite altered biotite porphyroblasts (up to 3 mm) which contain relict S_2 internal schistosity that has been rotated up to 90° relative to the external S_3 foliation ($S_0/S_1=S_3$) (Fig. 4-15). Thus peak metamorphism appears synkinematic to D_2 . Pressure shadows of fine grained strained quartz and muscovite-sericite flank biotite porphyroblasts and are interpreted as having formed in response to flattening and shearing associated with D_3 . Chlorite-biotite schists adjacent to the Antler-phyllite contact contain chlorite-altered biotite porphyroblasts which have been shredded and drawn out along their respective cleavages within S_2 (Fig. 4-16). Relict elongate pressure shadows contain fine grained polygonized strain-free quartz which in places show optical continuity and have therefore recrystallized from once larger grains. Small layers and lenses of quartz not associated with pressure shadow development are characterized by small ribbon grains and aggregates of smaller polygonized nearly strain-free quartz, all showing optical continuity.

Pelitic assemblages within the Antler consist mainly of small layers and lenses of fine grained micaceous quartzite and argillic phyllonite. Internally, layers of highly recrystallized-polygonized quartz are folded and often outline F_2 intrafolial microfolds within S_2 (Fig. 4-17). Muscovite and sericite are aligned parallel to the foliation and appear folded about F_2 . Small laths of pseudomorphic chlorite (after biotite) are similarly aligned within S_2 . Plagioclase of albitic composition (An_{8-15}) occurs in minor amounts throughout this rock type with minor amounts of sphene, apatite, and carbonaceous material present as accessories. The presence of garnet was not detected anywhere throughout rocks of this composition in the Antler and based upon the quartz-muscovite-chlorite-albite assemblage, it seems likely that the metamorphic grade did not exceed the middle greenschist facies. Parent rock types for these pelitic assemblages probably include silicious subgreywacke and argillaceous quartz sandstone. Relationships between mineral phases and the proposed deformation sequence are presented in Table 4-4.

Rock types within the Antler, though varied in composition, outline a general metamorphic transition from the albite-epidote amphibolite facies (upper-greenschist) within rocks adjacent to the lower amphibolite grade Snowshoe to the middle-lower greenschist within structurally higher Antler lithologies. Mineral assemblages also delineate a compositional change in the Antler from predominantly mafic-ultramafic (magnesian) rocks situated at the structural base of the exposed formation to a less mafic (Fe -rich) nature in central and



1 mm

Figure 4-15a. Photomicrograph (plane-light) of a rotated biotite porphyroblast in an Antler Formation chlorite-biotite schist. Relict internal schistosity ($S_0=S_2$) has been rotated approximately 90° relative to the external S_3 foliation ($S_2=S_3$).



1 mm

Figure 4-15b. Cross-nicols view of 4-15a showing the highly recrystallized nature of the groundmass (quartz, chlorite, muscovite-sericite).

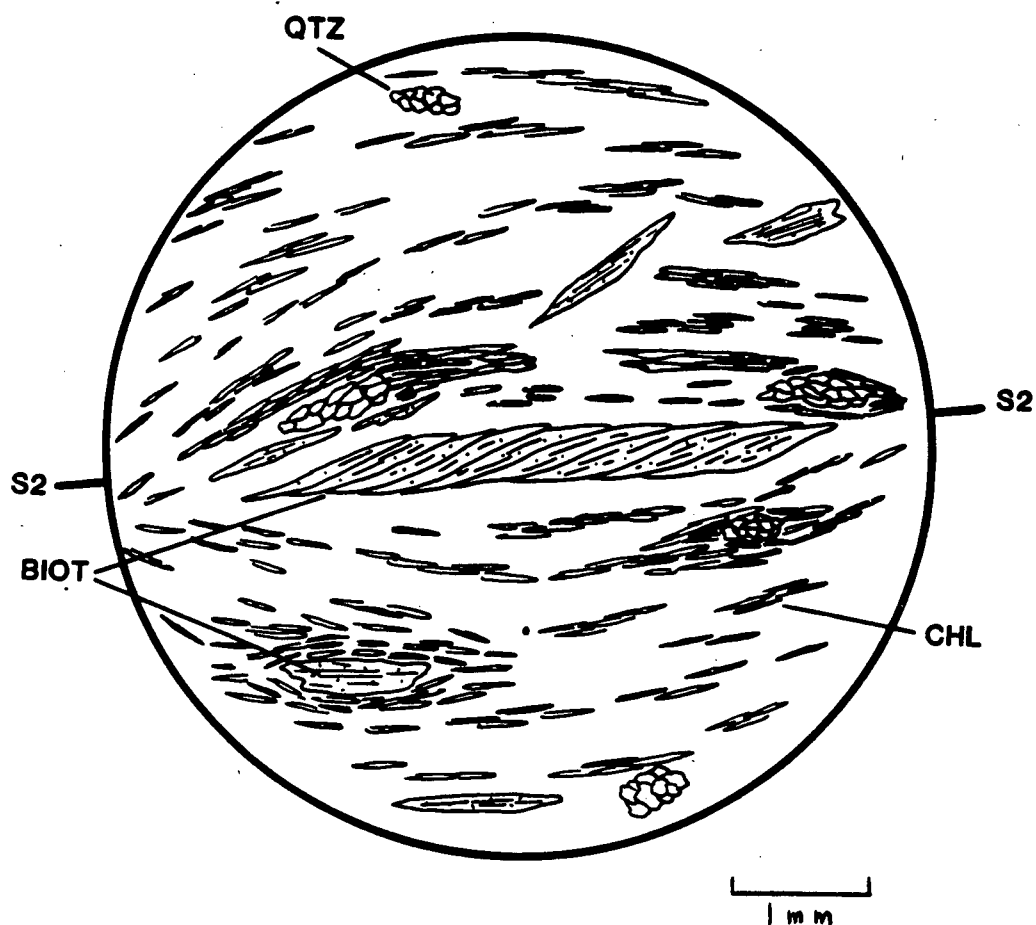
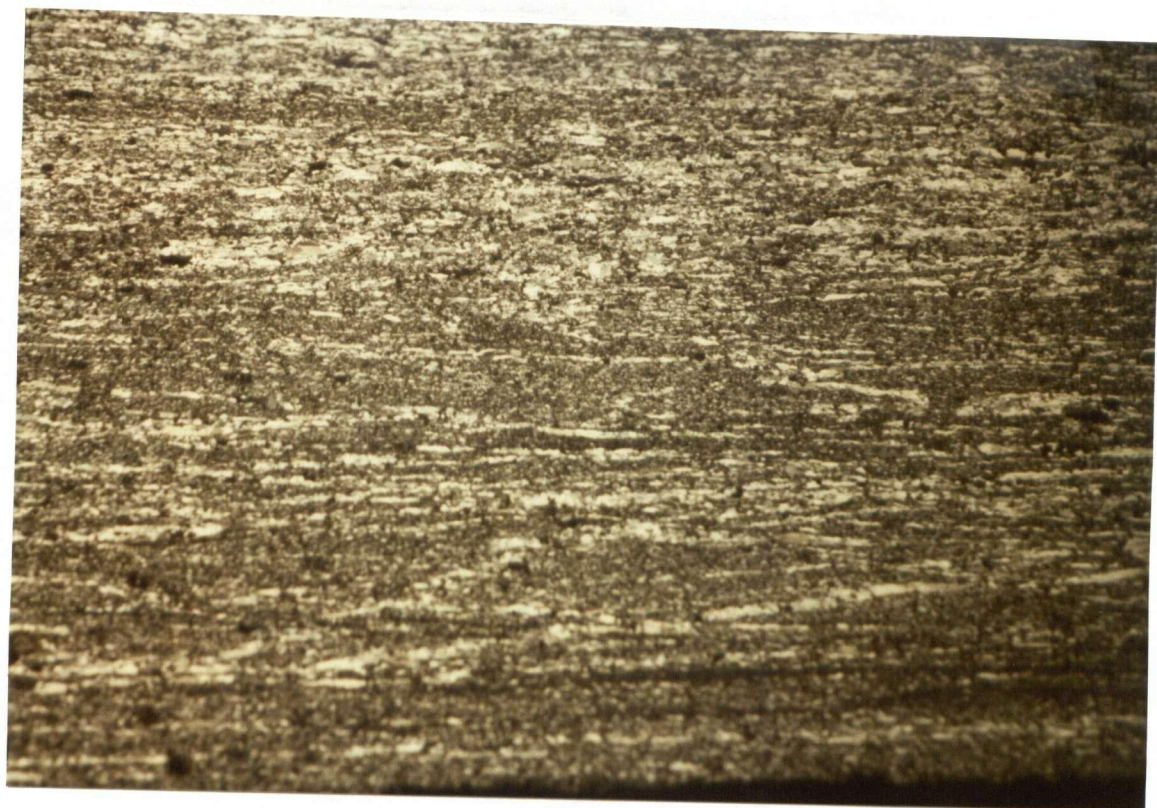


Figure 4-16. A sketch of a thin section of an Antler chlorite-biotite schist. Porphyroblasts of chlorite altered biotite have been shredded and drawn-out along their respective cleavages within the S_2 foliation.



┌
└ 1 mm

Figure 4-17a. Photomicrograph (plane-light) of folded rootless compositional layers within a micaceous quartzite of the Antler Formation. Microfolds are of the F_2 generation and deform S_0 compositional layers composed of highly recrystallized quartz and muscovite-sericite.



┌
└ 1 mm

Figure 4-17b. Cross-nicols view of Figure 4-17a. Microfolds serve to illustrate the transposed and recrystallized nature of the S_2 foliation.

upper stratigraphy. Microtextures indicate that peak metamorphism was synkinematic with D_2 and progressively waned during and after D_3 . Few post-deformational phases are present though post-deformational annealing is strongly developed in the lower portions of the Antler.

The formation of mylonites is largely related to D_2 and is mostly restricted to narrow zones adjacent to the formation's tectonic contacts. Lower-most units of the Antler appear most strongly deformed and annealed and thus represent a zone in which high strain was accommodated during the convergence of Quesnellia on to the Omineca terrane. Further deformation (D_3) associated with the folding of this convergent zone, was accommodated in part along this tectonic boundary and in the formation of small widespread subsidiary mylonite zones related to F_3 fold geometry.

This structural assemblage and succession of meta-igneous stratigraphy are similar in many respects to alpine-type ophiolite complexes observed in other orogenic belts. Interpretation of this nature would infer that the Antler Formation represents a slice of oceanic floor rock structurally emplaced (obducted) via low angle thrusting onto deformed continentally derived stratigraphy through the tectonic convergence of Omineca and Quesnellia terranes. Further discussion regarding this will be presented in the following chapter.

MINERAL PHASES		SYN ^{D₁} POST	SYN ^{D₂} POST	SYN ^{D₃} POST	SYN ^{D₄} POST
A N T L E R	BIOTITE		_____	_____	_____
	MUSCOVITE		_____	_____	_____
	CHLORITE		_____	_____	_____
	ACTINOLITE- TREMOLITE		?—?	_____	_____
	ACTINOLITE- HORNBLENDE		?—?	_____	_____
	CALCITE		_____	_____	
	TALC		_____	_____	

TABLE 4-4

Relation of mineral growth to proposed deformation scheme
in the Antler Formation, Mt. Perseus area, Crooked Lake, B.C.

Upper-Triassic Formation

Un-named Upper-Triassic graphitic phyllites and psammitic schists comprise the structurally highest formation within the confines of the Mt. Perseus area. They appear mostly concordant in both contact and metamorphic fabric with underlying Antler Formation and Snowshoe Group rocks. The lowermost or basal unit of the Upper-Triassic assemblage consists of thin pelitic layers of recrystallized quartzitic mylonite and graphitic phyllonite. Overlying pelitic units are composed of calcareous graphitic schist and graphitic phyllite which contain minor lenses of fine grained chlorite schist. Mylonitic versions of these rocks occur variably spaced in narrow shear zones related to D_3 folding.

Mineral assemblages within these units are indicative of the lower greenschist facies. The primary metamorphic fabric observed within the phyllites represents a transpositional foliation oriented parallel to compositional layering, formed during phase-two regional deformation (equivalent to the first deformational phase within Antler and Upper-Triassic rocks). Third phase deformation has produced an ubiquitous spaced cleavage related to disharmonic folds formed in both ductile and brittle environments. Phyllitic rocks also contain numerous quartz-filled hydraulic fractures, now folded by F_2 and F_3 and probably represent features associated with initial de-watering and pressure solution. Table 4-5 presents a summary of relevant stratigraphy, metamorphic rock types and typical mineral constituents.

	STRATIGRAPHIC UNIT	TYPICAL MINERALOGY	PROTOLITH ROCK TYPE
U P P E R - T R I A S S I C F O R M A T I O N	upper unit: graphitic phyllite	muscovite-sericite + quartz + graphite ± chlorite + plagioclase (albitic) ± biotite ± spinel	argillaceous mudstone, fine grained sandstone

	chlorite schist greenstone	chlorite + muscovite- sericite + quartz ± plagioclase ± (An ₁₀₋₂₀) ± sphene	fine grained basalt
	middle unit: calcareous graphitic schist	muscovite-sericite + calcite- dolomite + quartz + graphite ± plagioclase (albitic) + biotite ± spinel	calcareous mudstone
	lower unit: graphitic sericite schist	muscovite-sericite + graphite + quartz ± plagioclase (albitic) ± calcite ± biotite ± spinel	argillaceous mudstone
	graphitic phyllonite	muscovite + quartz + graphite + chlorite ± spinel	argillaceous mudstone

	micaceous quartzite mylonite	quartz + muscovite-sericite + calcite + chlorite ± biotite ± opaques	impure sandstone

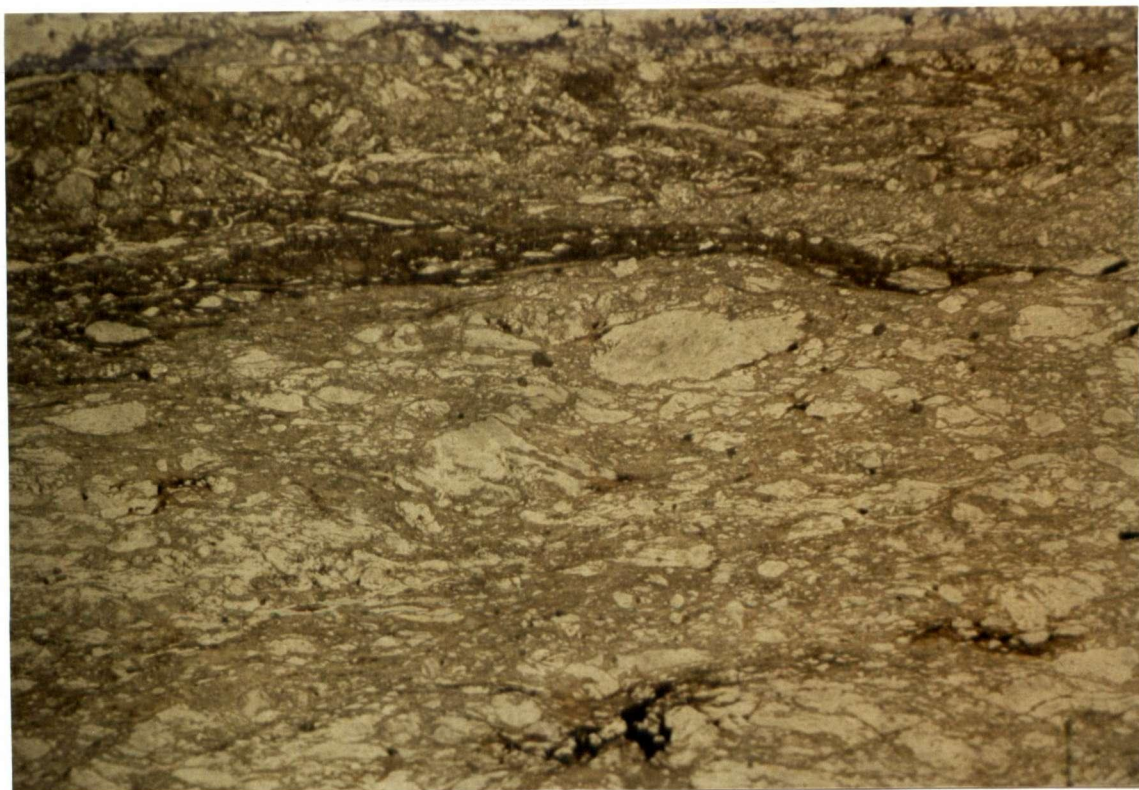
Table 4-5

Basal Quartzite Mylonite

Golden tan to light grey fine grained micaceous quartzite mylonite and minor graphitic phyllonite form the lowermost layer within the Upper-Triassic formation. Quartz and fine grained muscovite-sericite outline the S_2 foliation. Quartz occurs as highly strained individual grains exhibiting up to 100:1 elliptical elongation ratios parallel to the foliation (Fig. 4-18). These ribbon grains and other porphyroclasts are commonly situated in a mass of more fine-grained essentially strain free quartz subgrains. Most subgrains exhibit a dimensional preferred orientation and therefore indicate that they are

Muscovite-sericite occur as small laths and along with minor chlorite (after biotite) define S_2 . Fine grained laths of biotite, when not altered to chlorite are aligned primarily within S_2 though several samples contained large masses of biotite porphyroblasts which have overgrown muscovite within the S_3 cleavage plane. Plagioclase occurs as small irregular laths of An_{7-15} composition. Poikilitic K-feldspar and grains of calcite are found as minor constituents throughout this rock type.

Graphitic phyllonite is confined to small layers and lenses within the quartzite mylonite and is composed largely of quartz and muscovite/sericite with intercalations of carbonaceous material (Fig. 4-19). The



1 mm

Figure 4-18a,b,c. Photomicrographs (plane-light) of basal micaceous quartzite of the Upper Triassic assemblage. The prominent S_2 foliation is mylonitic and is outlined by individual quartz layers and ribbon grains. Several ribbon grains have elongation ratios in excess of 100:1. Mylonitization processes were initiated during the latter stages of D_2 and continued during D_3 . Recrystallization processes outlasted deformation.



Figure 4-18b.

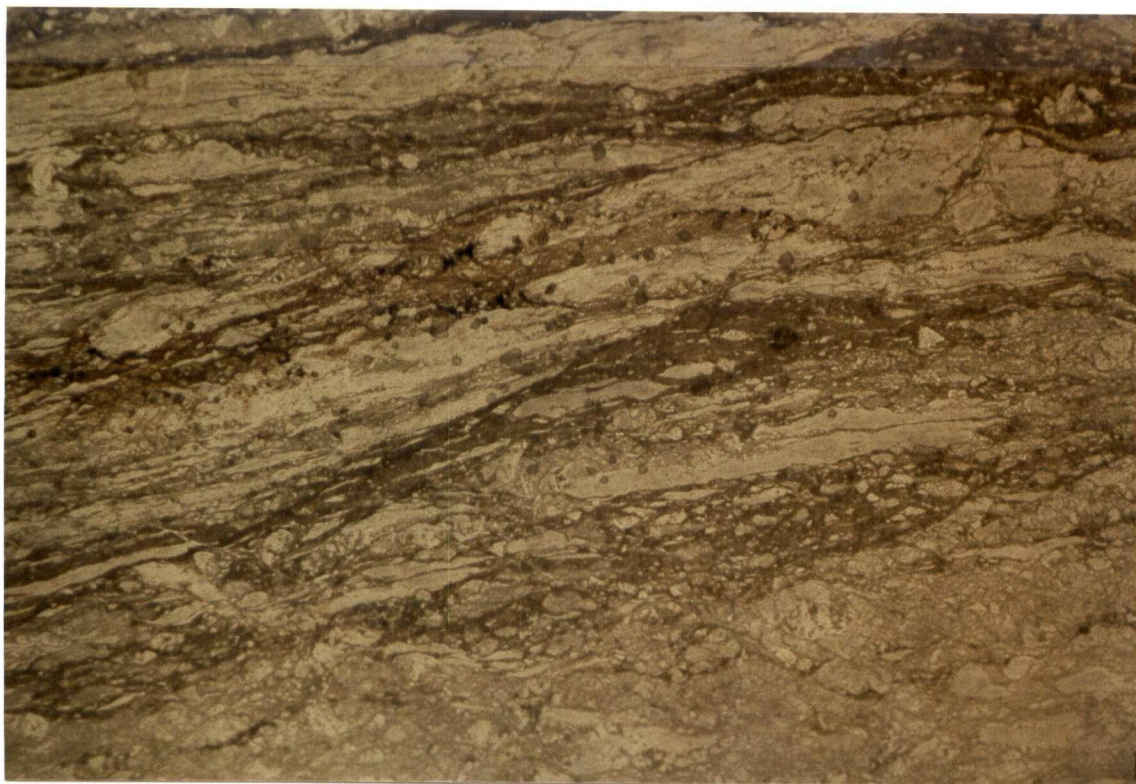


1 mm

Figure 4-18c.


1 mm

term phyllonite is used in that this rock type is largely recrystallized and has a mylonite fabric related to D_2 similar to overlying phyllites.

Mylonitic fabrics within this unit indicate that strong ductile shearing was active during D_2 . This may indicate that the present stratigraphic position of the phyllites may in large be the result of tectonic emplacement onto Antler rocks via low angle thrusting synkinematic to D_2 . Mylonites may also infer that a stratigraphic contact existed between Antler and phyllitic rocks prior to the tectonic convergence and was subjected to subsequent mylonitization during and after the convergence of the two terranes.

Lower Unit

Graphitic muscovite-sericite schist and minor argillite comprise the lower stratigraphic unit within the Upper Triassic formation. These rocks are typically dark grey to black and contain a well developed metamorphic foliation subparallel in orientation to S_2 foliation attitudes present within underlying Antler rocks. Fine grained muscovite-sericite outline the S_2 fabric in the phyllites along with layers and lenses of graphitic material and fine grained pods of recrystallized quartz. Phase-3 microfolds (buckle folds) deform the muscovite-sericite, graphitic material and quartz lenses (Fig. 4-20), hence, primary metamorphic crystallization was active primarily during the latter stages of D_2 . Hydraulic fractures filled with quartz are

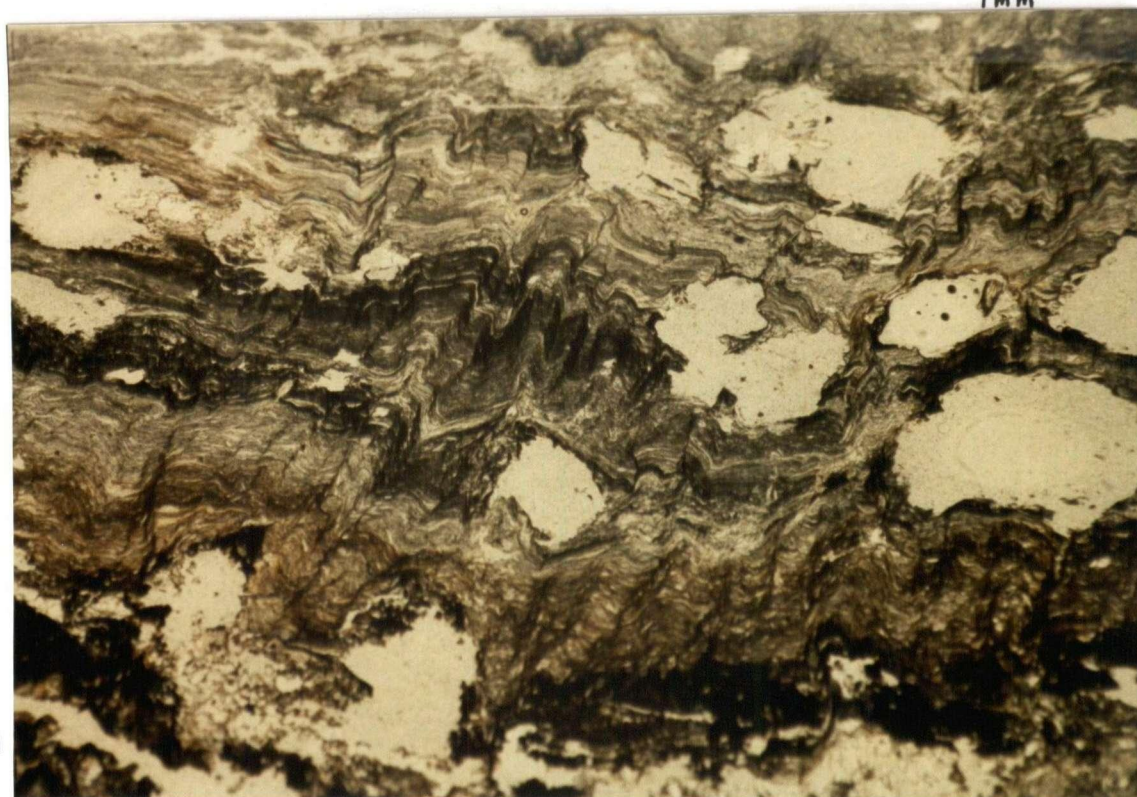


1 mm

Figure 4-19. Photomicrograph (x-nicols) of an Upper Triassic graphitic phyllonite. The prominent foliation, S_2 , is outlined by recrystallized quartz, muscovite-sericite, and graphite.



a



b

Figure 4-20a,b. Photomicrographs (plane-light) of typical graphitic phyllites of the Upper Triassic assemblage. Compositional layers, which represent a transposed foliation, are comprised of biotite, muscovite, sericite, and graphitic material. Phase 3 crenulations deform S_2 layering and have produced a spaced cleavage in photo (b). The large white patches represent holes which were once filled by hematite porphyroblasts, which have since been re-precipitated.

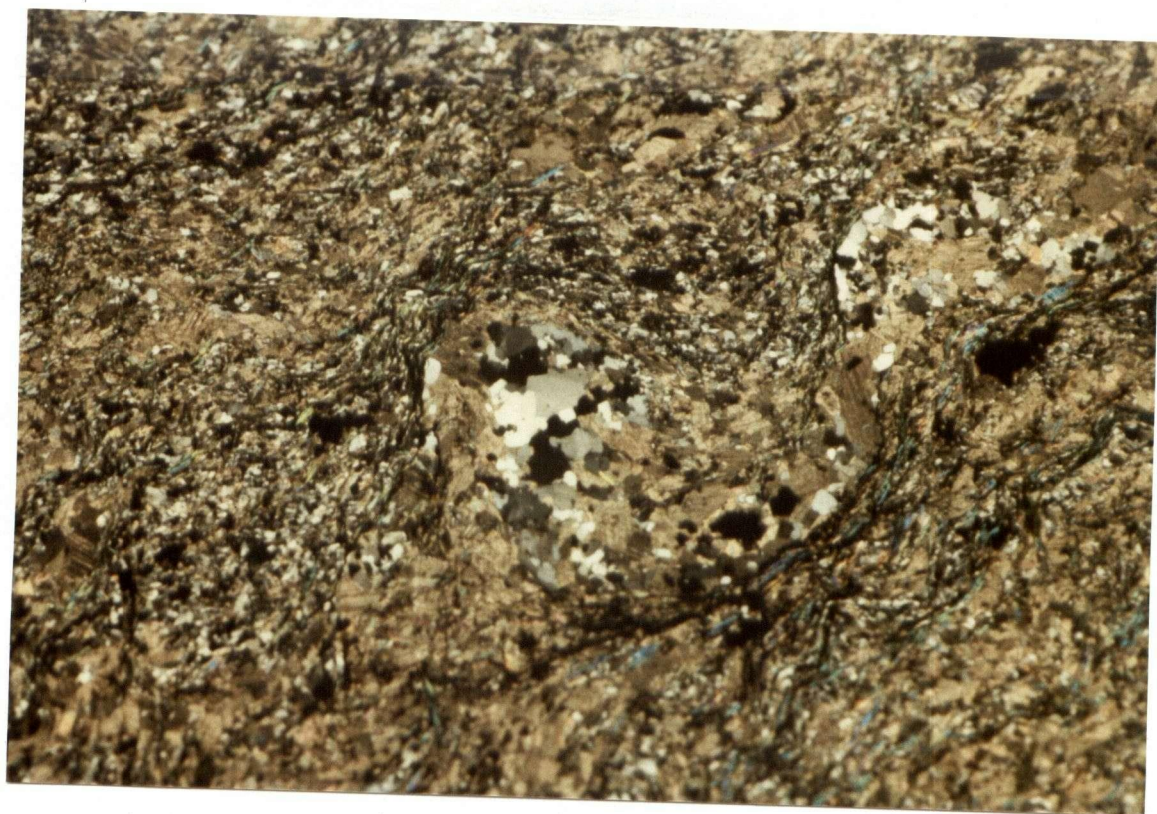
often deformed by F_2 and F_3 and represent relict features associated with initial de-watering and pressure solution phenomenon active during the early stages of deformation (D_2) (Fig. 4-21).

Middle Unit

Rocks within the middle unit consist largely of mixed graphitic phyllite and carbonate. Carbonates (calcite, dolomite) occur as lenses and knots, remnants of boudinaged phase-2 isoclinal folds, intercalated within graphitic muscovite-sericite schist. Quartz, when present in layers appears strained and relatively fine grained though no appreciable grain boundary migration or subgrain development was detected. Muscovite-sericite define the S_2 fabric and are deformed by phase-3 open buckle-fold-microcrenulations. Several zones of tightly folded (D_3) phyllites revealed metamorphic textures in which biotite has crystallized along S_3 crenulation cleavage. These zones are analogous to transposition (shear) zones observed within Antler and Snowshoe rocks adjacent to their respective contact. The nature of transposition in these areas involved more ductile folding and has, locally higher metamorphic grade, such that biotite grew along third phase cleavage whereas metamorphism in rocks involved in more open phase-3 folding at this structural level did not support biotite growth.



Figure 4-21a. Photomicrograph (plane-light) of graphite phyllite which contains a deformed quartz filled hydraulic fracture.



1 mm

Figure 4-21b. Cross-nicols view of Figure 4-21a illustrating the recrystallized nature of quartz.

Upper Unit

Upper-unit lithologies within Upper-Triassic rocks are composed of graphitic phyllite with intercalated layers of chlorite schist and greenstone lenses. Phyllites in this unit are similar in texture and mineralogy to underlying phyllite with the exception of the presence of only very small amounts of calcareous material. Chlorite schists are composed of quartz, chlorite, muscovite and occasional porphyroblasts of brown biotite. The primary foliation, S_2 , is outlined by and contains all of these phases. Minor phases include magnetite and sphene.

Finer grained rocks containing chlorite-sericite and quartz define massive lenses of greenstone. No recognizable foliation can be identified and it is generally assumed that these "pods" may represent the stratigraphic incorporation of fine grained basaltic material, (most likely associated with an arc environment) prior to the convergence of Quesnellia and Omineca terranes.

Table 4-6 presents the relationship between the growth of mineral phases and the proposed deformation sequence.

MINERAL PHASES		SYN ^{D₁} POST	SYN ^{D₂} POST	SYN ^{D₃} POST	SYN ^{D₄} POST
U Tr P H Y L L I T E	BIOTITE			-----	-----
	MUSCOVITE-SERICITE			-----	-----
	HEMATITE			-----	
	CHLORITE			-----	-----

TABLE 4-6

Relation of mineral growth to proposed deformation scheme in the
in the Upper Triassic Formation, Mt. Perseus area, Crooked Lake, B.C.

Microtextures: General Conclusions

From the previous discussion of metamorphism and microtextures, one can infer that a Barrovian-type prograde metamorphic sequence exists within the Mt. Perseus area that ranges from the middle greenschist in structurally highest rocks to lower amphibolite at deeper structural levels.

Snowshoe Group lithologies are characterized by coexisting phases of garnet and biotite which indicate that metamorphism most likely did not exceed the lower amphibolite facies (600°C). Two generations of garnet growth have been related to phase-two and phase-three deformation and outline a continuous recrystallization sequence, the peak of which occurred sykinematically to D₂. The presence of chlorite and post-kinematic biotite indicates that metamorphic activity within the Snowshoe Group was reduced to at least the upper greenschist after phase-three deformation and that metamorphism continued and outlasted deformation.

Antler metavolcanic assemblages show a range in metamorphism from the epidote amphibolite (albite-epidote-hornblende facies, 500°C) to the middle greenschist facies. Structurally lowest rocks (mylonites), in contact with upper Snowshoe mylonites are typically magnesian, ultramafic and contain a mineralogy (antigorite-actinolite-carbonate; actinolite-chlorite-talc-hornblende-epidote-albite) characteristic of

the transition between the upper-greenschist and epidote-amphibolite facies. Hence, an isograd based on the appearance-disappearance of these diagnostic phases exists within the lower units of the Antler Formation. Structurally higher lithologies appear less mafic more Fe enriched and contain albite, chlorite, epidote, calcite, and actinolite; phases more characteristic of the upper to middle greenschist facies (400°C). Pelitic compositions within the Antler contain albite, muscovite, and chlorite; minerals also diagnostic of the middle and upper greenschist facies. Microtextures indicate that peak metamorphic assemblages are associated with D_2 and recrystallization and annealing, during D_3 , was followed by further recrystallization which outlasted deformation.

Lithologic compositions indicate that basal Antler stratigraphy was derived principally from mafic-ultramafic igneous rock types which grade structurally upward into dominantly mafic meta-volcanic assemblages. This small cross-section is similar in many respects to ophiolite-type complexes associated with other convergent boundaries in the Cordillera.

Upper-Triassic rocks reflect deep water anaerobic depositional environments and contain minerals diagnostic of the lower to middle greenschist facies. Minerals such as muscovite, quartz, and albitic plagioclase outline a transpositional metamorphic foliation formed as a result of phase 2 regional deformation. Metamorphic recrystallization associated with phase 3 and later deformation (ductile and

brittle) is not widespread and is principally confined to narrow zones containing mylonites and ductile fold sets.

Metamorphism within the Mt. Perseus area thus appears to represent a prograde sequence whose grade is a function of structural depth and proximity to the convergent boundary. The crystallization of peak metamorphic assemblages in all formations is related to phase 2 regional deformation and isograds delineating the first appearance of garnet parallel the tectonic boundary. Recrystallization associated with and subsequent to phase 3 folding is widespread throughout the Snowshoe but is restricted to narrow mylonite zones in Antler and Upper Triassic lithologies.

The timing of metamorphism can only be inferred as having been initiated in the post-Upper-Triassic and probably continued throughout the mid-Mesozoic in association with the Columbian Orogeny.

SUMMARY AND DISCUSSION

Structural Conclusions

The central conclusions arising from this study are concerned with a detailed description of the structural relation across the Intermontane (Quesnellia)-Omineca Belt boundary and in the presentation of a coherent picture of the tectonic evolution of part of the Quesnel Lake region.

The Intermontane (Quesnellia)-Omineca boundary within the Mt. Perseus area is contained within an overturned fold limb associated with a series of regional northwesterly shallow plunging antiformal folds cored by metasediments of the westernmost extension of the Omineca Belt. These metasediments comprise members of the Snowshoe Group of rocks whose age may range from Hadrynian through lower Paleozoic (Campbell, 1978; Struik, 1984).

Immediately structurally overlying the Snowshoe Group is an exposure of basic meta-volcanic and ultramafic rocks that may be the southern equivalents of the Slide Mountain Group composed of basic volcanics and chert of late Paleozoic age (Struik, 1982). This volcanic sequence is in turn structurally overlain by black phyllites of uncertain Upper Triassic age.

Each of these major groups is separated from its neighbor by a well-defined fault zone that is usually outlined by zones of mylonitic rocks varying in width of up to 1 kilometer. The Snowshoe Group is thus considered to be basement to the overlying cover of younger late Paleozoic and early Mesozoic volcanic and sedimentary rocks.

Snowshoe Group metasediments within the field area consist largely of meta-pelitic rocks that envelope a layer of quartzo-feldspathic orthogneiss. This granitic gneiss may be related to the Quesnel Gneiss which has yielded zircons of mid-Paleozoic age (Montgomery, 1985). All rock types have been variably metamorphosed throughout the lower amphibolite facies and belong in part to the northernmost extremity of the Shuswap Complex.

A sequence of 5 deformational phases has been established within the Snowshoe. The earliest deformation phase is unique to the Snowshoe and consists of mesoscopic isoclinal folds that are commonly rootless, east-verging, and contain mineral lineations parallel with their hinge lines. A well developed axial foliation, outlined in part by compositional layering has not as yet been related to any large scale regional structure. Thus, the earliest surface that outlines any recognizable regional structure is a transposed foliation of regional nature.

The earliest deformation common to all formations in the study area, phase 2 deformation, is recognizable on all scales and is

associated with the widespread ductile behaviour in all rock types. This deformation is probably the main phase of penetrative deformation everywhere recognized in Snowshoe Group rocks and associated gneisses and is responsible in the formation of a large east-verging synform, later deformed into the Perseus antiform. Pronounced metamorphic foliation dips variably to the east and is axial planar to major and minor folds. Fold axes are curvilinear and are outlined by strongly developed mineral lineations throughout the area. Minor folds show consistent easterly vergence related to a major synformal closure outlined by the Perseus gneiss.

Associated with this penetrative deformation is a metamorphism, whose mineral assemblages in the Snowshoe are characteristic of the lower amphibolite and epidote-amphibolite facies. Microtextures indicate that this metamorphism peaked and outlasted the second phase of deformation and began to wane well into the third phase.

Nowhere within the field areas were phase-2 folds seen to deform the Intermontane (Quesnellia)-Omineca boundary. Thus, the formation of this boundary is related to the formation of large scale easterly-verging folds within the Snowshoe.

Third phase deformation consists of meso-macroscopic folds having westerly vergence with an associated well developed axial planar foliation which dips steeply to the northeast. Adjacent to the Intermontane (Quesnellia)-Omineca boundary phase 3 geometry consists of

large rounded antiformal closures separated by highly attenuated synforms into which overlying cover rocks have been drawn. Ductile shear zones of variable width and high flattening strain are located at and extend below the synform closures. Larger scale northwest plunging third phase folds define and control the present configuration of the convergent boundary. The Perseus antiform, an example of a large scale basement fold structure is dome-like in outcrop and overturned to the northeast.

Phase 2 easterly verging folds are refolded by these almost coaxial westerly verging third folds and their associated foliation. It is the superposition of this third phase stage on the pre-existing phase 2 folds that give rise to the curvilinear nature of these phase 2 axial structures and elongate dome geometry of the Perseus antiform. Phase 3 slip directions, determined from the locus of distorted phase 2 linear features are seen to make a high angle with the third axial direction, almost parallel with the dip direction of its associated axial foliation.

Phase 4 deformation is characterized by non-penetrative east verging folds and crenulations whose axial cleavages dip gently to the southwest across all previously developed surfaces. This deformation is particularly well developed with the core regions of large phase 3 structures and within cover rocks adjacent to the Intermontane-Omineca boundary.

Phase 5 deformation is represented by non-penetrative small scale vertical buckle folds whose axial surfaces dip steeply to the northwest. Folds of this generation are open and mildly deform all existing structures throughout the study area.

Thus, the Snowshoe Group, basement to the late-Paleozoic-early Mesozoic cover displays a deformation sequence whose vergence changes in direction with time, firstly and secondly to the northeast, then to the southwest and finally to the northeast again.

Structurally above and in tectonic contact with Snowshoe Group rocks is a highly deformed package of meta-mafic-ultramafic rocks of volcanic affinity believed to be of late Paleozoic age (Antler Formation). It has a variable thickness (150-800 metres) and has a well developed mylonitic lamination that is parallel with gross compositional layering which contain discrete rootless isoclinal folds. Metamorphism in these rocks varies between the middle and upper greenschist to the epidote-amphibolite facies. Immediately above and in tectonic contact with Antler rocks is a Mesozoic package of mixed sedimentary and basic volcanic rocks informally designated as Upper-Triassic Black Phyllites. This unit, metamorphosed within the middle greenschist facies, shows no gross structural inversion and near to its lower contact, the phyllite has a transposed foliation, parallel with the transposed foliation within the underlying volcanic assemblage. Both of these earliest recognizable axial foliations are parallel with the phase 2 axial foliation recognized within Snowshoe basement rocks.

Approximately 200 metres above the phyllite-volcanic contact, the degree of transposition becomes less so, and isoclinal folds gradually develop measurable angles between their limbs. Whereever present, these earliest cover folds - open or transposed - exhibit a north-easterly vergence.

The earliest recognizable cover folds, as described above, are refolded on all scales by a westerly verging second fold set characterized by disharmonic geometry and associated small scale ductile shear zones. A well developed axial foliation parallel to third phase foliation within the Snowshoe Group is characterized in large by a spaced crenulation cleavage. It is this fold set that controls the regional map pattern and gives the Intermontane (Quesnellia)-Omineca convergent zone its present regional configuration.

The last significant common deformation geometry consists of a mesoscopic crenulation and crenulation cleavage developed across all earlier surfaces. These small scale folds show consistent vergence to the northeast and become less well developed at higher structural levels within the cover rocks.

Regional Implications and Tectonic Conclusions

It is apparent that all three major groups of rocks, Snowshoe Group, the Antler Formation and the Upper Triassic Black Phyllites have common phases of deformation with the Snowshoe Group having an extra phase of deformation not present within the other two.

Prior to phase 1 deformation within the Snowshoe Group, presumably within the early to mid-Paleozoic, cratonic sediments of pelitic composition belonging to the leading edge of a westward prograding continental margin terrace wedge (Monger and Price, 1979; Monger et al., 1982) were intruded by large sills of quartz diorite and quartz monzonite porphyry of uncertain affinity. Zircons within the Quesnel Gneiss have placed the date of intrusion within the mid-Paleozoic (Montgomery, 1985).

Phase 1 folding may be associated with mild deformation during the mid-Paleozoic Caribooan orogeny in which pelitic rocks of the Snowshoe Group underwent initial dewatering accompanied by pressure solution. Incipient widespread mesoscopic folding developed in both pelites and igneous intrusions which at the onslaught of later deformation associated with tectonic convergence became progressively flattened, transposed, and subsequently metamorphosed.

As mentioned above, all the major rock groups share common phases

of deformation, however, the conditions wherein the common phases are accomplished are different for the Snowshoe Group (basement) and upper structural levels within the Antler and Upper-Triassic Formations (cover). At this time of the earliest common phase (phase 2 within the Snowshoe Group) prograde metamorphism is synkinematic with the Snowshoe, peaking at the lower amphibolite facies adjacent to the convergent boundary and middle amphibolite at deeper structural levels. Metamorphism in the Snowshoe began to wane during phase-3, whereas the cover deformation during this earliest time is accomplished through initial dewatering accompanied by pressure solution and folding of the mixed cover assemblage. The junction between the cover and basement during this deformation episode is itself not deformed but is outlined by mylonites. Thus one can infer that the cover assemblage was progressively thrust via low angle east-directed transport onto continental basement rocks. This thrusting occurred within a ductile regime and resulted in the formation of narrow mylonite zones adjacent to existing contacts between the respective cover lithologies.

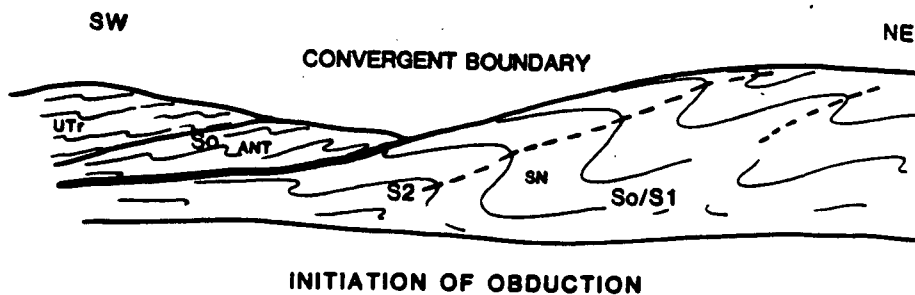
The junction between basement and cover becomes deformed during the second common phase of deformation and due to the extreme ductility contrast present during tectonic shortening, less competent cover rocks are drawn down into and occupy the cores of highly attenuated synforms between more open antiformal closures of the more competent basement. Below these nearly transposed synforms, basement shear zones contain isolated slivers of cover meta-volcanics.

The following concept of the tectonic evolution of the Mt. Perseus

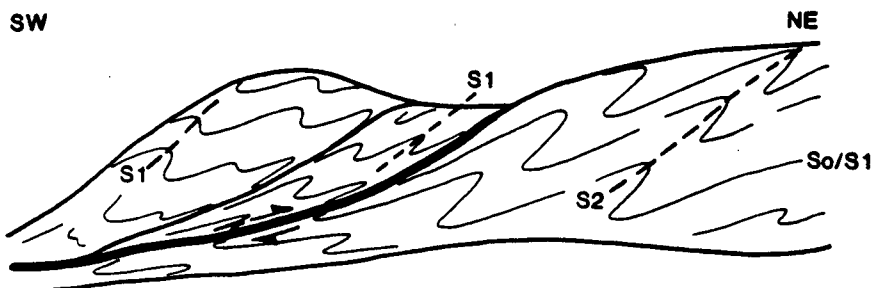
area and surrounding Quesnel Lake region is synthesized in combining the above geometry together with vergence directions of the different deformation phases to give one possible model.

The first common phase of deformation within the basement and cover involves the development of easterly verging folds without any visible shortening of the basement-cover boundary. From this it can be inferred that these two packages of rocks had likely undergone an initial phase of convergence (Fig. 5-1). This convergence, involving the emplacement of a late-Paleozoic mafic-ultramafic volcanic assemblage (ophiolite) together with early Mesozoic sediments and volcanics was likely an obduction process whereby continental Hadrynain rocks were subducted westwards below the easterly converging accretionary package. The association of deep water (anaerobic) argillic sediments with underlying mafic volcanics and ultramafics most likely infer that a subsiding marginal back-arc- type basin existed west of the continental margin prior to the mid- Mesozoic (Monger and Price, 1979). Subduction of continental rocks active during the mid-Mesozoic (Columbian Orogeny) resulted in the closing of this marginal basin and later obduction and accretion of sedimentary-volcanic assemblages of oceanic affinity.

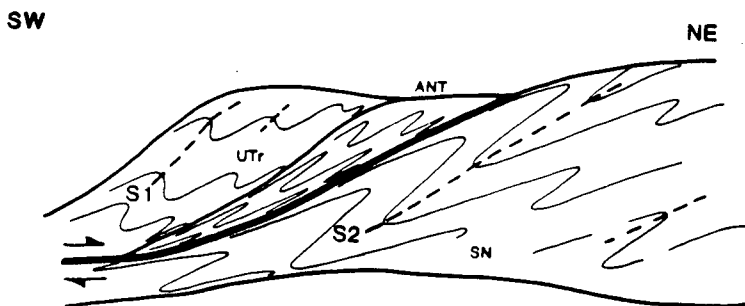
A change in transport direction is inferred from the next common phase of deformation, wherein westerly verging folds are developed throughout both basement and cover rocks and the basement-cover



1



2



3

Figure 5-1. Schematic cross-section across the Quesnellia-Omineca boundary during the time of initial convergence (obduction).

junction becomes markedly shortened. These westerly verging folds, shortening of the junction, and east-dipping shear zones within the basement and lower cover appear to indicate a reversal of the direction of subduction (Fig. 5-2). The development of the late crenulation cleavage is likely a consequence of late eastward thrusting of early Jurassic marine volcanics (outside of the field area) which overlie, with decollement, the Upper-Triassic phyllites.

The tectonic model described above is but one interpretation of the data, is simple and involves only a change in transport direction. However, regional tectonic models proposed by Monger et. al. (1982) involves not only convergence but also large scale lateral translation associated with the accretion process. In any convergent model the shortening direction observed in rocks is not directly related to the direction of convergence, rather it is perpendicular to the zone of convergence even when the process is oblique. Often the component of convergence parallel with the zone is evidenced by large scale strike-slip displacement in the arc region behind the subduction zone. No such strike-slip displacement has been recognized within the region under discussion and no evidence of lateral regional extension parallel with the zone of convergence has been seen. Thus, if large scale translation is involved in the accretion processes then the evidence for same has been destroyed during the convergence process or translation occurred before convergence began.

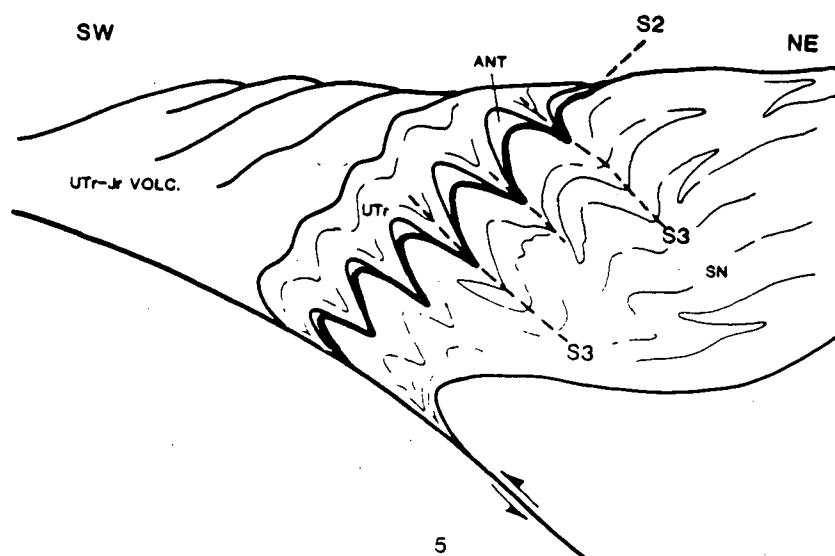
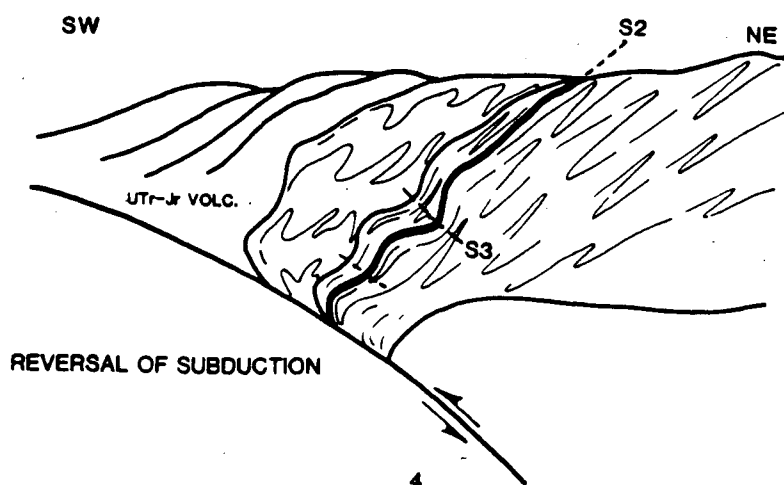


Figure 5-2. Schematic cross-sections across the Quesnellia-Omineca boundary after initial convergence. A reversal in subduction direction produced a shortening of the terrane boundary into the present day map configuration.

BIBLIOGRAPHY

- Archibald, D.A., Glover, J.K., Price, R.A., Farrar, E. and Carmichael, D.M., 1983. Geochronology and tectonic implications of magmatism and metamorphism southern Kootenay Arc and neighbouring regions, southeastern British Columbia. Part I: Jurassic to mid-Cretaceous. *Canadian Journal of Earth Science*, 20, pp. 1891-1913.
- Armstrong, R.L., 1982. Cordilleran metamorphic core complexes from Arizona to southern Canada. *Annual Review of Earth and Planetary Sciences*, 10, pp. 129-154.
- Bailey, David G., 1976. Geology of the Morehead Lake area, central British Columbia; Notes to accompany preliminary map no. 20; British Columbia Department of Mines and Petroleum Resources, July 1976, 6 p.
- Berthe, D., Chokroune, P. and Jegouzo, P., 1979. Orthogneiss, mylonite and non-coaxial deformation of granites: the example of the South American Shear Zone. *Journal of Structural Geology*, 1, 31-42.
- Brown, R.L., 1981. Metamorphic complex of SE Canadian Cordillera and relationship to foreland thrusting. In *Thrust and nappe tectonics*. The Geological Society of London, pp. 463-473.
- Brown, R.L. and Murphy, D.C., 1982. Kinematic interpretation of mylonitic rocks in part of the Columbia River fault zone, Shuswap Terrane, British Columbia. *Canadian Journal of Earth Sciences*, 19, pp. 456-465.
- Brown, R.L. and Read, P.B., 1983. Shuswap Terrane of British Columbia: a Mesozoic "core complex". *Geology*, 11, pp. 164-168.
- Campbell, K.V., 1971. Metamorphic petrology and structural geology of the Crooked Lake area, Cariboo Mountains, British Columbia. Ph.D. thesis, University of Washington, Seattle, Washington, 192 pages.
- Campbell, K.V. and Campbell, R.B., 1970. Quesnel Lake map area, British Columbia. In report of activities, part A. Geological Survey of Canada, Paper 70-1, pp. 32-35.
- Campbell, R.B., 1970. Structural and metamorphic transitions from infrastructure to suprastructure, Cariboo Mountains, British Columbia. Geological Association of Canada, Special Paper No. 6, pp. 67-72.
- Campbell, R.B., 1973. Structural cross-section and tectonic model of the southeastern Canadian Cordillera. *Canadian Journal of Earth Sciences*, 10, pp. 1607-1620.

- Campbell, R.B., 1977. The Shuswap Metamorphic Complex, British Columbia. Geological Society of America, Abstracts with Programs, 9, pp. 920.
- Campbell, R.B., 1978. Quesnel Lake (93A) map area, British Columbia. Geological Survey of Canada, Open File map 574.
- Campbell, R.B., Mountjoy, E.W. and Young, F.G., 1973. Geology of the McBride map area, British Columbia (93H). Geological Survey of Canada, Paper 72-35, 104 pages.
- Campbell, R.B. and Tipper, H.W., 1970. Bonaparte River, British Columbia. Geological Survey of Canada, Memoir 363.
- Coney, P.J., Jones, D.L. and Monger, J.W.H., 1980. Cordilleran suspect terranes. Nature, 288, pp. 329-333.
- Deer, W.A., Howie, R.A. and Zussman, J., 1977. An introduction to the rock forming minerals. Longman Group Ltd. 528 pages.
- Dewey, J.F., 1976. Ophiolite obduction Tectonophysics, 31, pp. 93-120.
- Durney, D.M. and Ramsay, J.G., 1972. Incremental strains measured by syntectonic crystal growths. In DeJong, K.A., and Scholten, R., eds., Gravity and tectonics, John Wiley and Sons, New York, pp. 67-96.
- Elliot, D., 1973. Diffusion flow laws in metamorphic rocks. Geological Society of America Bulletin, 84, pp. 2645-2664.
- Ferry, J.M. and Spear, F.S., 1978. Experimental calibration of the partitioning of Fe and Mg between biotite and garnet. Contributions to Mineralogy and Petrology, 66, 113-117.
- Fillipone, J.A., 1985. Structure and metamorphism at the Intermontane-Omineca boundary, near Boss Mountain, east-central British Columbia. M.Sc. thesis, University of British Columbia, Vancouver, British Columbia.
- Fletcher, C.J.N. and Greenwood, H.J., 1978. Metamorphism and structure of Penfold Creek area, near Quesnel Lake, British Columbia. Journal of Petrology, 20, part 4, pp. 743-794.
- Getsinger, J.S., 1985. Geology of the Three Ladies Mountain/Mount Stevenson area, Quesnel Highland British Columbia. Ph.D. thesis, University of British Columbia, Vancouver, British Columbia.
- Ghent, E.D., Simony, P.S. and Raeside, R.P. 1981. Metamorphism and its relation to structure within the core zone west of the Southern Rocky Mountains. Field guides to geology and mineral deposits, Calgary 81, Geological Association of Canada, Mineralogical Association of Canada, Canadian Geophysical Union.

- Hobbs, B.E., Means, W.D. and Williams, P.F., 1976. An outline of structural geology. John Wiley and Sons, 571 pages.
- Holland, S.S. 1954. Geology of the Yanks Peak- Roundtop Mountain area, Cariboo District, British Columbia. British Columbia Department of Mines Bulletin, 34, 90 pages.
- Mason, R., 1978. Petrology of the metamorphic rocks. George Allen and Unwin Ltd., London, 254 pages.
- Miyashiro, A., 1961. Evolution of metamorphic belts. Journal of Petrology, 2, pp. 277-311.
- Monger, J.W.H. and Price, R.A., 1979. Geodynamic evolution of the Canadian Cordillera progress and problems. Canadian Journal of Earth Sciences, 16, pp. 770-791.
- Monger, J.W.H., Price, R.A. and Tempelman-Kluit, D., 1982. Tectonic accretion and the origin of two major metamorphic and plutonic welts in the Canadian Cordillera. Geology, 10, pp. 70-75.
- Montgomery, J.R., 1985. Structural relations of the southern Quesnel Lake Gneiss, Isoceles Mountain area, central British Columbia. M.Sc. thesis, University of British Columbia, Vancouver, British Columbia.
- Montgomery, S.L., 1978, Structural and metamorphic history of the Dunford Lake map area, Cariboo Mountains, British Columbia. M.S. thesis, Cornell University, Ithaca, New York.
- Morton, R.L., 1976. Alkalic volcanism and copper deposits of the Horsefly area, central British Columbia; unpublished Ph.D. thesis, Carleton University, 196 p.
- Murphy, D.C and Rees, C.J., 1983. Structural transition and stratigraphy in the Cariboo Mountains, British Columbia. In Current Research, Part A., Geological Survey of Canada, Paper 83-1A, pp. 245-252.
- Okulitch, A.V., 1984. The role of the Shuswap Metamorphic Complex in Cordilleran tectonism. Canadian Journal of Earth Sciences, 21, pp. 1171-1193.
- Pigage, L.C., 1977. Rb-Sr dats for granodiorite intrusions of the northeast margin of the Shuswap Metamorphic Complex, Cariboo Mountains, British Columbia. Canadian Journal of Earth Sciences, 14, pp. 1690-1695.
- Pigage, L.C., 1978. Metamorphism and deformation on the northeast margin of the Shuswap Metamorphic Complex, Azure Lake, British

- Columbia. Ph.D. thesis, University of British Columbia, Vancouver, British Columbia, 289 pages.
- Pigage, L.C. and Greenwood, H.J., 1982. Internally consistent estimates of pressure and temperature: the staurolite problem. *American Journal of Science*, 282, pp. 943-969.
- Price, R.A. and Douglas, R.J.W., 1972. Variations in Tectonic Styles in Canada. Geological Association of Canada, Special Paper No. 2, pp. 1-81.
- Price, R.A., Monger, J.W.H. and Roddick, J.A., 1985. Cordilleran cross-section; Calgary to Vancouver. In Field guides to geology and mineral deposits in the Southern Canadian Cordillera. Geological Society of America Cordilleran Section Meeting, Vancouver, British Columbia, May 1985.
- Ramsay, J.G., 1962a. The deformation of earlier linear structures in areas of repeated folding. *Journal of Geology*, 68, 75-93.
- Ramsay, J.G., 1962b. The geometry and mechanics of "similar" type folds. *Journal of Geology*, 70, pp. 309-327.
- Ramsay, J.G., 1967. Folding and fracturing of rocks. McGraw-Hill, New York, N.Y., 568 pages.
- Ramsay, J.G., Casey, M. and Kligfield, R., 1983. Role of shear in the development of the Helvetic fold-thrust belt of Switzerland. *Geology*, 11, pp. 439-442.
- Read, P.B. and Brown, R.L., 1981. Columbia River fault zone; southeast margin of the Shuswap and Monashee Complexes, southern British Columbia. *Canadian Journal of Earth Sciences*, 18, pp. 1127-1145.
- Rees, C.J., 1981. Western margin of the Omineca Belt at Quesnel Lake, British Columbia. In Current Research, Part A., Geological Survey of Canada, Paper 81-1A, pp. 223-226.
- Rees, C.J. and Ferri, F., 1983. A kinematic study of mylonitic rocks in the Omineca-Intermontane Belt tectonic boundary in east-central British Columbia. In Current Research, Part B, Geological Survey of Canada, Paper 83-1B, pp. 121-125.
- Rosenfeld, J.L. 1970. Rotated garnets in metamorphic rocks. Geological Society of America Special Paper, 129, 105 pages.
- Ross, J.V., 1968. Structural relations at the eastern margin of the Shuswap Complex, near Revelstoke, southeastern British Columbia. *Canadian Journal of Earth Sciences*, 5, pp. 831-849.
- Ross, J.V., 1981. A geodynamic model for some structures within and adjacent to the Okanagan Valley, southern British Columbia. *Canadian Journal of Earth Sciences*, 18, pp. 1581-1598.

- Ross, J.V. and Christie, J.S., 1979. Early recumbent folding in some westernmost exposures of the Shuswap Complex, southern Okanagan, British Columbia. *Canadian Journal of Earth Sciences*, 16, pp. 877-894.
- Ross, J.V., Fillipone, J.A., Montgomery, J.R., Elsby, D.C. and Bloodgood, M.A., 1985. Geometry of a convergent zone, central British Columbia, Canada. *Tectonophysics*, in press.
- Simpson, C. and Schmid, S.M., 1983. An evaluation of criteria to deduce the sense of movement in sheared rocks. *Geological Society of America Bulletin*, 94, pp. 1281-1288.
- Struik, L.C., 1981. Snowshoe Formation, central British Columbia. In *Current Research, Part A*, Geological Survey of Canada, Paper 81-1A, pp. 213-216.
- Struik, L.C., 1982. Bedrock geology of Cariboo Lake (93A/14), Spectacle Lakes (93H/3), Swift River (93A/13), and Wells (93H/4) map-areas, central British Columbia. Geological Survey of Canada, Open File 858.
- Struik, L.C., 1982. Snowshoe Formation (1982), central British Columbia. In *Current Research, Part B*, Geological Survey of Canada, Paper 82-1B, pp. 117-124.
- Struik, L.C., 1983a. Bedrock geology of Spanish Lake (93A/11) and parts of adjoining map areas, central British Columbia. Geological Survey of Canada, Open File Map 920.
- Struik, L.C., 1983b. Bedrock geology of Quesnel Lake (93A/10) and part of Mitchell Lake (93A/15) map areas, central British Columbia. Geological Survey of Canada, Open File Map 962.
- Struik, L.C., 1984. Geology of Quesnel Lake and part of Mitchell Lake, British Columbia. Geological Survey of Canada, Open File Map, 962.
- Struik, L.C., 1985. Pre-Cretaceous terranes and their thrust and strike slip contacts, Prince George east half and McBride west half, British Columbia. In *Current Research, Part A*, Geological Survey of Canada, Paper 85-1A.
- Sutherland-Brown, A., 1957. Geology of the Antler Creek area, Cariboo District, British Columbia. British Columbia Department of Mines, Bulletin 38, 105 pages.
- Sutherland-Brown, A., 1963. Geology of the Cariboo River area, British Columbia. British Columbia Department of Mines, Bulletin 47.
- Tempelman-Kluit, D.J., 1979. Transported cataclasite, ophiolite and granodiorite in Yukon: evidence of arc-continent collision; Geological Survey of Canada, Paper 79-14, 27 p.

- Thompson, A.B., 1975. Mineral reactions in calc-mica schist from Gassetts, Vermont, U.S.A. *Contributions to Mineralogy and Petrology*, 53, pp. 105-127.
- Thompson, A.B., 1976a. Mineral reactions in pelitic rocks: I. Prediction of P-T-X (Mg/Fe) phase relations. *American Journal of Science*, 276, pp. 401-424.
- Thompson, A.B., 1976b. Mineral reactions in pelitic rocks: II. Calculation of some P-T-X (Mg/Fe) phase relations. *American Journal of Science*, 276, pp. 425-454.
- Tipper, H.W., 1960. Prince George map area. Geological Survey of Canada, map 49-1960.
- Tipper, H.W., Woodsworth, G.J. and Gabrielse, H., 1978. Tectonic assemblage map of the Canadian Cordillera and adjacent parts of the United States of America. Geological Survey of Canada, Map 1505A.
- Turner, F.J., 1981. *Metamorphic petrology*. McGraw-Hill, second edition, 524 pages.
- Vernon, R.H., 1977. Relationships between microstructures and metamorphic assemblages. *Tectonophysics*, 39, pp. 439-452.
- Wheeler, J.O., 1970. Summary and discussion. Geological Association of Canada, Special Paper No. 6, pp. 155-166.
- Wheeler, J.O., Campbell, R.B., Reesor, J.E. and Mountjoy, E.W., 1972. Structural style of the southern Canadian Cordillera. In *Guidebook for Excursion A-01 - X-01*. 24th International Geological Congress, Montreal, Quebec, 118 pages.
- Wheeler, J.O. and Gabrielse, H., 1972. The Cordilleran structural province. Geological Association of Canada, Special Paper 11, pp. 1-81.
- White, S.H., Burrows, S.E., Carreras, J., Shaw, N.D., and Humphreys, F.J., 1980. On mylonite in ductile shear zones; *Journal of Structural Geology*, v. 2, pp. 175-187.
- Williams, P.F., 1976. Relationship between axial plane foliations and strain. *Tectonophysics*, 30, pp. 181-196.
- Williams, H.J.F., 1979. *Petrogenesis of metamorphic rocks*. Springer Verlag, New York, N.Y., fifth edition, 348 pages.
- Williams, H., Turner, F.J. and Gilbert, C.M., 1954. *Petrography, and introduction to the study of rocks in thin sections*. W.H. Freeman and Company, San Francisco, California, p. 224.